

STRATIGRAPHIC AND PALEOENVIRONMENTAL CONTEXT OF THE
INGERSOLL SHALE, AN UPPER CRETACEOUS CONSERVATION
LAGERSTÄTTE, EUTAW FORMATION,
EASTERN ALABAMA

Except where reference is made to the work of others, the work described in this thesis is my own or was done in collaboration with my advisory committee. This thesis does not include proprietary or classified information.

Patrick Sean Bingham

Certificate of Approval:

Ronald D. Lewis
Associate Professor
Geology and Geography

Charles E. Savrda, Chair
Professor
Geology and Geography

William J. Frazier
Professor
Chemistry and Geology
Columbus State University

Joe F. Pittman
Interim Dean
Graduate School

STRATIGRAPHIC AND PALEOENVIRONMENTAL CONTEXT OF THE
INGERSOLL SHALE, AN UPPER CRETACEOUS CONSERVATION
LAGERSTÄTTE, EUTAW FORMATION,
EASTERN ALABAMA

Patrick Sean Bingham

A Thesis

Submitted to

the Graduate Faculty of

Auburn University

in Partial Fulfillment of the

Requirements for the

Degree of

Master of Science

Auburn, Alabama
August 4, 2007

STRATIGRAPHIC AND PALEOENVIRONMENTAL CONTEXT OF THE
INGERSOLL SHALE, AN UPPER CRETACEOUS CONSERVATION
LAGERSTÄTTE, EUTAW FORMATION,
EASTERN ALABAMA

Patrick Sean Bingham

Permission is granted to Auburn University to make copies of this thesis at its discretion, upon request of individuals or institutions and at their expense. The author reserves all publications rights.

Signature of Author

Date of Graduation

VITA

Patrick Sean Bingham, son of William Edward Bingham and Mattie Louise (Pat) Finney, was born on July 1, 1970, in Columbus, Georgia. He graduated from William Henry Shaw High School, in Columbus, Georgia, in 1988. On March 30, 1995, he became the proud father of Alexandra Nichole Bingham. He married Joani Maria Blair on June 22, 1995. On March 20, 1999, he became the proud father of Devin Fernand Marshall Bingham. He attended Columbus State University in Columbus, Georgia, and graduated in May 2004, summa cum laude, with a Bachelor of Science degree in Geology. He started his graduate program at Auburn University in August, 2004.

THESIS ABSTRACT

STRATIGRAPHIC AND PALEOENVIRONMENTAL CONTEXT OF THE
INGERSOLL SHALE, AN UPPER CRETACEOUS CONSERVATION
LAGERSTÄTTE, EUTAW FORMATION,
EASTERN ALABAMA

Patrick Sean Bingham
Master of Science, August 4, 2007
(B.S., Columbus State University, 2004)

134 Typed Pages

Directed by Charles Savrda

The Ingersoll shale, a thin (<1 m) clay-dominated lens within the Upper Cretaceous Eutaw Formation exposed in Russell County, Alabama, contains an exceptionally well-preserved, primarily terrestrial biota that includes a diverse, carbonized and variably pyritized flora, abundant amber with fossil inclusions, and common feathers. Stratigraphic, sedimentologic, and geochemical studies were undertaken in an attempt to determine the conditions under which this conservation Lagerstätte formed.

Geometry of the Ingersoll shale lens and its position between high-energy tidal sand facies below and estuarine central bay sediments above indicate that deposition

occurred in a shallow, narrow channel in the lower reaches of a bay-head delta in response to estuarine transgression. Well-developed tidal laminites in the lower part of the shale lens and textural analysis of the entire unit indicate that the channel filled very rapidly (up to 77 cm/yr), under progressively waning energy regimes, in response to diurnal tidal rhythms. Ichnofabrics, high organic carbon, and abundant pyrite indicate that sediments in the channel were likely highly fluid and oxygen deficient. Abundance of marine palynomorphs, sulfide contents, and stable isotopic signatures of pyrite sulfur indicate that waters within the channel were characterized by normal to near-normal marine salinities.

Environmental factors and sedimentary processes contributing to unusual preservation of the Ingersoll shale biota include (1) extremely rapid tidal deposition and burial of organic remains (obstruction); (2) reducing conditions in pore waters (stagnation), which limited bioturbation and scavenging, resulted in pyritization of some fossils (diagenetic mineralization), and facilitated the growth of bacterial mats on fossil feathers and, possibly, other fossil elements (bacterial sealing); and (3) concentration of allochthonous or para-autochthonous amber clasts (preservation traps) by tidal currents.

Documented conservation Lagerstätten differ significantly in terms of paleoenvironments, fossil biotas, and modes and causes of preservation. Nonetheless, knowledge gained from the study of the Ingersoll shale may help prospect for similar isolated marginal deposits that may contain comparable well-preserved, predominately terrestrial fossil assemblages.

ACKNOWLEDGMENTS

The author would like to thank the Gulf Coast Association of Geological Societies, the Geological Society of America, and the National Science Foundation for grants that supported this research. Michael Ingersoll allowed the author access to his property. Fellow Auburn University geology student Terry Knight was an integral part of this research and acted as a sounding board for ideas. The following individuals assisted in the field: Jerry Smith, Carl Mehling, John Interlandi, David Grimaldi, Christine Bean, William Bevil, David Leuth, Dent Williams, Michael Brocato, David Schwimmer, William Montante, Greg Mestler, Vicki Lais, Robert Monrreal, Will Newton, Dan Evans, Tom Hart, and Bobby Norris. The following individuals prepared, identified, analyzed, and/or photographed specimens for this thesis: Richard Lupia, David Grimaldi, Mary Schweitzer, Darla Zelenitski, Raymond Christopher, Barton Prorok, and Michael Miller. The following individuals provided information critical to the completion of this thesis: Andy Rindsberg, Allen Archer, Neal Landman, Neal Larson, Trisha Weaver, Royal Mapes, Jody Martin, Stephen Weeks, Thomas Demchuk, Vaughn Bryant, Mike Everhart, Peter Allison, Herbert Summesberger, Bruce Saunders, Peter Jones, Brian Axsmith, Earl Manning, and Patrick Herendeen. The author's thesis committee members provided guidance with field work, laboratory analyses, and writing. The author's family provided their never-ending love, support, and encouragement. The author dedicates this thesis and M.S. Degree to his late mother, Pat Bingham.

Journal style used: Palaios

Computer software used: Microsoft Word 2003, Microsoft Excel 2003, Corel PHOTO-PAINT 11, Adobe Photoshop 7.0, Merge eFILM, 2003, Gradistat v 4.0

TABLE OF CONTENTS

LIST OF FIGURES	xi
LIST OF TABLES	xvii
1.0 INTRODUCTION	1
2.0 EUTAW FORMATION	3
2.1 General Stratigraphy	3
2.2 Sequence Stratigraphy	3
2.3 Depositional Facies	6
3.0 INGERSOLL SHALE	10
3.1 Location	10
3.2 Fossil Assemblage	10
3.3 Paleoenvironmental and Taphonomic Conditions	16
4.0 METHODS	17
4.1 General Approach	17
4.2 Field Studies	17
4.2.1 Section Measurement and Description	17
4.2.2 Excavation and Description of the Ingersoll Shale	18
4.2.3 Sample Collection	19
4.3 Laboratory Studies	20
4.3.1 Analysis of Tidal Rhythmicity and Other Fabrics	20
4.3.2 Textural Studies	21
4.3.3 Carbonate and Organic Analyses	22
4.3.4 Sulfur and Sulfur Isotope Analysis	22
4.3.6 Microscopy	23
5.0 FIELD OBSERVATIONS	24
5.1 General Section Description	24
5.1.1 Tuscaloosa Formation	24
5.1.2 Eutaw Formation	27
5.2 Geometry of the Ingersoll Shale	35
5.3 Internal Stratigraphy of the Ingersoll Shale	42
5.3.1 Subunit A	42
5.3.2 Subunit B	46
5.3.3 Subunit C	48

5.3.4 Distribution of Fossils in the Ingersoll Shale.....	52
6.0 LABORATORY OBSERVATIONS.....	57
6.1 Fabric Analyses.....	57
6.1.1 Tidal Rhythmicity in Subunit A.....	57
6.1.2 Subunit B and C Fabrics	62
6.2 Textural Studies	64
6.3 Organic Studies.....	64
6.3.1 Carbonate and Organic Carbon Contents	64
6.3.2 Types of Organic Matter.....	67
6.4 Pyrite and Sulfur Analyses.....	71
6.4.1 Pyrite.....	71
6.4.2 Sulfur and Sulfur Isotopic Analyses	71
7.0 INTERPRETATIONS	78
7.1 General Environmental Settings	78
7.1.1 Tuscaloosa Formation.....	78
7.1.2 Eutaw Formation.....	78
7.1.3 Ingersoll Shale Channel Complex (Units 6 and 7)	81
7.2 Sea-Level Dynamics.....	83
7.3 Conditions in the Channel.....	85
7.3.1 Depositional Processes and Environmental Energy	85
7.3.2 Sedimentation Rates.....	86
7.3.3 Substrate Consistency	87
7.3.4 Salinity	88
7.3.5 Oxygenation.....	90
8.0 DISCUSSION.....	92
8.1 Factors Controlling Fossil Preservation in Fossil Lagerstätten	92
8.1.1 Previous Studies.....	92
8.1.2 Factors Controlling Fossil Preservation in the Ingersoll Shale.....	95
8.2 Comparison with Other Lagerstätten.....	97
8.2.1 Burgess Shale.....	97
8.2.2 Francis Creek Shale	98
8.2.3 Messel Shale	99
8.2.4 South Amboy Fire Clay	100
8.3 Prospecting for Comparable Conservation Lagerstätten	101
9.0 SUMMARY AND CONCLUSIONS	103
10.0 REFERENCES	106

LIST OF FIGURES

<p>FIGURE 1—Distribution of Cretaceous strata (light-colored belt), including the Eutaw Formation (darker colored belt), in the eastern Gulf coastal plain. The site of the current study (red square) is in Phenix City, eastern Alabama.....</p>	4
<p>FIGURE 2—Generalized stratigraphy of Upper Cretaceous strata across Alabama. Position of the study section is shown by the red rectangle (modified from Savrda and Nanson, 2003)</p>	5
<p>FIGURE 3—Sequence stratigraphic context of the Eutaw and superjacent formations as interpreted by King (1993) and Mancini et al. (1995)</p>	7
<p>FIGURE 4—Paleoenvironmental reconstruction of Santonian-age shoreline with study area indicated by white arrow and star. Reconstruction is based on previous work by Frazier and Taylor (1980), King and Skotnicki (1986), Frazier (1997), and Bingham and Frazier (2004)</p>	8
<p>FIGURE 5—Location of the Ingersoll shale exposure (star) near Highway 431, Phenix City, eastern Alabama (downloaded from MapQuest, 2006)</p>	11
<p>FIGURE 6—Outcrop containing the Ingersoll shale. Basal and top contacts of Ingersoll shale are approximated with yellow and orange lines, respectively (dashed where inferred)</p>	12
<p>FIGURE 7—Examples of Ingersoll shale fossils. (A) Large intact angiosperm leaf (c.f. <i>Manihotites georgiana</i>). (B) Angiosperm leaf (<i>Ficus?</i> sp.) showing marginal insect damage. (C) Fruit wing. (D) Small flower. (E) Taxodeaceous branch with leaflets (c.f. <i>Geinitzia</i>). (F) Three-dimensionally preserved taxodeaceous cones articulated on stems. (G) Three-dimensionally preserved, pyritized conifer shoot. (H) Fern pinnatifid. (I) Water-fern sporocarp containing articulated mega- and microsporangia. (J) Female scale insect preserved in amber. (K) Araneoid spider appendage in amber. (L) Taxodeaceous conifer stem with <i>in situ</i> amber rods. (M) Internal mold of bivalve. (N-P) Representative feathers. (Q) SEM image of fossilized <i>Bacillus</i>-like structures replacing feathers.....</p>	13
<p>FIGURE 8—Stratigraphic column for the measured section of outcrop including the Ingersoll shale (unit 7), Russell County, Alabama</p>	25

FIGURE 9—Representative photos of units 1-4, Tuscaloosa Formation. (A) Sandy mud of unit 1 characterized by red mud intraclasts. (B) Fine to medium sand of unit 2 showing medium-scale trough cross-stratification. (C) Homogeneous sandstone of unit 3 characterized by iron-cemented rhizoliths. (D) Homogeneous and mottled silty clay of unit 4. Scale bars in A, B, and D = 10 cm.....	26
FIGURE 10—Disconformable contact separating silty clay (unit 4) of the Tuscaloosa Formation from the coarse- to very coarse-grained gravelly sands (unit 5) of the Eutaw Formation.....	28
FIGURE 11—Clay drapes (gray), herringbone cross-stratification, and sparse <i>Ophiomorpha</i> (arrows) in gravelly sand of unit 5. Scale bar ~10 cm long	29
FIGURE 12—Unit 6 (oxidized clay and sand) and unit 7 (Ingersoll shale). Note erosional contact (yellow line) between units 6 and 7 and distinct sand laminae near the base of the Ingersoll shale. Height of trench exposure is ~30 cm.....	30
FIGURE 13—Thoroughly bioturbated muddy sands of unit 8. Ichnofossils visible in this view include large <i>Thalassinoides</i> (arrow). Scale bar is ~5 cm long	32
FIGURE 14—Fine micaceous sand of unit 9. (A) Orange lines show approximate upper and lower contacts of unit 9. (B) Large flame structure containing sand-breccia entrained in flow (outlined in orange). (C-D) Large ball-and-pillow structures in the finely layered sands. Scale bars are ~20 cm long.....	33
FIGURE 15—Representative fabrics of units 10-12. (A) Heavily bioturbated unit 10. (B) Heavily bioturbated, pale greenish-yellow, fine, micaceous sand of unit 11. (C) Bioturbated sandy zone of unit 12. (D) Weakly bioturbated shale at top of unit 12. Scales in A-C are graded in cm. Scale bar in D is ~10 cm long.....	34
FIGURE 16—Representative photos of unit 13. (A) Highly bioturbated sand above contact with unit 12 (orange line). (B) Large <i>Thalassinoides</i> in unit 13. Scale bars are ~10 cm long	36
FIGURE 17—East-west backhoe trench cut perpendicular to the hill slope to the north of the fossil quarry (see Fig. 20). The yellow and red dotted lines denote the lower and upper contacts of the Ingersoll shale, respectively. View is toward the NE	37
FIGURE 18—Detailed cross-section of the Ingersoll shale and associated units constructed from trench exposure shown in Fig. 17. Note the asymmetry of the shale body (trees depict ground surface and are not to scale).....	38

FIGURE 19—Portion of trench cut parallel to slope on western side of fossil quarry (see Fig. 20). The yellow and red dotted lines indicate lower and upper contacts of the Ingersoll shale, respectively. View is to the NE.....	39
FIGURE 20—Map of quarry and trenches. Quarry map shows location of bedding-plane strike and dip orientations, orientations of the long axes of plant macro-detritus (double-headed arrows), and presumed position of the long axis of the Ingersoll shale lens.....	40
FIGURE 21—Three-dimensional reconstruction of the channel-form complex containing the Ingersoll shale. Diagram shows location of quarry and the spatial arrangement of units 4-8	41
FIGURE 22—Stratigraphic column of the Ingersoll shale showing general character of three subunits (subunits A-C)	43
FIGURE 23—Graded sand-mud laminae couplets in subunit A of the Ingersoll shale. A starved current-ripple (?) is indicated with an arrow. The thicknesses of these couplets were the focus of the tidal rhythmicity study. Scale bar is ~1 cm long	44
FIGURE 24—Comminuted plant detritus on bedding-plane parting surface of shale in subunit A (Brunton compass for scale)	45
FIGURE 25— <i>Rosselia</i> -like structures in subunit A. (A) and (B) Circular, concentrically laminated areas of displaced silt-sand with central cores of pyrite exposed on bedding surfaces of shale. (C) Close-up of burrow showing plant detritus organized in concentric rings around a central core of pyrite. (D) View perpendicular to bedding shows pyrite core of burrow with pelletized texture similar to <i>Ophiomorpha nodosa</i> . Scale bars ~2 cm long.....	47
FIGURE 26—Bedding surface in subunit B showing cusped current ripple with plant macrodetritus on the lee side. Arrow shows paleocurrent direction. Paleocurrent directions varied from NE to NW but overall trend (n=22) was determined to be NNW	49
FIGURE 27—Burrows in subunit B. (A) Horizontal to subhorizontal, meandering burrows preserved as hyporeliefs on a leaf fossil exposed on bedding surface of shale. (B) Pyritized meandering burrows preserved as epireliefs on the surface of a leaf fossil exposed on a parting surface. Scale bar ~1 cm long	50

FIGURE 28—Ichnofossils extending from the upper erosional surface into subunit C. (A) *Thalassinoides* passively filled with iron-oxide stained, gravelly coarse-grained sand. (B) Close-up of sand-filled, sharp-walled *Thalassinoides*. Red line denotes contact with unit 8. (C) Three *Rhizocorallium*. (D) Close-up of *Rhizocorallium* showing patterned scratch marks (arrows) on the burrow walls. This wall ornamentation indicates firmground conditions. Scale bars are ~2 cm long51

FIGURE 29—Soft-sediment deformation in subunit C of the Ingersoll shale. Dashed line approximates hinge of large synsedimentary fold. Note that unit 8 is deformed along with the upper surface of the Ingersoll shale53

FIGURE 30—Distributions and relative abundances of fossils vertically through the Ingersoll shale. Note the absence of fossil material in the lower ~ 9 cm of subunit A due to weathering and oxidation. Bar widths qualitatively reflect abundances based on observations during quarrying.....54

FIGURE 31—Lateral distribution and abundances of fossils in the Ingersoll shale. Bar widths qualitatively reflect abundances based on observations during quarrying. Note fossil abundance generally decreases away from axis of the clay lens56

FIGURE 32—CT scans of 3.2-cm and 7.6-cm diameter cores taken from the Ingersoll shale. The cores show iron-cemented laminae (red arrows) and pyrite nodules (yellow arrows). The cores show alleged tidal laminae, but resolution is inadequate for measuring sand-mud couplets. Scale bar ~3.0 cm long.....58

FIGURE 33—Photographs of Ingersoll shale core halves. Core on the left, encapsulated in paraffin wax, yielded poor resolution of individual lamina. Core on the right, encapsulated in epoxy resin, allowed for detailed observations of the graded sand-mud couplets. Red polygon highlights the interval used for tidal laminae analysis. S1-S7 refers to peaks in couplet thickness identified in figure 34..... 59

FIGURE 34—Histogram of graded sand-mud couplet thickness versus couplet number. Spring-neap cycles are shown in red lettering. Yellow histogram bars represent oxidized portion of Ingersoll shale core, gray bars represent unoxidized portion of core. Red lines and notations reflect possible interpretations of tidal signals. (A) C1 through C6 likely reflect semimonthly spring tide-to-spring tidal cycles (S1-S7 denote spring tide peaks). Note alternating high (S2, S4, S6) and low (S1, S3, S5) spring peaks that likely reflect perigee (P) and apogee (A), respectively. (B) A less likely alternate interpretation involving a higher number of incomplete cycles (C1-C11). As in A, S indicates spring tide peaks and A and P reflect apogee and perigee, respectively 61

FIGURE 35—Subunit B and C fabrics. (A) CT scan of 3.2-cm core from subunit C shows high density (pyrite) anomalies (arrow). (B) Photomicrograph of thin-section from subunit C showing thin, discrete quartz silt lamina. Opaque objects are pyritized organic detritus. Scale bar ~1 mm long. (C) SEM image of subunit B showing strong preferred grain orientation parallel to bedding. M, Q, and L indicate mica plates, quartz grain, and lignite clast, respectively.....	63
FIGURE 36—Textural data plotted against stratigraphic column of the Ingersoll shale. Peaks in weight percent sand are labeled 1 through 25. Red box indicates area of core containing sand-mud couplets used to study tidal rhythmicity and TL= tidal laminae.....	66
FIGURE 37—Total organic carbon (TOC) and sulfide sulfur (S) contents plotted against textural data	68
FIGURE 38—Photomicrographs of palynomorphs and megaspores isolated from the Ingersoll shale. (A-D) Pollen of the <i>Sohlipollis</i> Taxon Range Zone. (E-H) Megaspores, including <i>Ariadnasporites</i> sp. (E), <i>Paxillitriletes</i> sp. (F), <i>Molaspora lobata</i> (G), and <i>Paxillitriletes</i> sp. (H). (I-K) Marine dinoflagellate cysts. (L) Acritarch. Scale bars are ~20 μm long in A-D and ~100 μm long in E-L	70
FIGURE 39—Pyrite concretion from subunit A of the Ingersoll shale. (A) Primary laminae (dashed yellow lines) are compacted around the pyrite concretion. (B) Same concretion shown in top photograph, rotated horizontally ~90° and enlarged to show horizontal traces of laminae within the concretion (dashed yellow lines). Scale bars are ~1 cm long.....	72
FIGURE 40—Forms of pyrite in Ingersoll shale. (A) Pyritized, compacted burrow(?). (B) Pyritized wood clasts. (C) Pyrite framboids from feather specimen. Image on right shows pyrite as bright white framboids and clusters, highlighted by backscatter elemental imaging (BSE). Clay matrix remains light gray. (D) False color image of a pyrite framboid in clay matrix. Scale bars are ~1 mm long in A and B, and 10 μm long in C and D.....	73
FIGURE 41—C versus S contents for Ingersoll shale samples (blue dots). Sulfur contents are generally much higher than those characteristic of normal marine and freshwater mudrocks as described by Berner and others (Berner, 1983, 1985; Berner and Raiswell, 1984)	75
FIGURE 42—Generalized geologic cross-section of Eutaw lithofacies in east central Alabama and west central Georgia. Cross-section illustrates transition from bayhead delta facies to distal bay sediments down-dip and up section (modified from Frazier, 1997)	80

FIGURE 43—Interpretation of estuarine depositional setting for the Ingersoll shale. (A) Estuarine complex including bayhead delta in the Chattahoochee Valley. Red dot indicates inferred tidal creek setting for the Ingersoll shale. (B) Outcrop-scale reconstruction of the Ingersoll tidal creek in relation to quarry and trenches (lines A-A' and B-B') 82

FIGURE 44—Reconstruction of estuary development within the Chattahoochee Valley in relation to the study location (red dots). (A) Subaerial exposure and erosion of the Tuscaloosa Formation during lowstand. (B) Initial transgressive flooding of river mouth and development of bayhead delta. (C) Cutting and progressive filling of tidal creek within bayhead delta. (D) Continued landward migration of bay shoreline and deposition of estuarine central bay deposits on top of truncated Ingersoll shale 84

LIST OF TABLES

TABLE 1—Weight percent sand and organic carbon in the Ingersoll shale.....65

TABLE 2—Palynomorphs identified in the Ingersoll shale.....69

TABLE 3—Weight percent organic carbon, sulfide sulfur, and sulfate sulfur from
the Ingersoll shale74

TABLE 4—Sulfur isotopic compositions of Ingersoll shale pyrite samples.....77

1.0 INTRODUCTION

Fossil Lagerstätten are defined as “rock bodies unusually rich in paleontological information, either in a quantitative [*Konzentrat-Lagerstätten*] or qualitative [*Konservat-Lagerstätten*] sense” (Seilacher et al., 1985: p. 5). *Konzentrat-Lagerstätten*, or concentration deposits, are those wherein fossils were concentrated by sedimentological and/or biological processes. Although concentration deposits do not necessarily exclude organic remains, the conditions that lead to their formation usually preclude preservation of soft-bodied organisms. *Konservat-Lagerstätten*, or conservation deposits, are those that contain exceptionally preserved fossils. These rare fossil deposits commonly preserve soft parts and, hence, provide otherwise unavailable information about soft-bodied organisms and the paleoenvironments in which they lived (e.g., Bottjer et al., 2002). The development of conservation deposits may result from a variety of factors, the most important of which include stagnation, obrution (rapid burial), bacterial sealing, and early diagenetic mineralization (Seilacher et al., 1985; Allison, 1988; Babcock, 2001; Briggs, 2003).

The conservation Lagerstätte addressed herein, the Ingersoll shale, is a thin (< 1 m), discontinuous, carbonaceous clay lens within the Eutaw Formation exposed in Russell County, eastern Alabama. The Ingersoll shale, discovered by the author during the course of an undergraduate research project (for Dr. William Frazier, Columbus State University), contains an extraordinarily rich and well-preserved, mainly terrestrial fossil

assemblage. The biota includes a diverse flora consisting of plant macrofossils, megaspores, palynomorphs, and abundant fossilized plant resins (amber), marine dinoflagellates, and a fauna that includes mollusks, arthropods, and vertebrates. Unusually well-preserved vertebrate fossils recovered from the Ingersoll shale include fish scales and, more remarkably, abundant theropod feathers.

Paleontologic and taphonomic studies of the Ingersoll Lagerstätte by the author and collaborator Terrell Knight were performed concurrent with this research (Knight, 2007). Terrell Knight's companion thesis documents the composition and modes of preservation of the biota. The primary objectives of the thesis research described herein were to establish (1) the paleoenvironmental setting within which the Ingersoll shale accumulated, and (2) the depositional and early diagenetic conditions that resulted in exquisite fossil preservation. These objectives were achieved via detailed stratigraphic, sedimentologic, and geochemical studies of the Ingersoll shale and the strata that envelop it. Results not only provide an improved understanding of the genesis of an important new Cretaceous Lagerstätte but also may be of value in predicting the distribution of comparable deposits in the Gulf coastal plain and beyond.

2.0 EUTAW FORMATION

2.1 General Stratigraphy

The Upper Cretaceous (Santonian-Campanian) Eutaw Formation crops out in an arcuate belt that extends from Georgia, through Alabama, and into Mississippi (Savrda and King, 1993) (Fig. 1). Hilgard (1860) was the first geologist to describe this heterolithic package of micaceous sands and pyritiferous, laminated, and lignitic clays, and he named it for the town of Eutaw in western Alabama (Eargle, 1955).

The Eutaw Formation rests disconformably upon the Cenomanian Tuscaloosa Formation. It is overlain disconformably by marginal marine clastic sediments of the Blufftown Formation in western Georgia and eastern Alabama, and by coeval marine shelf deposits of the Mooreville Chalk in western parts of the outcrop belt (Reinhardt et al., 1994) (Fig. 2).

In the western part of the outcrop belt, the Eutaw Formation is divided into two members: an unnamed lower member and the Tombigbee Sand Member (Hilgard, 1860). In easternmost Alabama and western Georgia, including the current study area, the Eutaw Formation is not differentiated into members (Fig. 2).

2.2 Sequence stratigraphy

According to Mancini et al. (1995), the Eutaw Formation represents the lower transgressive parts of a single Upper Cretaceous depositional sequence. They interpret the basal Tuscaloosa-Eutaw contact as a type I sequence boundary. Mancini et al. (1995)



FIGURE 1—Distribution of Cretaceous strata (light-colored belt), including the Eutaw Formation (darker colored belt), in the eastern Gulf coastal plain. The site of the current study (red square) is in Phenix City, eastern Alabama.

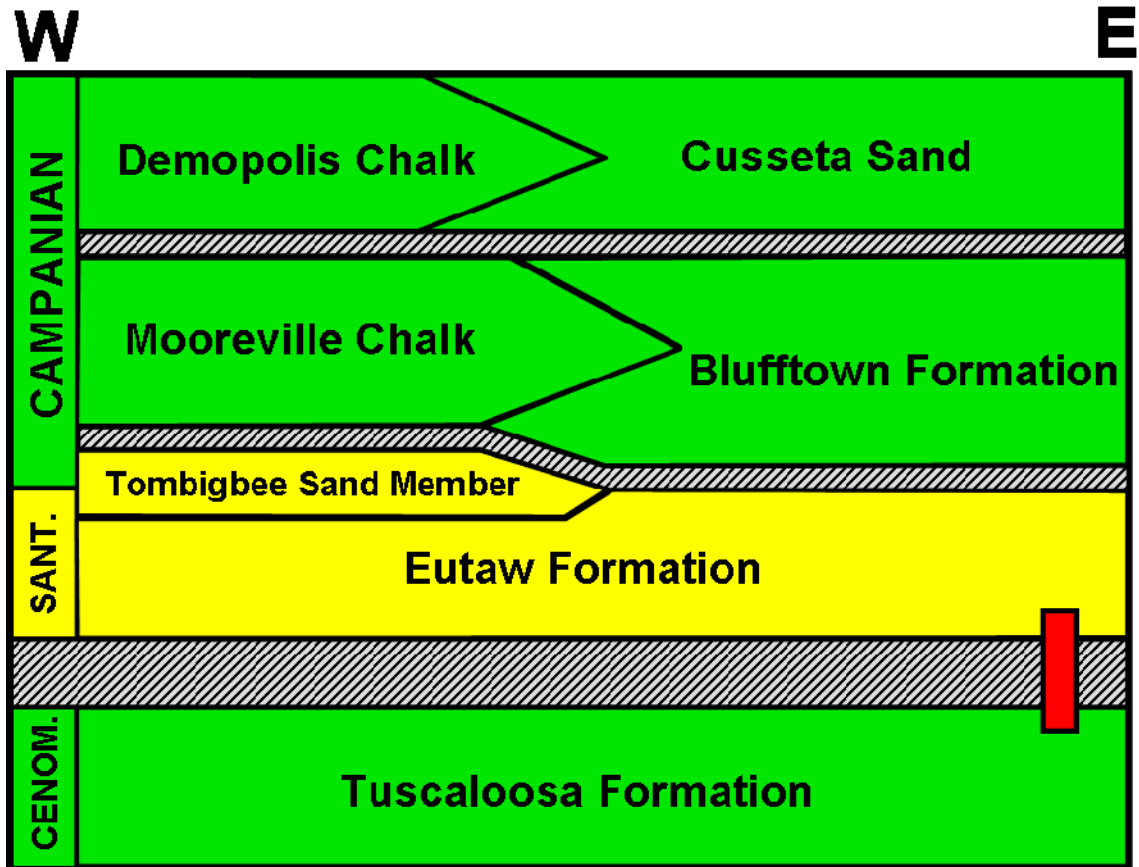


FIGURE 2—Generalized stratigraphy of Upper Cretaceous strata across Alabama. Position of the study section is shown by the red rectangle (modified from Savrda and Nanson, 2003).

assigned the bulk of the Eutaw to the lowstand systems tract, the Tombigbee Sand and the basal Mooreville Chalk to the transgressive systems tract, and the Mooreville Chalk and basal parts of the superjacent Demopolis Chalk to the highstand systems tract (Fig. 3). In contrast, King (1993) delineated two depositional sequences within the Eutaw. In addition to the basal type I sequence boundary recognized by Mancini et al. (1995), King (1993) recognized two additional type II or low-relief sequence boundaries, one within the Eutaw and the other at the contact between the Eutaw Formation and the overlying Mooreville Chalk / Blufftown Formation (Fig. 3). Differences in these sequence stratigraphic interpretations likely resulted from differences in scale of observation.

2.3 Depositional Facies

The Eutaw Formation is heterolithic, reflecting a variety of shallow-marine and marginal-marine settings associated with a barrier-island coast (Frazier and Taylor, 1980; King, 1990, 1993) (Fig. 4). In eastern and central Alabama, the lower member of the Eutaw was interpreted to represent a transition from back-barrier and barrier-island environments to shoreface and inner-shelf settings during marine transgression (Frazier and Taylor, 1980). The Tombigbee Sand is interpreted to have been deposited in barrier-island and back-barrier settings produced during shoreline progradation (King, 1990; Savrda et al., 1998). In eastern Alabama and western Georgia, the Eutaw Formation is thought to record deposition mainly in tidally influenced estuarine environments during marine transgression (Frazier, 1982, 1996, 1997; Savrda and Nanson, 2003). Facies were interpreted to record deposition in bayhead-delta, central bay or lagoon, and upper- and lower-shoreface environments (Frazier, 1982, 1997; King, 1990; Savrda and Nanson, 2003). As will be described later, the Ingersoll shale lens appears to be part of an

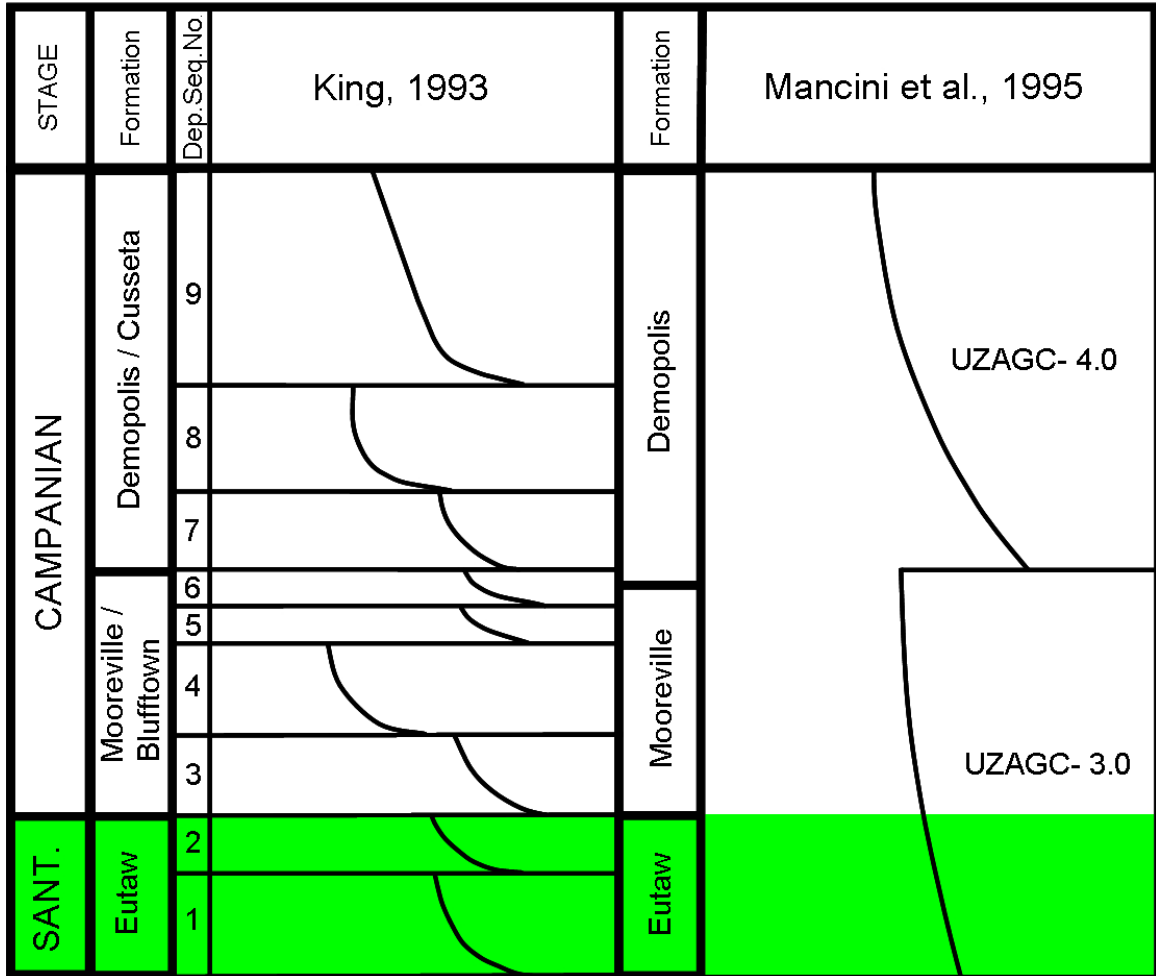


FIGURE 3—Sequence stratigraphic context of the Eutaw and superjacent formations as interpreted by King (1993) and Mancini et al. (1995).



FIGURE 4—Paleoenvironmental reconstruction of Santonian-age shoreline with study area indicated by white arrow and star. Reconstruction is based on previous work by Frazier and Taylor (1980), King and Skotnicki (1986), Frazier (1997), and Bingham and Frazier (2004).

estuarine bayhead-delta system (Fig. 4).

3.0 INGERSOLL SHALE

3.1 Location

The Ingersoll shale is located within a hillslope exposure in Phenix City, Russell County, Alabama (Fig. 5), on private property owned by Mr. Michael Ingersoll. This exposure includes the uppermost ~21 m of the Tuscaloosa Formation and the lower ~11 m of the Eutaw Formation. The Tuscaloosa Formation is composed here of weakly indurated, coarse-grained and cross-stratified to massive fluvial sands, and homogeneous and mottled mudstones. The Eutaw Formation at this locality is composed of sands, muddy sands, sandy muds, and shales. The Ingersoll shale occurs ~1.0 m above the disconformable Tuscaloosa/Eutaw contact. It varies from 0-80 cm in thickness and is dominated by olive-black, carbonaceous, pyritiferous clay-shale with subordinate silt/sand laminae. As described in greater depth below, the Ingersoll shale rests upon coarse-grained sands and is overlain by a package of muddy sands, sandy muds, and fine sands (Fig. 6).

3.2 Fossil Assemblage

Since its initial discovery by the author in 2003, the Ingersoll shale has yielded a diverse, mainly terrestrial biota that is dominated by plants but also includes various invertebrate and vertebrate components (Fig. 7). Detailed descriptions of the flora and fauna can be found in Knight (2007). Hence, only a short summary is provided here.



FIGURE 6—Outcrop containing the Ingersoll shale. Basal and top contacts of Ingersoll shale are approximated with yellow and orange lines, respectively (dashed where inferred).

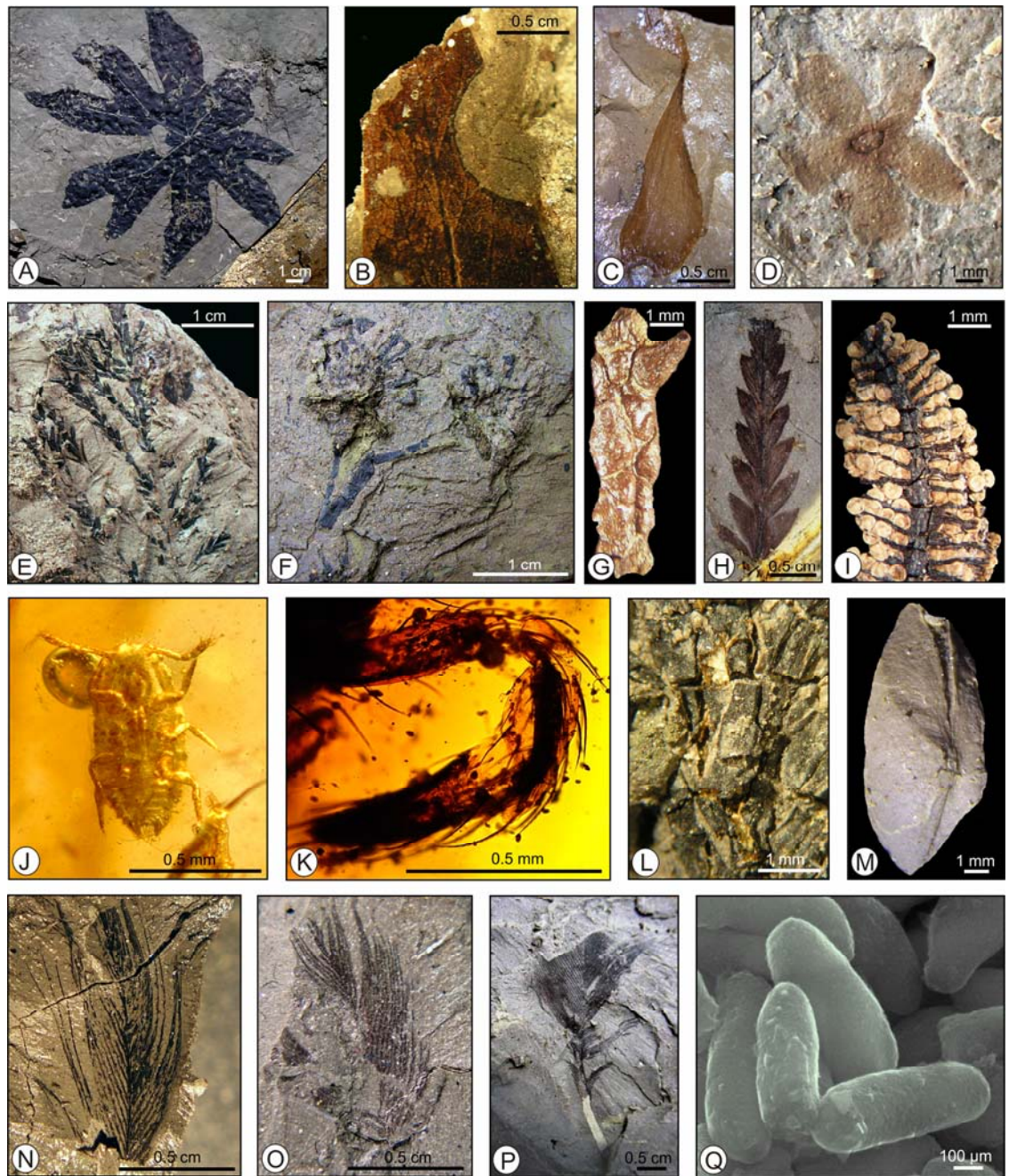


FIGURE 7—Examples of Ingersoll shale fossils. (A) Large intact angiosperm leaf (c.f. *Manihotites georgiana*). (B) Angiosperm leaf (*Ficus?* sp.) showing marginal insect damage. (C) Fruit wing. (D) Small flower. (E) Taxodeaceous branch with leaflets (c.f. *Geinitzia*). (F) Three-dimensionally preserved taxodeaceous cones articulated on stems. (G) Three-dimensionally preserved, pyritized conifer shoot. (H) Fern pinnatifid. (I) Water-fern sporocarp containing articulated mega- and microsporangia. (J) Female scale insect preserved in amber. (K) Araneoid spider appendage in amber. (L) Taxodeaceous conifer stem with *in situ* amber rods. (M) Internal mold of bivalve. (N-P) Representative feathers. (Q) SEM image of fossilized *Bacillus*-like structures replacing feathers.

The preserved macroflora includes leaves and reproductive structures of angiosperms, water ferns, and gymnosperms. Fossil angiosperm leaves, including relatively large forms (e.g., dinner plate-size c.f. *Manihotites georgiana*), are commonly whole (Fig. 7A) and, in some cases, are found articulated on stems. Some leaves show evidence of marginal insect damage (Fig. 7B) and associated reactivation tissue, while others exhibit evidence of parasitism (e.g., insect-induced galls and fungi-induced leaf spot). Additional plant organs at least tentatively attributed to angiosperms include seeds, seed pods, fruit wings (Fig. 7C), and small flowers (Fig. 7D), some of which are articulated on stems. Angiosperm fossils are compressions, impressions, carbonized, and/or variably pyritized. Some leaf cuticle is remarkably flexible and can be separated easily from sediment matrix.

Gymnosperms are represented by four forms and are tentatively assigned to two extant families—Araucariaceae and Cupressaceae (which includes Taxodiaceae)—and the extinct family Cheirolepidiaceae. All of these forms are manifest as isolated leaflets or as articulated leaflets and stems (e.g., Fig. 7E). Both the Araucariaceae and Cupressaceae also are represented by isolated or articulated cones (Fig. 7F). Gymnosperm fossils are compressions, impressions, carbonized, and/or variably pyritized. Pyritized specimens commonly exhibit three-dimensional preservation (Fig. 7G).

Lower vascular plants are represented by carbonized and locally pyritized horsetails and ferns (Fig. 7H), including a water fern. Megaspores, provisionally attributed to both water ferns and isoetalean and selaginellean lycosids, are also

common and typically exhibit three-dimensional preservation. Some water-fern sporocarps contain articulated mega- and microsporangia (Fig. 7I).

Isolated amber clasts are common, particularly in the lower parts of the Ingersoll shale where amber concentrations are as high as 360 g/m³ of sediment. Amber occurs as small (1 to 15 mm), highly fractile, light yellow to light red chips, drops, and rods. Inclusions are common and dominated by plant debris. However, Ingersoll shale amber thus far also has yielded fecal pellets, well-preserved fungal mycelia, mites, a female scale insect with well-developed legs and antennae (Fig. 7J), and an araneoid spider (Fig. 7K), which is the oldest found in association with its web (D. Grimaldi, personal communication, 2006).

In addition to isolated clasts, the lower part of the Ingersoll shale also hosts weakly compacted plant parts that contain *in situ* amber rods (Fig. 7L). Amber-bearing plant parts include lignitized stems and cone scales, most of which appear to be linked to the family Cupressaceae.

Remains of resident invertebrates are absent in the Ingersoll shale, excepting rare bivalves. The latter are preserved as molds and casts (Fig. 7M) and, rarely, via pyritization.

Vertebrate remains found within the Ingersoll shale include abundant fish scales and theropod feathers (Fig. 7N-P). Aside from feathered dinosaurs and birds from the Liaoning Province, China (Norell and Xu, 2005), feather fossils are exceedingly rare in Mesozoic strata. Known occurrences usually consist of only a few isolated individuals (Kellner, 2002, table 16.1). Notably, the Ingersoll shale has yielded the largest collection (14 specimens) of fossil feathers from North American Mesozoic strata. Most of these

feathers appear to be carbonized. However, preliminary scanning electron microscopy indicates that at least some are replaced by mats of small ($\sim 1 \mu$), carbonized rod-shaped structures (Fig. 7Q). These *Bacillus*-like structures, which resemble those preserving feathers from the Eocene Messel Shale (see Davis and Briggs, 1995) are most likely fossilized bacteria.

3.3 Paleoenvironmental and Taphonomic Conditions

The Ingersoll shale clearly contains an unusually diverse and well-preserved biota. General stratigraphic context of this deposit suggests that this Lagerstätte formed in a marginal marine, estuarine setting. In what specific depositional environment did this shale accumulate? What physiochemical processes operating in these depositional and diagenetic regimes led to exceptional fossil preservation? What role did sea-level dynamics play in the genesis and preservation of this deposit? This thesis research project was designed to provide some answers to these questions.

4.0 METHODS

4.1 General Approach

This project involved both field work and subsequent laboratory studies. Field studies, which focused on the stratigraphic context and geometry of the Ingersoll shale, involved detailed measurement, description, and selective sampling of the section and of strategically excavated trench and quarry exposures. Laboratory studies, designed to evaluate depositional and diagenetic conditions that resulted in unusual fossil preservation, included further analyses of sediment fabrics, textures, composition, and geochemistry. All analyses, except where noted, were conducted by the author at Auburn University.

4.2 Field Studies

4.2.1 Section Measurement and Description

In order to better establish the stratigraphic context of the Ingersoll shale, the entire section of Tuscaloosa and Eutaw formations exposed at the study locality was measured and described. Measurements were made using a Brunton compass, a clinometer, and a Jacob's staff; lithologic descriptions were made with the aid of a grain-size/texture estimation chart and a Munsell rock-color chart. Observations were used to construct a detailed stratigraphic column that includes general lithology and textures, primary sedimentary structures, and body and trace fossil content.

4.2.2 Excavation and Description of the Ingersoll Shale

Detailed descriptions of the Ingersoll shale were made during systematic hand-tool excavation for fossils and after trenching with a rented bulldozer and backhoe. Initial hand-tool excavation focused on a 6x10-m area of Ingersoll shale above which there was little or no overburden. To facilitate mapping, this area was divided into a 1-m² grid-system using wooden stakes to mark 1-m intervals along three sides. Using the NE corner stake as a reference, 1-m² sections were designated by letters and numbers (e.g., N0/W0 denotes the original NE corner, N3/W5 denotes a position 3 m south and 5 m west of the N0/W0, etc.). After thicker overburden was cleared with a bulldozer, the area of shale excavation was progressively expanded to 11x20 m. Expansion beyond the original NE reference stake necessitated the use of negative coordinates (e.g., N-2/W-4 denotes denotes a position 2 m north and 4 m east of the N0/W0).

As each 1-m² section was excavated from the top down, observations were placed in general vertical stratigraphic context using a discrete marker horizon (e.g., prominent, laterally continuous sand laminae). Field descriptions included observations of sediment texture and composition, primary sedimentary structures, paleocurrent indicators (e.g., the trend of the long axes of plant detritus), ichnofabrics (e.g., presence/absence of bioturbation, burrow types, and size parameters), and the strike and dip of accessible bedding planes. Observations were integrated to produce a detailed outcrop map of the Ingersoll shale.

Concurrent with hand-tool excavation, a bulldozer and a backhoe were used to cut two trenches through the shale lens and into the subjacent sediment. The trenches, one cut along the presumed longitudinal axis of the shale lens and the other normal to the first,

were used to establish the three-dimensional geometry of the Ingersoll shale. The thickness of the shale was measured at 1-m intervals along both trenches. Trench walls were cleaned with hand picks and putty knives to view and photographically document the Ingersoll shale, immediately subjacent strata, and their contact relationships. Stratigraphic cross sections derived from trench observations were combined with the outcrop map to create a 3-dimensional representation of the Ingersoll shale lens.

4.2.3 Sample Collection

Collection of samples focused on the Ingersoll shale and the immediately subjacent and superjacent sediments. Large (>500 cm³) sample blocks representing a continuous vertical section of the Ingersoll shale and a small portion of the enveloping strata were extracted from the outcrop. Collection of block samples was accomplished by hand-excavation of small trenches to form a vertical pedestal of the Ingersoll shale. The pedestal was then separated along prominent bedding-parallel partings to facilitate removal of blocks. These stratigraphically continuous block samples, hereafter referred to as master sample blocks, were taken back to Auburn University, and subsamples were extracted for laboratory analyses summarized below. Additional samples (~9.0 kg) of the shale were removed from the quarry and sent to Richard Lupia (University of Oklahoma) for standard palynological studies.

As will be described below, field observations of the lower part of the Ingersoll shale indicated the presence of sedimentary fabrics suggestive of tidal cyclicity (i.e., tidal rhythmites; Archer, 1998). In order to better describe and analyze these fabrics, several cores were extracted from this interval using homemade coring tools prepared from 1.25-in (3.2-cm) and 3.0-in (7.6-cm) diameter PVC pipes. Sections of pipe up to 61 cm in

length were beveled at one end using a bench grinder, lined with Pam® cooking oil, and driven into the lower part of the shale using a 25-lb sledge hammer. PVC corers and their contents were extracted after removal of surrounding shale. Corers recovered continuous, relatively undisturbed intervals up to ~30.5 cm thick that were used to test for tidal rhythmicity and to make supplementary observations of other primary and biogenic fabrics in the lower part of the Ingersoll shale.

4.3 Laboratory Studies

4.3.1 Analysis of Tidal Rhythmicity and Other Fabrics

PVC core samples were treated in various ways in the laboratory in an attempt to optimize observations of apparent tidal rhythmicity. Initially, all core samples were retained in their PVC core barrels and subjected to CT scanning at the Auburn University Small Animal Clinic. Subsequently, all core barrels were split to expose the recovered sediment. Due to the coring process and/or subsequent desiccation and shrinkage, core material was generally very fragile and required impregnation prior to further analysis. Impregnation techniques tested included: (1) immersion of wet shale in liquid paraffin wax; (2) immersion of dry shale in liquid paraffin wax; (3) encapsulation of wet shale in polyester resin; and (4) impregnation of desiccated shale in epoxy resin. The latter technique, performed commercially by Wagner Petrographic, produced the best results.

After epoxy impregnation, technicians at Wagner Petrographic cut the 7.6-cm diameter core in half along its longitudinal axis. One half was polished and the other half was used to produce a continuous series of oversized (2x3-inch) thin sections. At Auburn University, the polished half of the core was scanned at high resolution (1200 dpi) using a flatbed scanner. Resulting digital images were enlarged to >5X their original size, printed

on glossy paper, and laminated with plastic film. Thin sections were also photographed and used to produce enlarged images. Analysis of fabrics observed on polished core surfaces and in thin sections will be described in greater depth below (section 6.1.1).

4.3.2 Textural Studies

Textural analyses were conducted on a continuous series of 69 subsamples of the Ingersoll shale. Small (1 to 2 cm³) subsamples were extracted from the master block samples at 1-cm intervals. These subsamples were oven dried, weighed, and then disaggregated in distilled water for 24 hours. The samples were then wet-sieved through 1-Ø and 4-Ø screens. The 1-Ø screen was used to remove large pyrite masses and organic detritus, while the 4-Ø screen was used to isolate the detrital sand fraction. Fractions retained in the 1-Ø and 4-Ø screens were dried for 24 hours and weighed. Relative weight percent sand in each subsample was determined by the formula:

$$\text{weight \% sand} = \frac{4\text{-}\text{Ø wt}}{\text{Twt} - 1\text{-}\text{Ø wt}} \times 100$$

where 4-Ø wt = weight of the sand retained in the 4-Ø screen, Twt = total weight of sample prior to wet sieving, and 1-Ø wt = weight of the detritus retained on the 1-Ø screen. Weight % sand was plotted versus stratigraphic height in the Ingersoll shale.

A limited number of grain-size analyses were also conducted on sand samples collected immediately below and above the Ingersoll shale. Sand samples weighing ~450 gm were split using the quartering method to acquire representative ~ 50-to-70-gm subsamples. The subsamples were then dry-sieved at 1-Ø intervals through the range of 4.0 to -2.0 Ø using a sieve shaker. General grain-size parameters (e.g., mean grain size, sorting) were determined using the Gradistat software package (Blott and Pye, 2001).

4.3.3 Carbonate and Organic Analyses

Carbonate and organic carbon analyses were conducted on subsamples extracted from master sample blocks at the same intervals used for textural analyses. Small (~ 1-cm³) subsamples were placed in metal weighing trays and dried in an oven at ~ 82.0 °C for 24 hours. The dried samples were manually powdered with a mortar and pestle. Approximately 0.25 gm of powdered subsample was then weighed, digested in dilute (10%) HCl acid, and vacuum filtered through pre-weighed, carbon-free borosilicate glass filters. Filters and residues were oven dried and weighed immediately upon removal from the oven. Carbonate contents were determined by weight loss after acid digestion. Organic carbon contents were determined via combustion of filters and residues in a LECO CS-200 analyzer.

Additional data on organic matter were acquired via palynologic studies performed by Dr. Richard Lupia at the University of Oklahoma. Palynomorphs were isolated using standard palynological techniques (i.e., sequential digestion in HCl and HF; Sims et al., 1999) and digitally photographed. Photographs of the palynomorphs were sent electronically to Dr. Raymond Christopher (Clemson University), who aided in the identification and age determination of the palynomorphs.

4.3.4 Sulfur and Sulfur Isotopic Analyses

Sulfur contents were determined for 11 representative samples extracted from the master sample blocks. These samples, weighing between 15 and 22 grams, were oven dried and powdered to the consistency of talcum powder using a mortar and pestle. Sulfate and sulfide contents of samples were determined commercially by ACME Analytical Labs using a LECO sulfur analyzer.

Stable isotopic analyses were performed on three pyrite samples isolated from the shale during wet sieving (> 1-Ø fraction). Pyrite samples weighing ~ 0.1 gm each were selected from shale intervals that contained abundant, small (~ 1 mm) pyrite masses. Samples were analyzed commercially at Geochron Laboratories using a dual collector, dual inlet, ratio mass spectrometer. Data were reported in $\delta^{34}\text{S}$ notation relative to the Canyon Diablo Troilite (CDT) standard.

4.3.6 Microscopy

Observations of selected samples were made using both petrographic and scanning electron microscopes. Standard petrographic observations were made using the oversized thin sections prepared for the aforementioned fabric analysis, as well as three standard-size thin sections prepared by Wagner Petrographic from samples derived from the upper portions of the Ingersoll shale.

Scanning electron microscope (SEM) studies were performed on several small (~1 cm³) subsamples of shale extracted from master sample blocks. Subsamples were prepared using mudrock preparation techniques described by O'Brien and Slatt (1990) for clay microfabric analyses. SEM studies were made using a JEOL JSM 7000 housed in the College of Engineering (Wilmore Laboratories) at Auburn University.

Microscopic analyses provided data to supplement that derived from field and other laboratory studies. Sedimentologic aspects observed in these analyses include general sediment textures and microfabrics, primary and diagenetic mineralogy, and organic constituents

5.0 FIELD OBSERVATIONS

5.1 General Section Description

The slope exposure in the study area includes ~31 m of strata that can be assigned to the Cenomanian Tuscaloosa Formation (~19 m), Eutaw Formation (~11 m), and Quaternary alluvium (>1 m). Owing to housing development in the lower part of the exposure, only the upper ~20 m of the section were measured and described (Fig. 8). This Cretaceous interval of the section was divided into thirteen informal units, four units in the Tuscaloosa and nine units in the Eutaw Formation.

5.1.1 Tuscaloosa Formation

The lowermost unit in the measured section, unit 1 (Fig. 8), is a deeply weathered, massive, mottled light gray to dusky red, sandy mud that contains locally common mud intraclasts and lacks body fossils and obvious trace fossils (Fig. 9A). Unit 2, which rests in sharp contact with unit 1, is a relatively thick (4.2 m) poorly indurated, unbioturbated and unfossiliferous, light gray to dark yellowish-orange, medium sand characterized by well-developed, medium-scale trough cross stratification (Figs. 8, 9B). Cross-stratification generally indicates southerly paleocurrent flow directions. Unit 2 grades upward into unit 3, a thinner (~1.5 m), more indurated, homogeneous, medium to fine-grained sandstone with common iron-cemented rhizoliths (Figs. 8, 9C). In turn, unit 3 grades into a thin (~1.5 m), homogeneous to mottled, light gray and dusky-red to dark yellowish-orange silty clay (unit 4; Figs. 8, 9D). Like unit 1, unit 4 lacks body fossils and

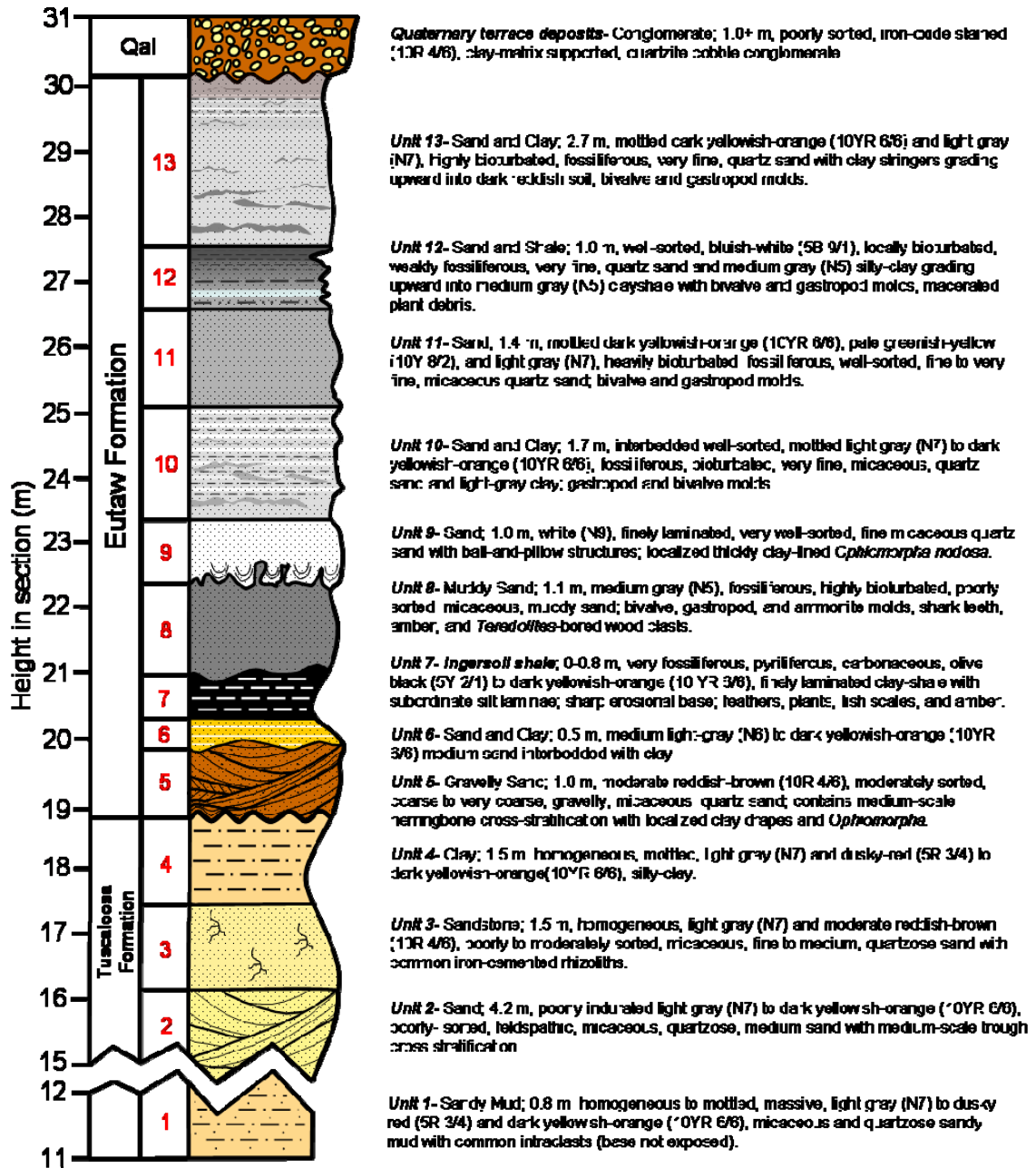


FIGURE 8—Stratigraphic column for the measured section of outcrop including the Ingersoll shale (unit 7), Russell County, Alabama.

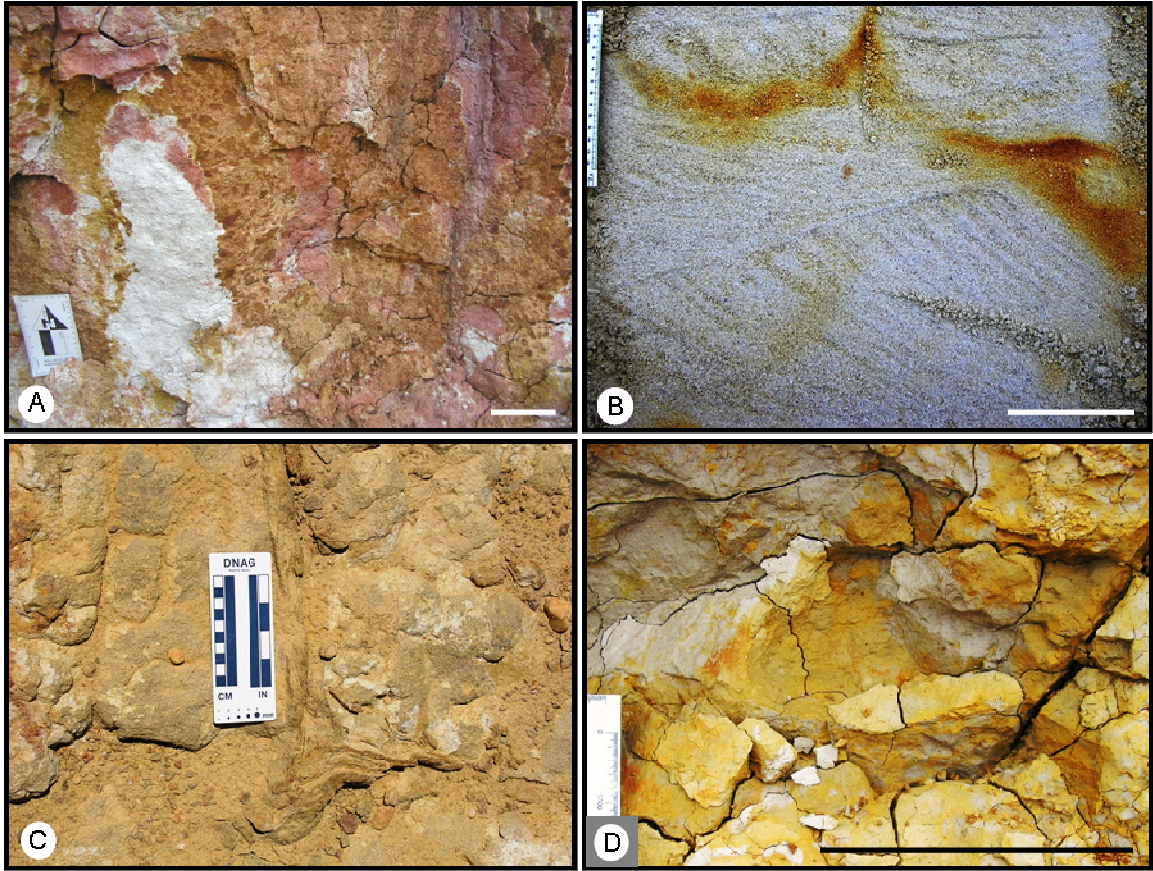


FIGURE 9—Representative photos of units 1-4, Tuscaloosa Formation. (A) Sandy mud of unit 1 characterized by red mud intraclasts. (B) Fine to medium sand of unit 2 showing medium-scale trough cross-stratification. (C) Homogeneous sandstone of unit 3 characterized by iron-cemented rhizoliths. (D) Homogeneous and mottled silty clay of unit 4. Scale bars in A, B, and D = 10 cm.

obvious ichnofossils. The top of unit 4 marks the disconformable contact between the Tuscaloosa Formation and the Eutaw Formation (Fig. 10).

5.1.2 Eutaw Formation

The Eutaw Formation is characterized by a range of lithologies including sands, muds, clays, and shales (Fig. 8). The basal unit of the Eutaw, unit 5, is dominated by moderate reddish-brown, moderately-sorted, coarse to very coarse, gravelly, micaceous, quartz sand with subordinate clay. The sand is characterized by medium-scale trough and wedge sets of cross-stratification, including herringbone cross-stratification. Clay occurs as discrete thin (<2 cm) beds and as intraclasts and foreset clay drapes within sand (Figs. 10 and 11). Stratification in unit 5 is weakly disrupted by bioturbation; it contains an impoverished *Skolithos* ichnofacies assemblage dominated by small-diameter (<1 cm), clay-lined burrows assigned to *Ophiomorpha nodosa* (Fig. 11). The contact between units 5 and 6 is erosional.

Unit 6 and unit 7 (the Ingersoll shale proper) form a laterally discontinuous, channel-form complex. Unit 6 (0 to 0.5 m thick) is an unfossiliferous package of massive, gray silty clays, and thinly planar laminated, medium light-gray to yellowish-orange sand and clay (Figs. 8, 12). Planar lamination is weakly disrupted by bioturbation, but no distinct ichnofossils could be identified. Stratification within unit 6 is locally truncated at internal erosional surfaces as well as at the contact with the Ingersoll shale (Fig. 12).

The Ingersoll shale ranges (unit 7) from 0 to ~80 cm in thickness. It grades from partly oxidized, laminated, pyritiferous, carbonaceous fine sands and clays at its base through an olive-black, faintly laminated, weakly bioturbated, pyritiferous clay at its top (Fig. 12). The contact between the Ingersoll shale and unit 8 is sharp and erosional

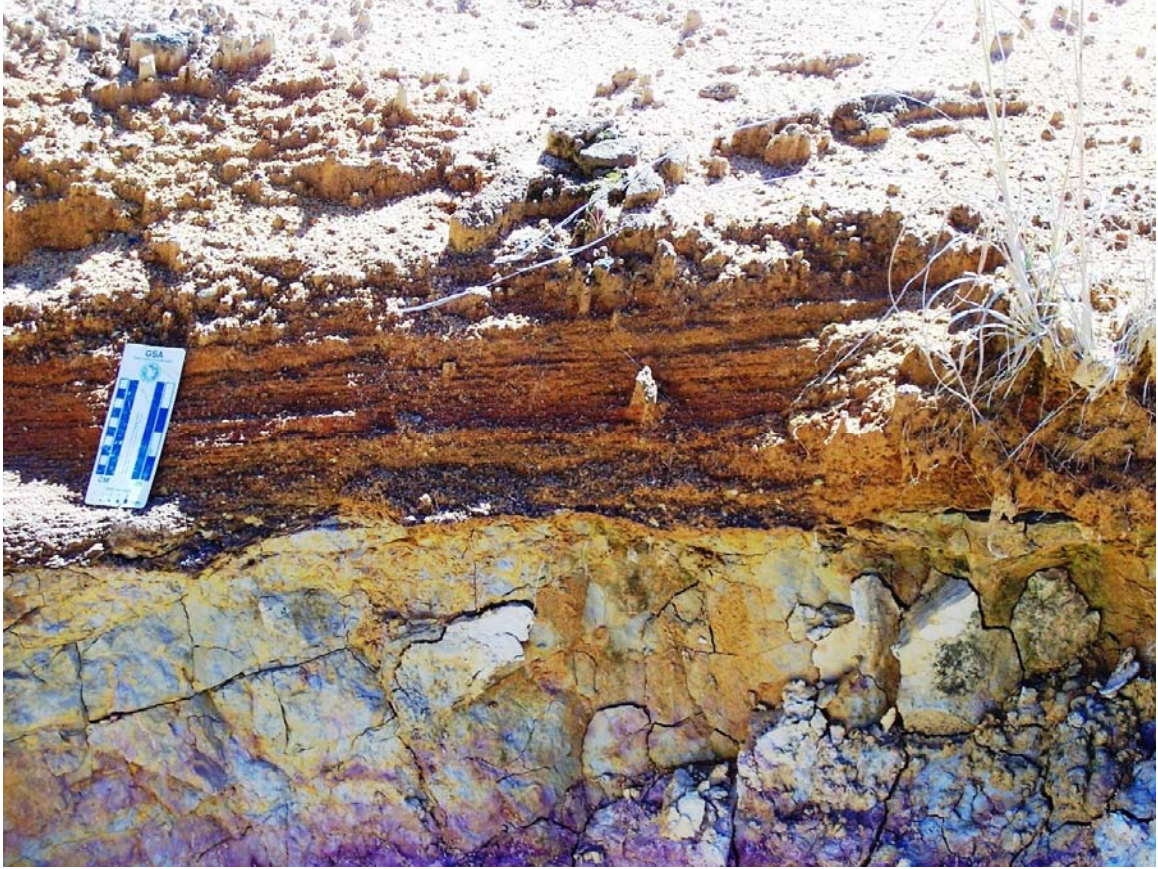


FIGURE 10—Disconformable contact separating silty clay (unit 4) of the Tuscaloosa Formation from the coarse- to very coarse-grained gravelly sands (unit 5) of the Eutaw Formation.

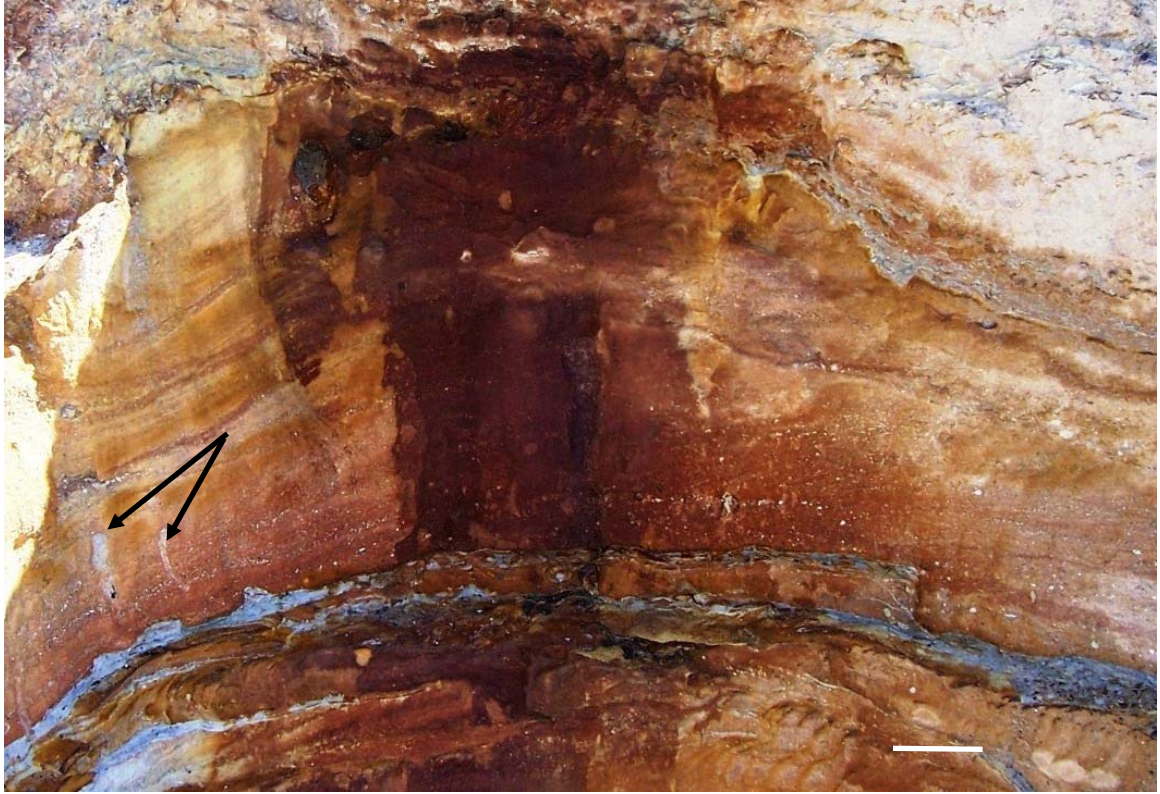


FIGURE 11—Clay drapes (gray), herringbone cross-stratification, and sparse *Ophiomorpha* (arrows) in gravelly sand of unit 5. Scale bar ~10 cm long.



FIGURE 12—Unit 6 (oxidized clay and sand) and unit 7 (Ingersoll shale). Note erosional contact (yellow line) between units 6 and 7 and distinct sand laminae near the base of the Ingersoll shale. Height of trench exposure is ~30 cm.

and cut by relatively large burrows (*Thalassinoides* and *Rhizocorallium*; see section 5.3). The geometry and detailed stratigraphy of the Ingersoll shale will be described in greater depth below (sections 5.2 and 5.3, respectively).

Units of the Eutaw Formation above the Ingersoll shale (units 8-13; Fig. 8) are laterally continuous across the exposure and consist of variably gray, medium to fine sands and clays that vary with respect to extent of bioturbation, sedimentary structures, and fossil content. Unit 8 is a relatively thick (~1.1 m) medium gray, fossiliferous, and highly bioturbated, micaceous muddy sand (Fig. 13). It contains common finely comminuted, carbonized plant detritus, larger *Teredolites*-bored wood clasts, amber clasts, and mollusks. Molluscan fossils, which include bivalves, gastropods, and less common ammonites, are preserved mainly as casts and molds. Identifiable ichnofossils include *Teichnichnus*, *Thalassinoides*, and *Rosselia*(?).

Unit 9 is a thin (~0.5 m), apparently unfossiliferous, nearly white to light gray, finely laminated, very fine, micaceous sand. Bioturbation in this unit is weak; burrows include only rare, thickly clay-lined *Ophiomorpha nodosa*. The base of unit 9 is sharp, irregular, and characterized by relatively large ball-and-pillow structures (Fig. 14). The contact with unit 10 is relatively sharp and only weakly bioturbated.

Unit 10 is approximately 1.7 m thick and characterized by moderately bioturbated interbeds of well-sorted, mottled light gray to dark-yellowish orange, very fine, micaceous quartz sands and light gray clay (Figs. 8, 15A). Like unit 8, unit 10 contains common molds of bivalves and gastropods. The contact with unit 11 is gradational.

Unit 11, approximately 1.4 m thick, is similar to unit 10 but bioturbation is more intense and discrete clay layers are generally lacking (Figs. 8, 15B). It is a mottled dark

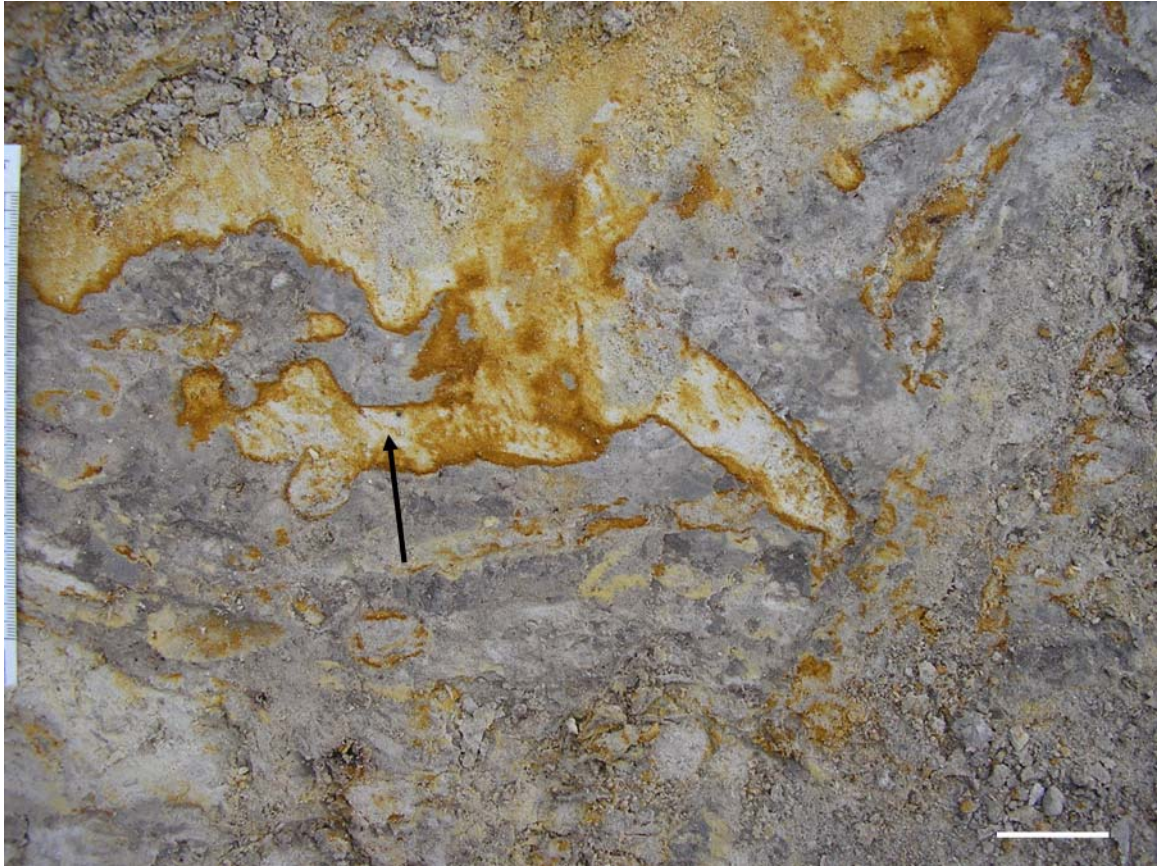


FIGURE 13—Thoroughly bioturbated muddy sands of unit 8. Ichnofossils visible in this view include large *Thalassinoides* (arrows). Scale bar is ~5 cm long.

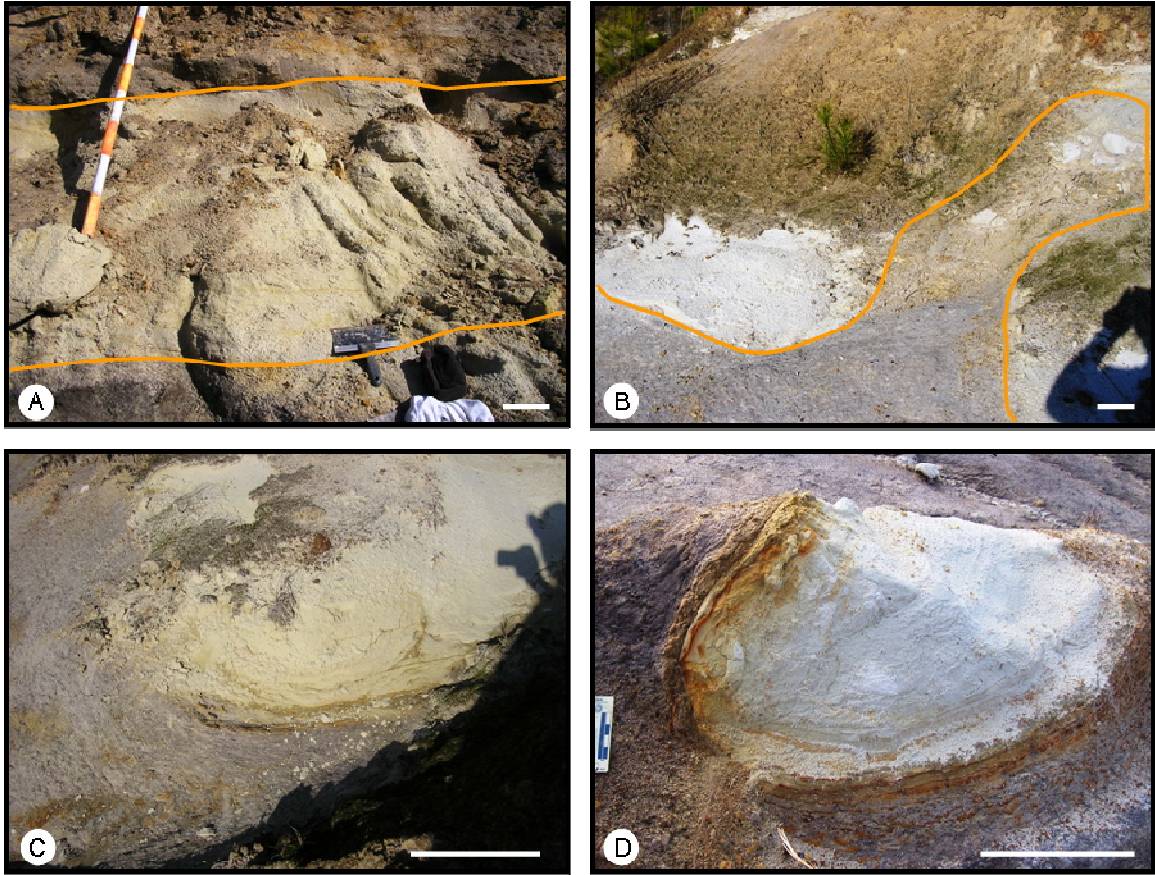


FIGURE 14—Fine micaceous sand of unit 9. (A) Orange lines show approximate upper and lower contacts of unit 9. (B) Large flame structure containing sand-breccia entrained in flow (outlined in orange). (C-D) Large ball-and-pillow structures in the finely layered sands. Scale bars are ~20 cm long.

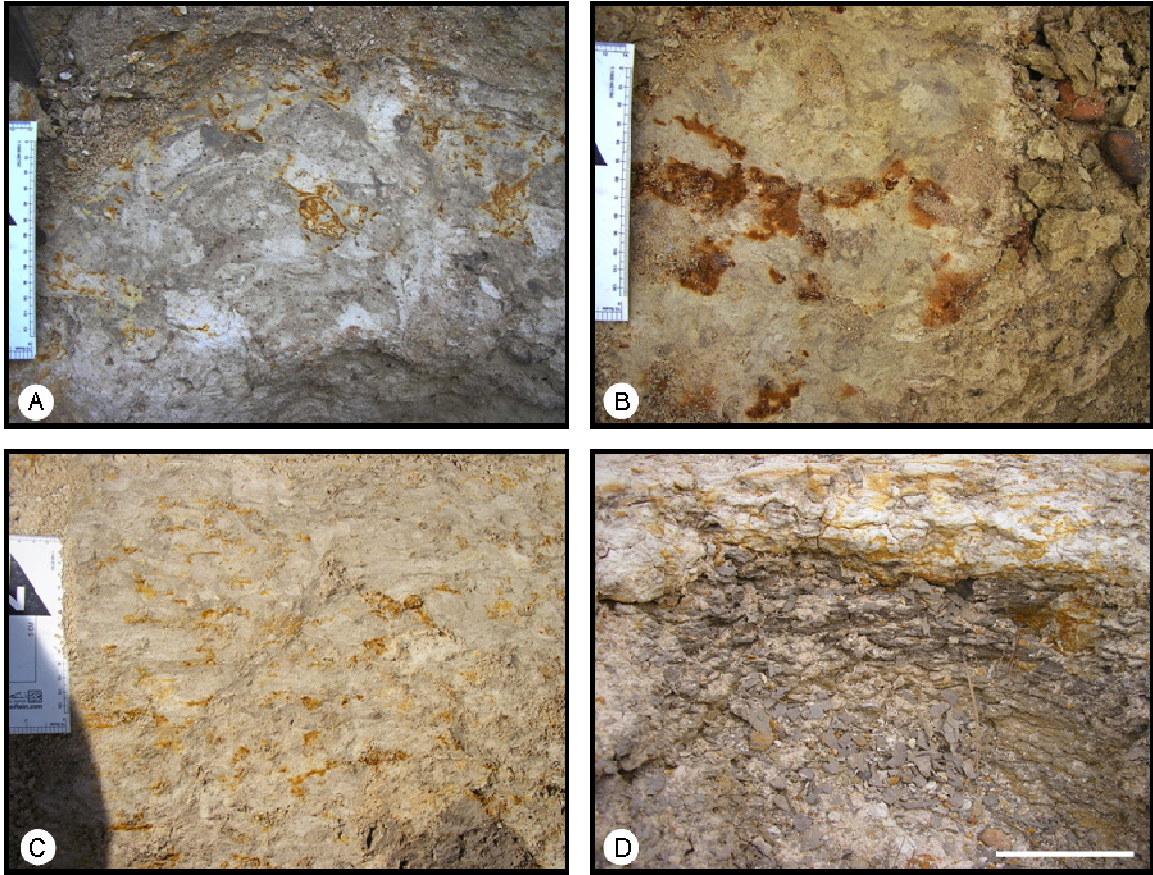


FIGURE 15—Representative fabrics of units 10-12. (A) Heavily bioturbated unit 10. (B) Heavily bioturbated, pale greenish-yellow, fine, micaceous sand of unit 11. (C) Bioturbated sandy zone of unit 12. (D) Weakly bioturbated shale at top of unit 12. Scales in A-C are graded in cm. Scale bar in D is ~10 cm long.

yellowish orange (oxidized), pale-greenish yellow, to light gray, fine to very fine, well-sorted, micaceous sand. Like unit 8, unit 11 contains common casts and molds of mollusks and distinct ichnofossils that include *Teichichnus*, *Thalassinoides*, and *Rosselia*(?). The contact between units 11 and 12 is gradational.

Unit 12 is a thin (~1.0 m), thinly bedded and relatively weakly bioturbated package of well-sorted quartz sands and medium gray clayshales (Figs. 8, 15C, D). Although the sands are apparently unfossiliferous, clays contain common macerated plant debris and molds of bivalves and gastropods. Its contact with unit 13 is relatively sharp.

Unit 13, the uppermost unit of the Eutaw, is comparatively thick (~2.7 m). It is dominated by mottled dark yellowish orange and light gray, highly bioturbated, fossiliferous, very fine quartz sand (Figs. 8, 16A,B). It is similar to unit 11, but contains thin, discrete lenses and discontinuous laminae of medium gray clay. The upper part of unit 13 grades into a reddish soil capped by a Quaternary terrace deposit consisting of iron-stained, matrix-supported, quartzite pebble conglomerate.

5.2 Geometry of the Ingersoll Shale

Exposures provided by trenching (e.g., Figs. 17-19) and fossil excavation (Fig. 20) provided the basis for evaluating the three-dimensional geometry of the Ingersoll shale (unit 7). As reconstructed, the shale forms a narrow, elongate channel-form body, the long axis of which trends approximately north-south (N04E) and hence is oblique to the slope of the exposure (Fig. 21). The lens is asymmetrical (Figs. 17, 18). The axis of the lens, where the shale reaches maximum thickness (~80 cm), is skewed to the west. Shale on the west side of the axis dip eastward toward the center of the lens (Figs. 18, 20) and thin relatively abruptly before they abut the unit 6 contact or are truncated at the

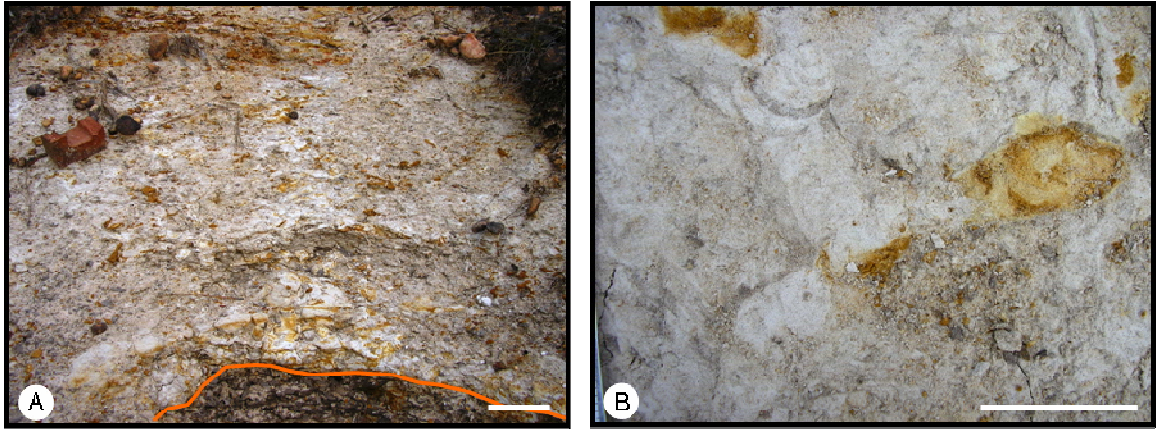


FIGURE 16—Representative photos of unit 13. (A) Highly bioturbated sand above contact with unit 12 (orange line). (B) Large *Thalassinoides* in unit 13. Scale bars are ~10 cm long.

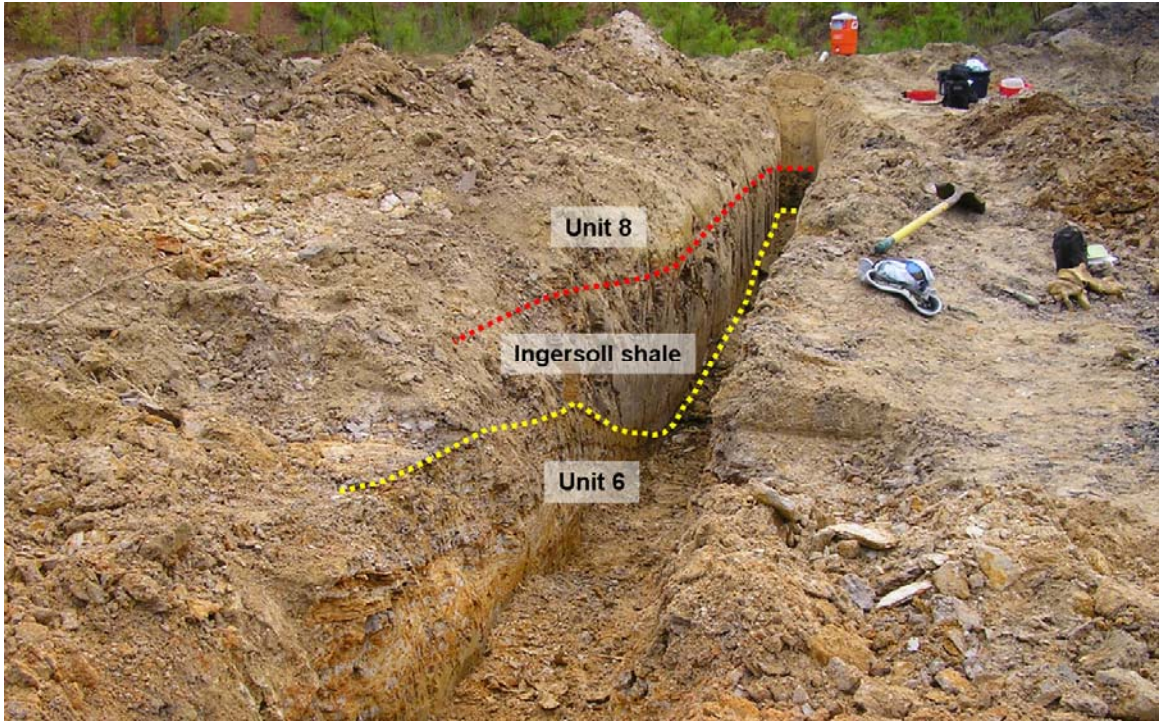


FIGURE 17—East-west backhoe trench cut perpendicular to the hill slope to the north of the fossil quarry (see Fig. 20). The yellow and red dotted lines denote the lower and upper contacts of the Ingersoll shale, respectively. View is toward the NE.

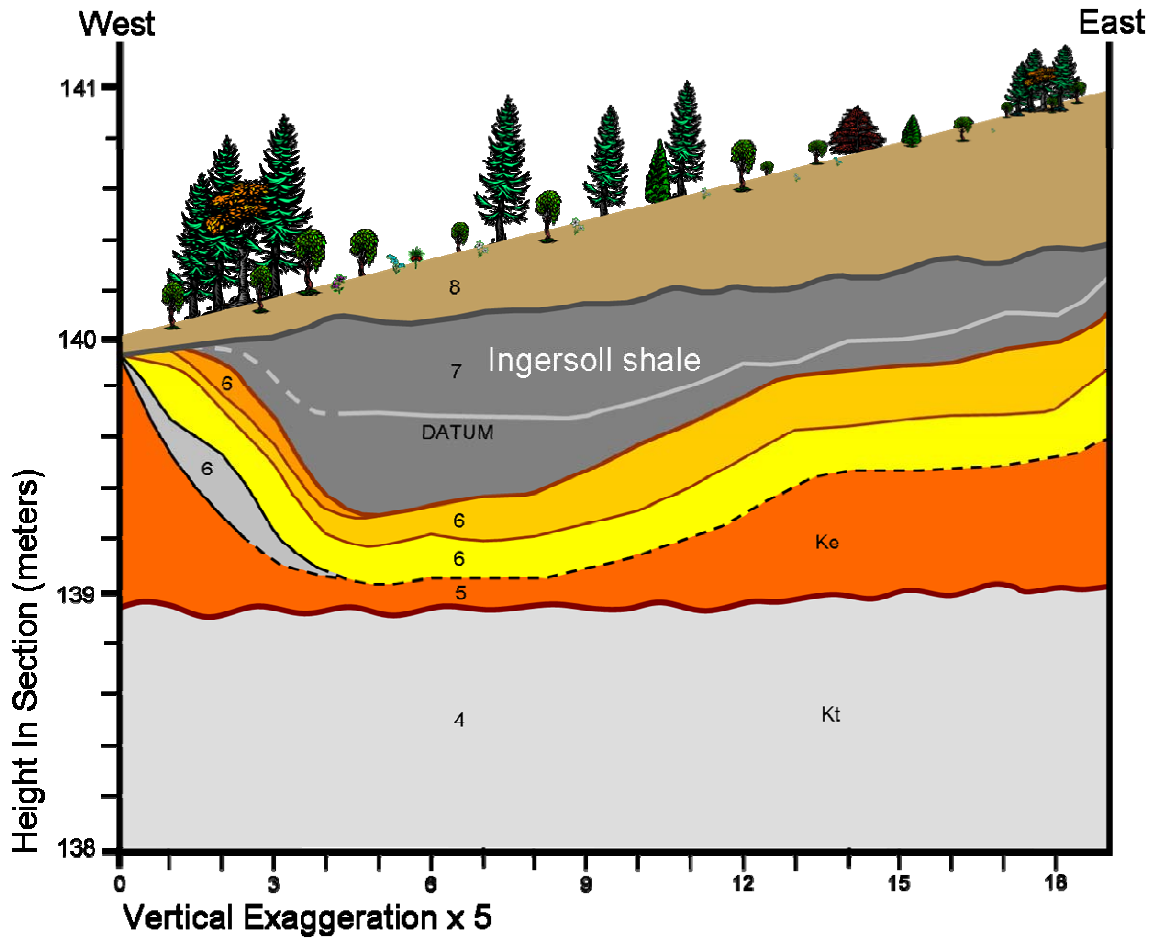


FIGURE 18—Detailed cross-section of the Ingersoll shale and associated units constructed from trench exposure shown in Fig. 17. Note the asymmetry of the shale body (trees depict ground surface and are not to scale).

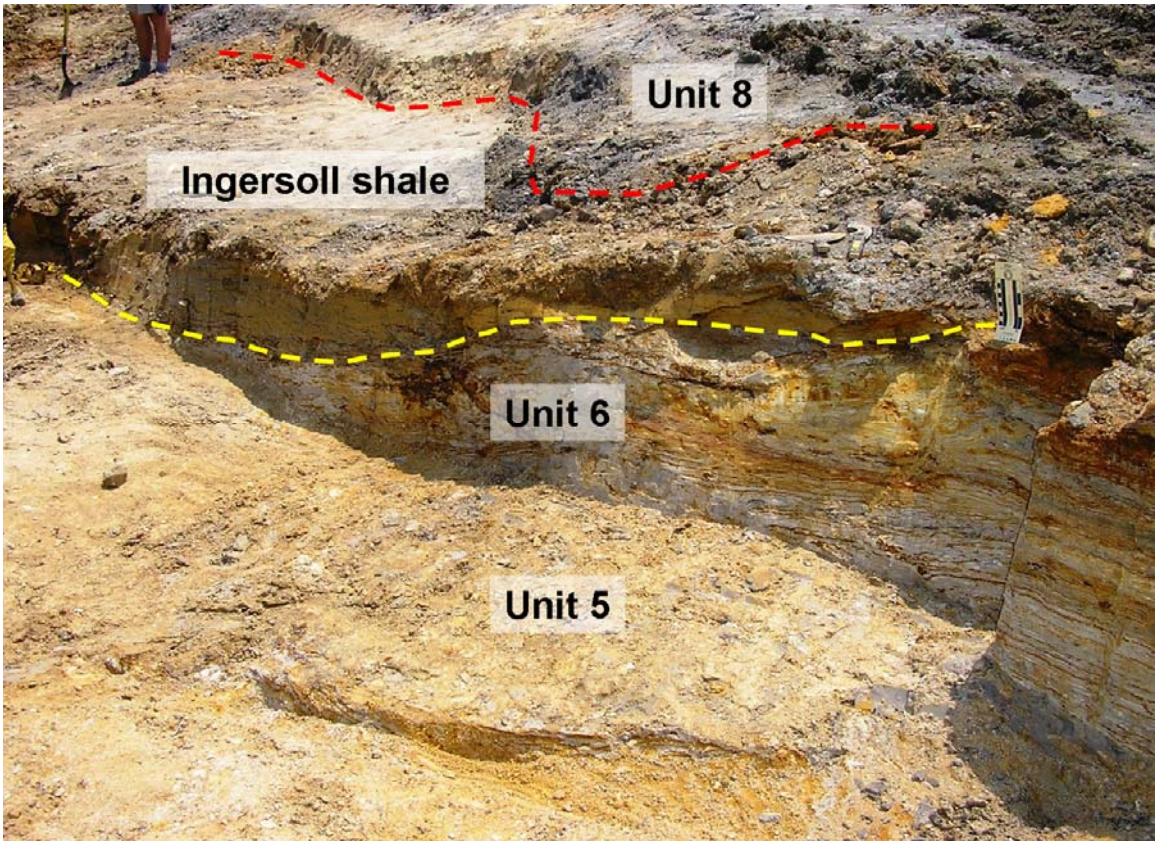


FIGURE 19—Portion of trench cut parallel to slope on western side of fossil quarry (see Fig. 20). The yellow and red dotted lines indicate lower and upper contacts of the Ingersoll shale, respectively. View is to the NE.

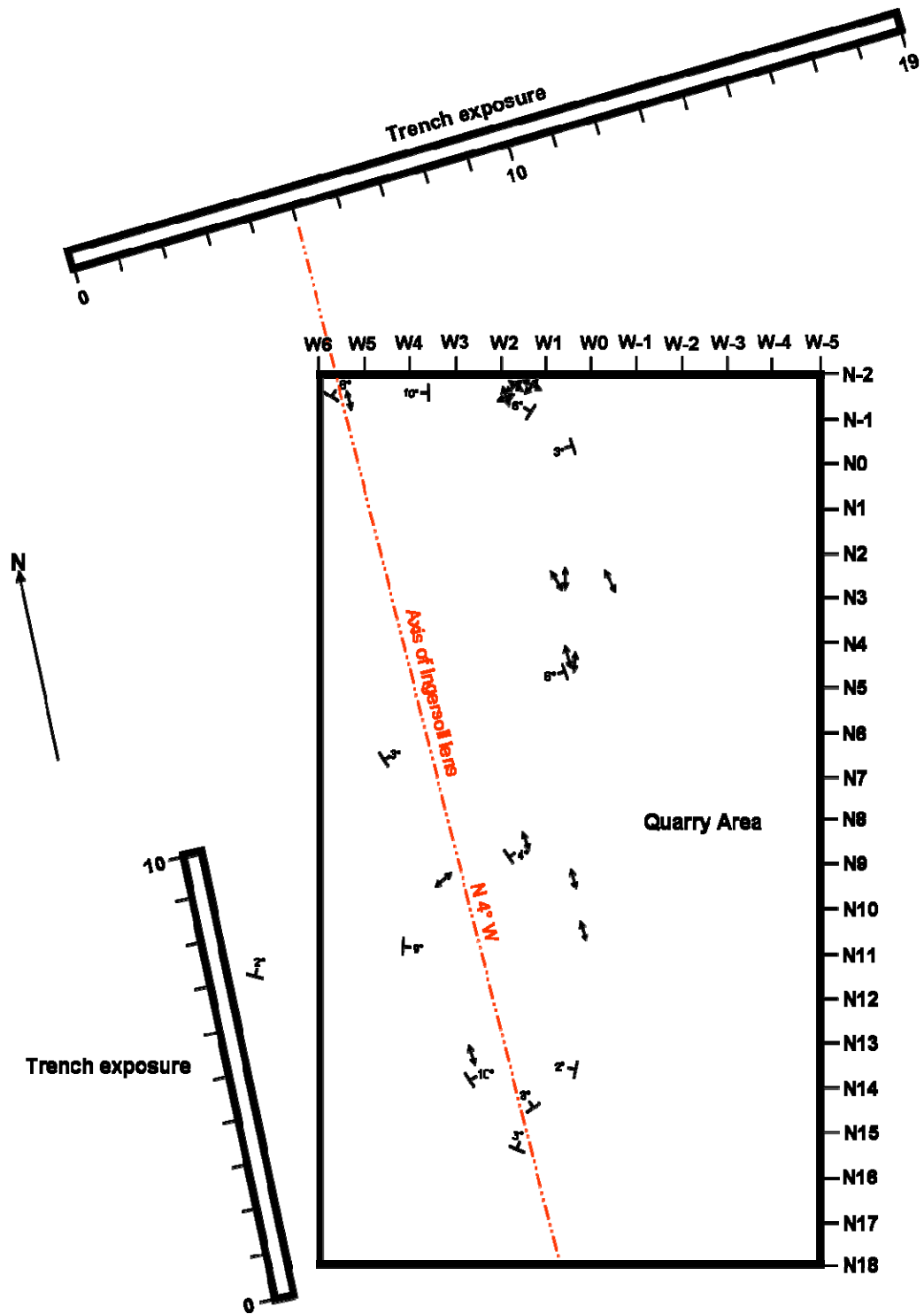


FIGURE 20—Map of quarry and trenches. Quarry map shows location of bedding-plane strike and dip orientations, orientations of the long axes of plant macro-detritus (double-headed arrows), and presumed position of the long axis of the Ingersoll shale lens.

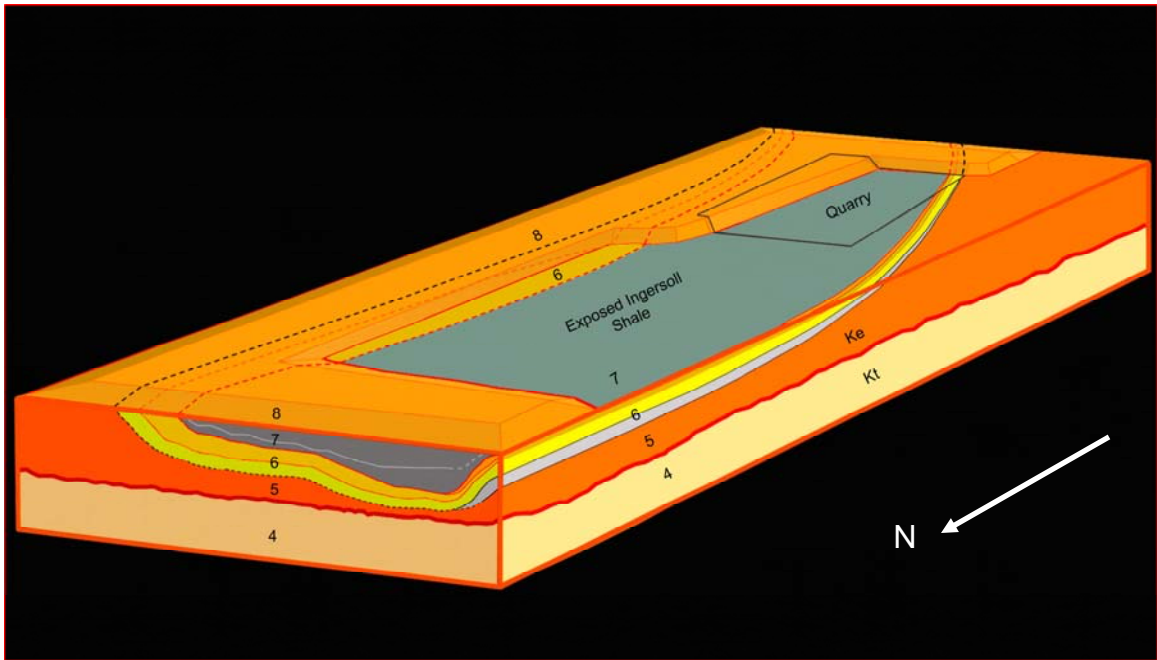


FIGURE 21—Three-dimensional reconstruction of the channel-form complex containing the Ingersoll shale. Diagram shows location of quarry and the spatial arrangement of units 4-8.

unit 7/unit 8 contact (Fig. 18). Bedding within the eastern part of the shale lens dip more gently westward towards the axis (Figs. 18, 20) and thin gradually towards the east (Fig. 18). The easternmost edge of the lens extended into the hillslope and was not exposed in trenching. However, based on rate of thinning, the width of the Ingersoll shale lens (normal to the lens axis) is estimated to be 20 to 25 m.

5.3 Internal Stratigraphy of the Ingersoll Shale

Based on field observations of sediment textures and fabrics, the Ingersoll shale is divided into three parts, referred to as subunits A, B, and C, in ascending order (Fig. 22). Contacts between these subunits are gradational.

5.3.1 Subunit A

Subunit A, the basal part of the Ingersoll shale, is thickest (~23 cm) near the axis of the lens, where it is dominated by thin (millimeter-scale), graded sand-mud couplets (Figs. 12, 22, 23). Sand laminae, dominated by very fine sand and coarse silt-sized quartz grains, are commonly separated from overlying mud counterparts by thin laminae of comminuted and locally pyritized plant detritus (Fig. 24). Parting surfaces along these organic-rich laminae commonly reveal a preferred current alignment of elongate plant parts that roughly parallels the shale-lens axis (Fig. 20). Variations in sand-mud couplet thickness define a crude bundling that is reminiscent of tidal laminites (Fig. 23). The tidal origin of sand-mud couplets is addressed in greater depth below (see section 6.1.1).

The upper parts of subunit A are generally light to medium gray, reflecting the abundance of plant detritus. However, the lower parts (up to 15 cm thick) commonly are yellowish-orange, reflecting the flow of oxidizing groundwaters through the relatively permeable sands (Figs. 12, 23).

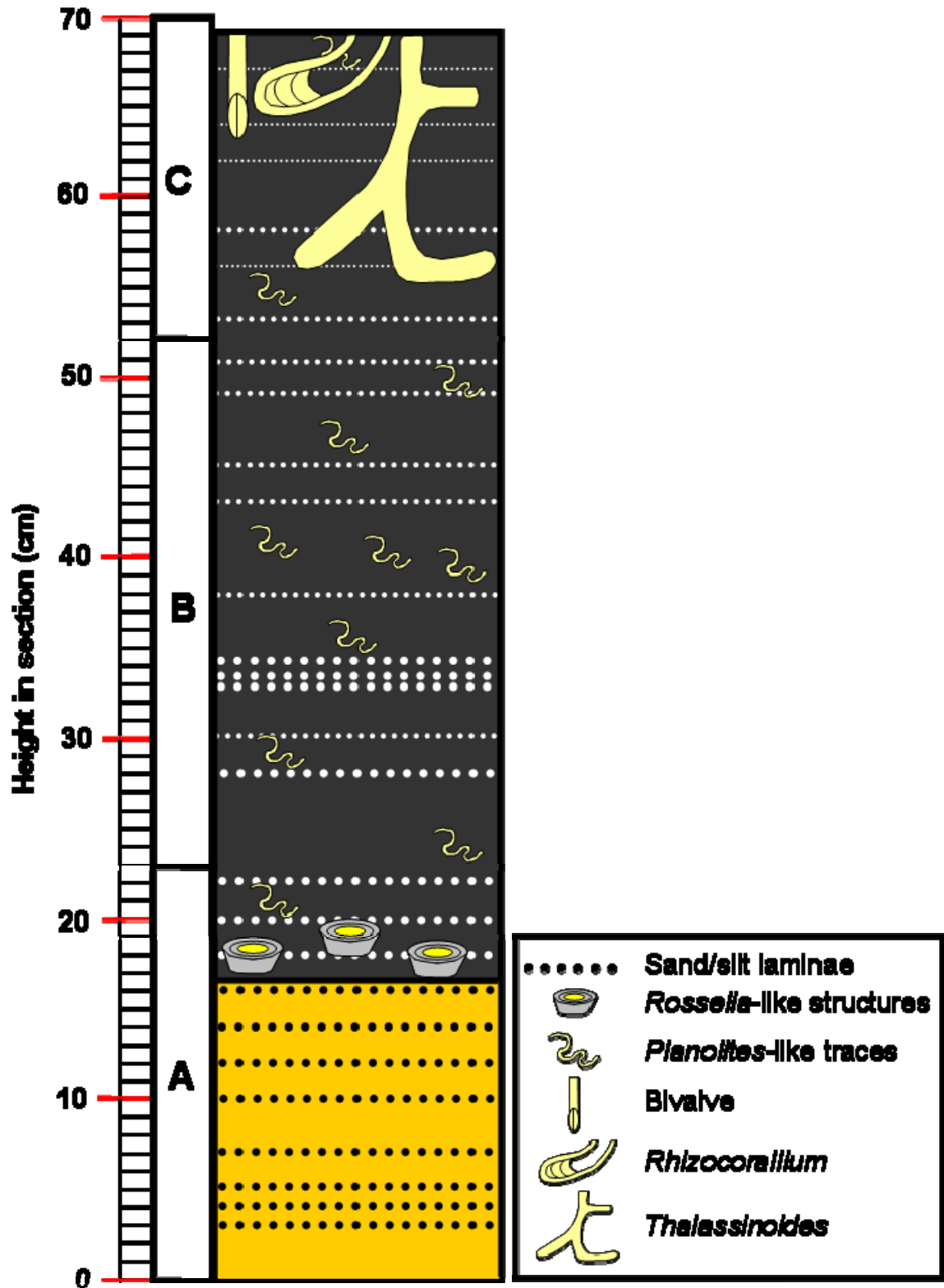


FIGURE 22—Stratigraphic column of the Ingersoll shale showing general character of three subunits (subunits A-C).

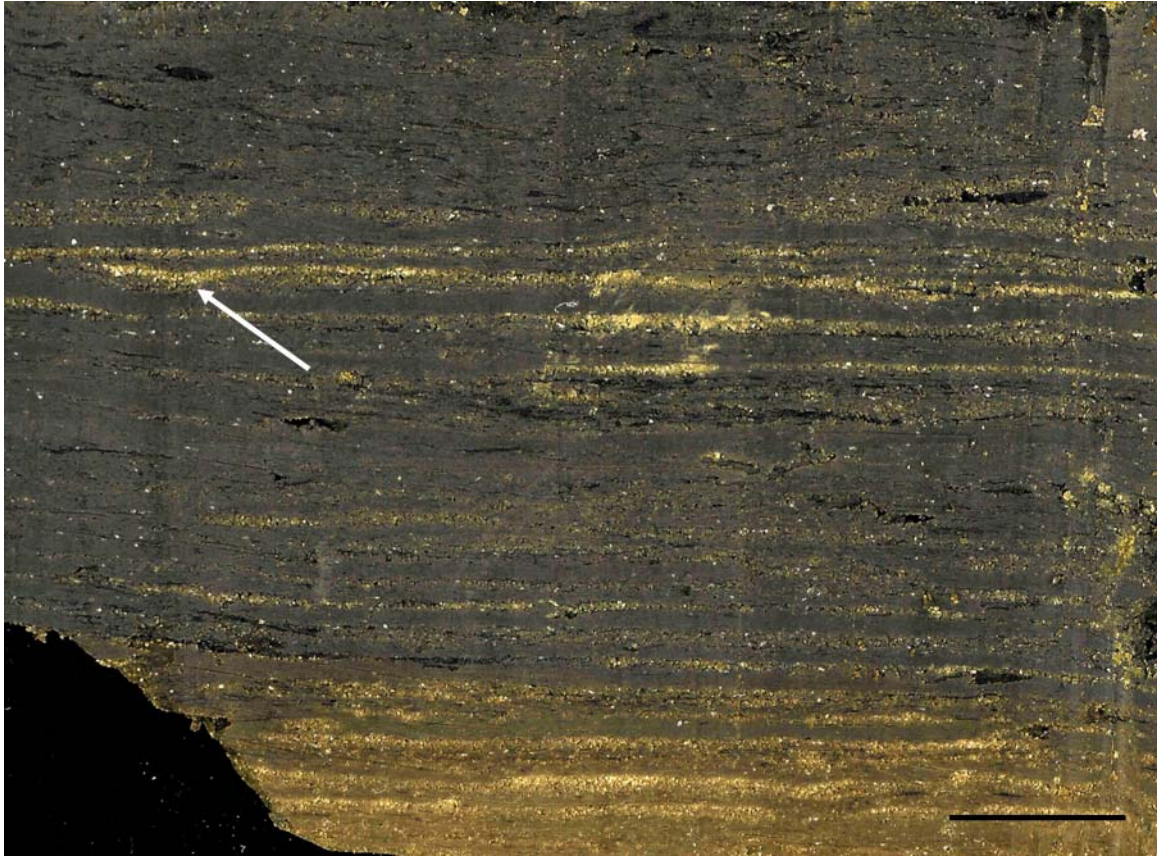


FIGURE 23—Graded sand-mud laminae couplets in subunit A of the Ingersoll shale. A starved current-ripple (?) is indicated with an arrow. The thicknesses of these couplets were the focus of the tidal rhythmicity study. Scale bar is ~1 cm long.



FIGURE 24—Comminuted plant detritus on bedding-plane parting surface of shale in subunit A (Brunton compass for scale).

Subunit A generally becomes thinner towards the margins of the lens. On the western margin of the lens, sand-mud couplets become steeply inclined (up to 35°). Some laminae lap onto the unit 6/unit 7 contact, while others seemingly grade into thin sets of (ripple-scale) cross stratification. Towards the eastern margin of the lens, subunit A progressively thins, but planar laminae appear to be concordant with the basal contact.

Evidence for bioturbation in subunit A is relatively sparse and limited to rare enigmatic *Rosselia*-like structures and simple pyritized burrows. *Rosselia*-like structures are shallow (<4 cm deep), narrow (1 to 2 cm), vertical to subvertical, cylindrical structures consisting of a sandy, commonly pyritized central shaft surrounded by a zone of concentrically laminated sediment that contains abundant oriented plant detritus (Fig. 25A-C). Some central shafts locally exhibit nodose (pelleted?) exteriors (Fig. 25D). Simple pyritized burrows appear as narrow (1-3 mm), short (<3 cm), straight to curved, horizontal to subhorizontal, cylindrical to highly flattened tube segments. These burrows are comparatively rare in the lower part of the subunit but become more common, or at least more obvious, near the top.

5.3.2 Subunit B

Subunit B is clay dominated but does contain rare, thin (<1 mm) laminae of quartzose and micaceous fine sand and silt (Fig. 22). Three distinct, closely-spaced sand/silt laminae that extend throughout the lens provided an important marker horizon (vertical datum) during shale excavation and fossil collection. Most other sand laminae are notably discontinuous. Owing to the relative lack of textural heterogeneity, strata of subunit B do not part along bedding planes as readily as in subunit B. Some parting surfaces reveal poorly-defined, very low-amplitude, short-crested, cusped current

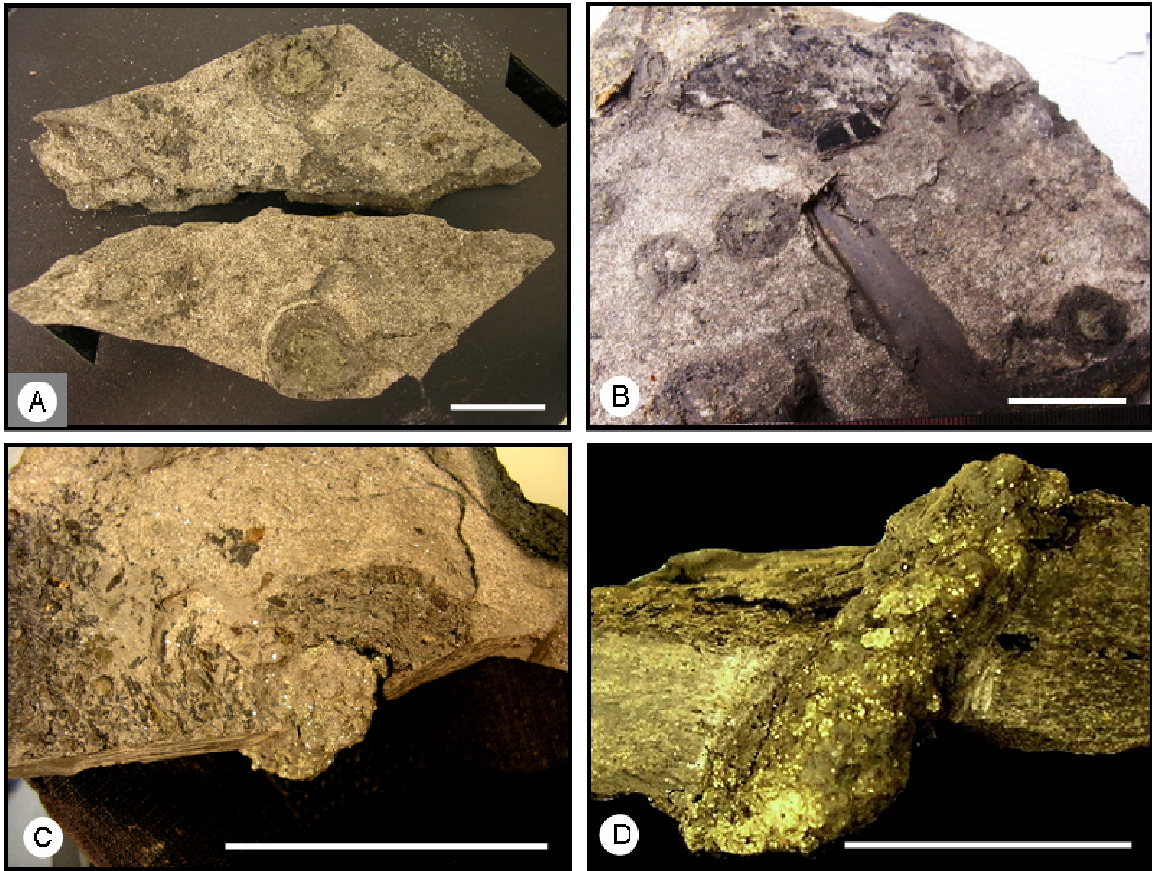


FIGURE 25—*Rosselia*-like structures in subunit A. (A) and (B) Circular, concentrically laminated areas of displaced silt-sand with central cores of pyrite exposed on bedding surfaces of shale. (C) Close-up of burrow showing plant detritus organized in concentric rings around a central core of pyrite. (D) View perpendicular to bedding shows pyrite core of burrow with pelletized texture similar to *Ophiomorpha nodosa*. Scale bars ~2 cm long.

ripples defined by isolated concentrations of fine sand, silt, and/or comminuted plant detritus (Fig. 26). Paleocurrent data derived from these starved ripples indicate current flow to the NNW, generally coincident with the axis of the shale lens.

Evidence for bioturbation in subunit B is limited to simple, narrow (1-3 mm), meandering, horizontal to subhorizontal burrows (Fig. 27). These structures are generally only visible on bedding parallel surfaces where they are manifest as short (3-33 mm), straight to curved, typically highly flattened, pyritized, and locally silt-filled tube segments. Burrows are particularly well expressed where they are preserved in relief on large fossil leaves (Fig. 27).

5.3.3 Subunit C

Subunit C is a dark, relatively massive clay; silt and fine sand laminae are not apparent in the field or in samples blocks. The clay contains evidence of two discrete phases of the bioturbation. The first phase is reflected by discontinuous, straight to curved, narrow, subhorizontal to horizontal, typically flattened, pyritized tubes that are identical to those in subunits A and B. The second phase is reflected by larger *Thalassinoides* and *Rhizocorallium* that extend down into the subunit C from the erosional contact with unit 8 (Fig. 28). These larger burrows are most common in the upper 8 cm of subunit C but locally penetrate as deep as 20 cm below the unit 8 contact. Burrows in irregularly branching *Thalassinoides* systems range from 1 to 4 cm in diameter, exhibit sharp walls, and are filled with gravelly, coarse-grained sand (Fig. 28A, B). *Rhizocorallium* are horizontal to subhorizontal, straight to sinuous, u-shaped spreiten structures. Widths of these structures vary from 2.0-3.9 cm, and lengths range up to



FIGURE 26—Bedding surface in subunit B showing cusped current ripple with plant macrodetritus on the lee side. Arrow shows paleocurrent direction. Paleocurrent directions varied from NE to NW but overall trend (n=22) was determined to be NNW.

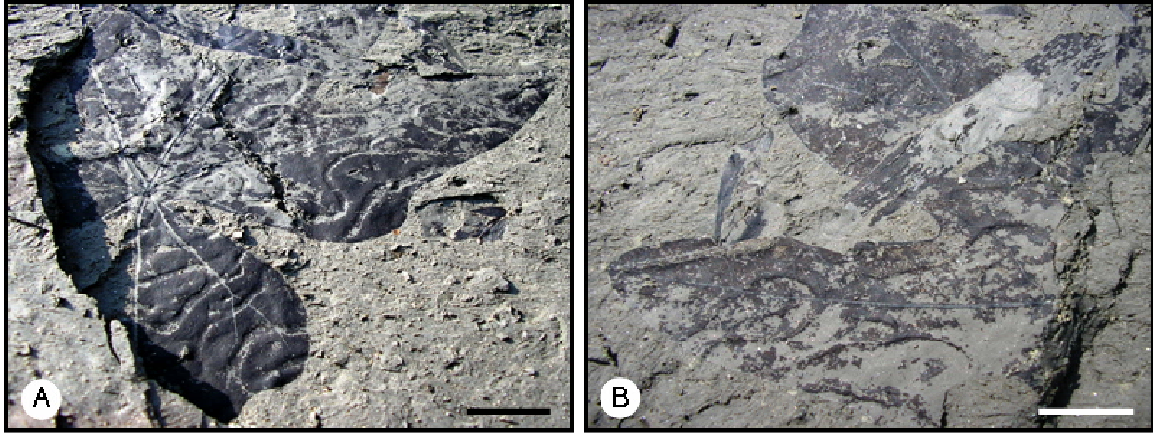


FIGURE 27—Burrows in subunit B. (A) Horizontal to subhorizontal, meandering burrows preserved as hyporeliefs on a leaf fossil exposed on bedding surface of shale. (B) Pyritized meandering burrows preserved as epireliefs on the surface of a leaf fossil exposed on a parting surface. Scale bar ~1 cm long.

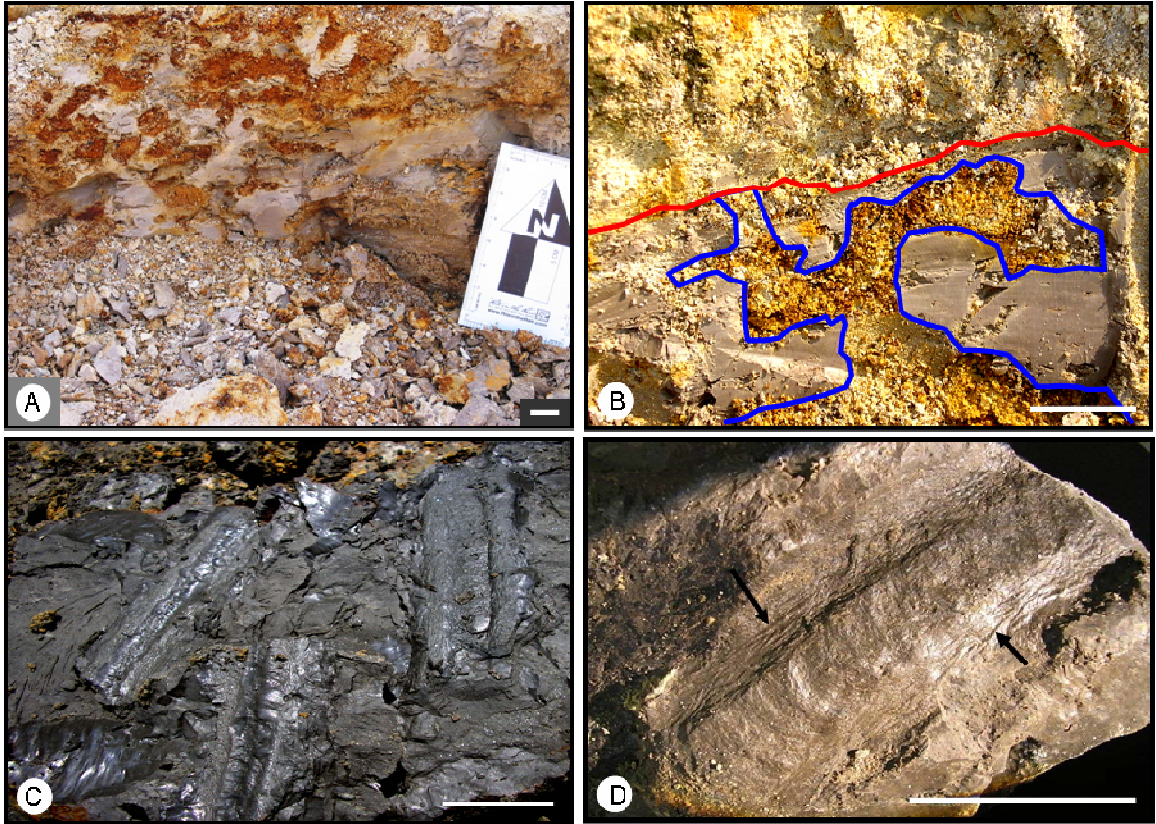


FIGURE 28—Ichnofossils extending from the upper erosional surface into subunit C. (A) *Thalassinoides* passively filled with iron-oxide stained, gravelly coarse-grained sand. (B) Close-up of sand-filled, sharp-walled *Thalassinoides*. Red line denotes contact with unit 8. (C) Three *Rhizocorallium*. (D) Close-up of *Rhizocorallium* showing patterned scratch marks (arrows) on the burrow walls. This wall ornamentation indicates firmground conditions. Scale bars are ~2 cm long.

several decimeters. U-shaped burrows that bound the spreiten range from 4 to 10 mm in diameter and are commonly filled with sand. Where burrows remained unfilled or fills have been removed, burrow walls generally display patterned scratch marks (Figs. 28C-D).

Subunit C locally experienced soft-sediment deformation. It contains synsedimentary folds, one of which has an amplitude of ~10 cm and trends northwest across the entire exposure (Fig. 29). Subunit C also contains common irregular slickensided joints associated with differential compaction.

5.3.4 Distribution of Fossils in Ingersoll Shale Subunits

The relative abundance of fossil constituents is closely related to subunit stratigraphy in the Ingersoll shale (Fig. 30). Fossil material in subunit A is dominated by relatively abundant and well-preserved angiosperm and conifer reproductive organs, spores, and amber clasts (Fig. 30). Angiosperm leaves, conifer foliage, and ferns are relatively rare and are usually not as well-preserved as in the other subunits. Vertebrate remains in this subunit are rare and consist only of fish scales. Large pieces of lignite (> 15 cm) and abundant macerated plant debris mark the boundary between the olive-black shale of subunit A and the lower oxidized portion of this subunit. Fossils in the lower portions of subunit A are either poorly preserved (as impressions and/or stains) or absent altogether (e.g., in the lowermost ~9 cm) due to oxidation.

Angiosperm leaves and conifer foliage dominate the fossil assemblage in subunit B (Fig. 30). The foliage is generally found intact and extremely well-preserved. Angiosperm and conifer reproductive organs and spores are found in moderate abundance throughout this subunit. Amber clasts are rare, and when present, they are



FIGURE 29—Soft-sediment deformation in subunit C of the Ingersoll shale. Dashed line approximates hinge of large synsedimentary fold. Note that unit 8 is deformed along with the upper surface of the Ingersoll shale.

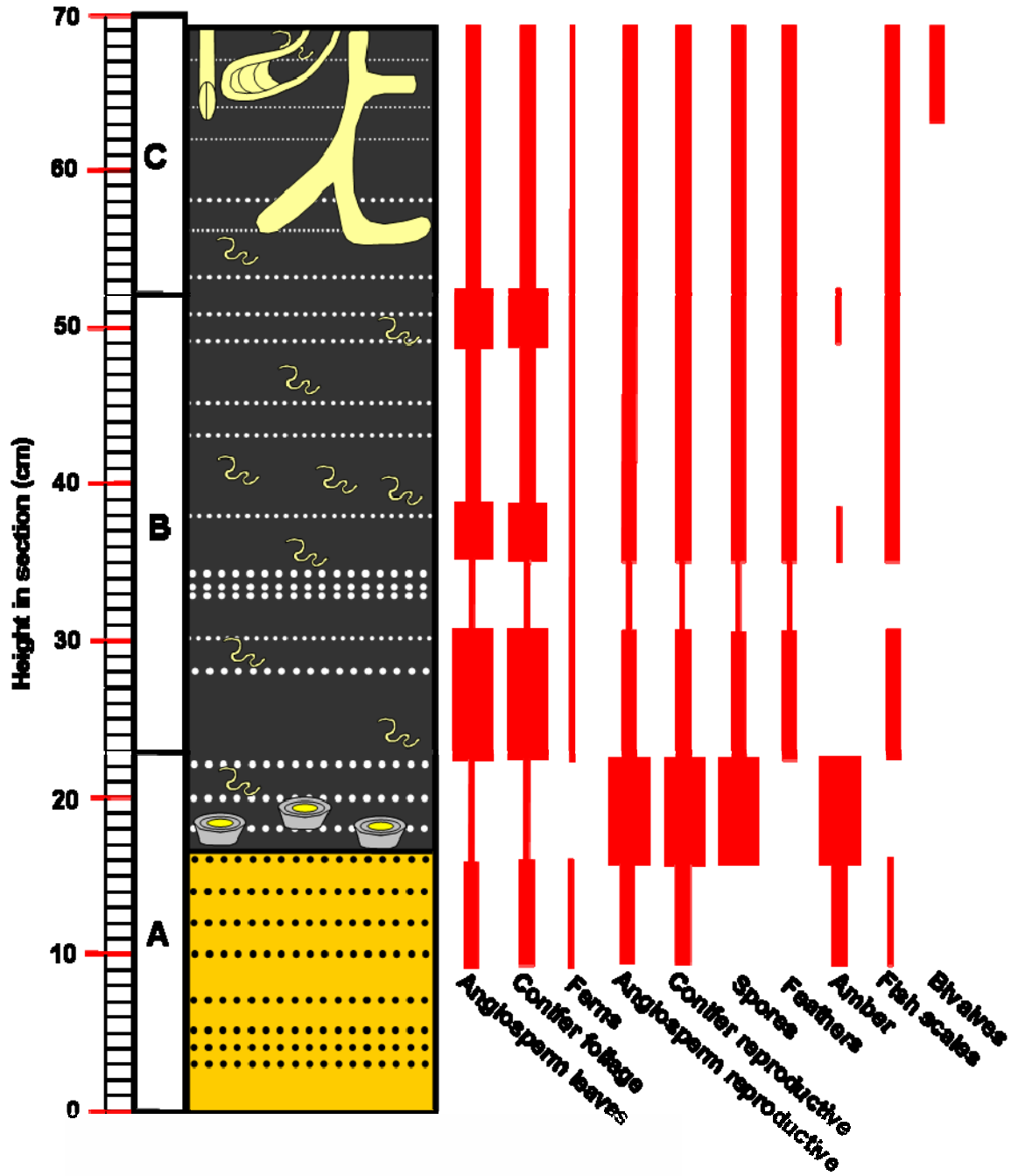


FIGURE 30—Distributions and abundances of fossils vertically through the Ingersoll shale. Note the absence of fossil material in the lower ~9 cm of subunit A due to weathering and oxidation. Bar widths qualitatively reflect abundances based on observations during quarrying

much smaller (< 1 mm) than those found in subunit A. Plant macrodetritus is common but reduced in both quantity and size relative to subunit A. Ferns are relatively rare. Vertebrate remains are moderately abundant and include fish scales and extremely well-preserved feathers.

Fossils are least abundant in subunit C. This may be due in part to bioturbation (Fig. 30) and jointing, both of which inhibit bedding-parallel splitting of the shale. Angiosperm leaves and reproductive organs, conifer foliage and reproductive organs, and spores are moderately abundant. Ferns are a minor component of the fossil assemblage, and amber is absent altogether. Vertebrate remains are moderately abundant and, as in subunit B, include feathers and fish scales. Fossil preservation is generally good. However, some fossils have been deformed due to differential compaction of clay around sand-filled burrows. Bivalves, preserved as internal molds and rarely via pyritization, are found mainly in the upper 8 cm of subunit C.

Fossils are not distributed evenly across the lateral extent of the Ingersoll shale. Rather, they are generally most abundant in sediments where the clay lens is thickest (i.e., near the axis of the lens, Fig. 31). Amber clasts and large pieces of lignite are found principally within the medial part of the lens, while plant foliage occurs throughout the lateral extent of the unit. On the western side of the lens, fossils are moderately abundant but are commonly deformed due to bioturbation. Fossil abundances gradually decrease laterally from the longitudinal axis towards the eastern side of the lens.

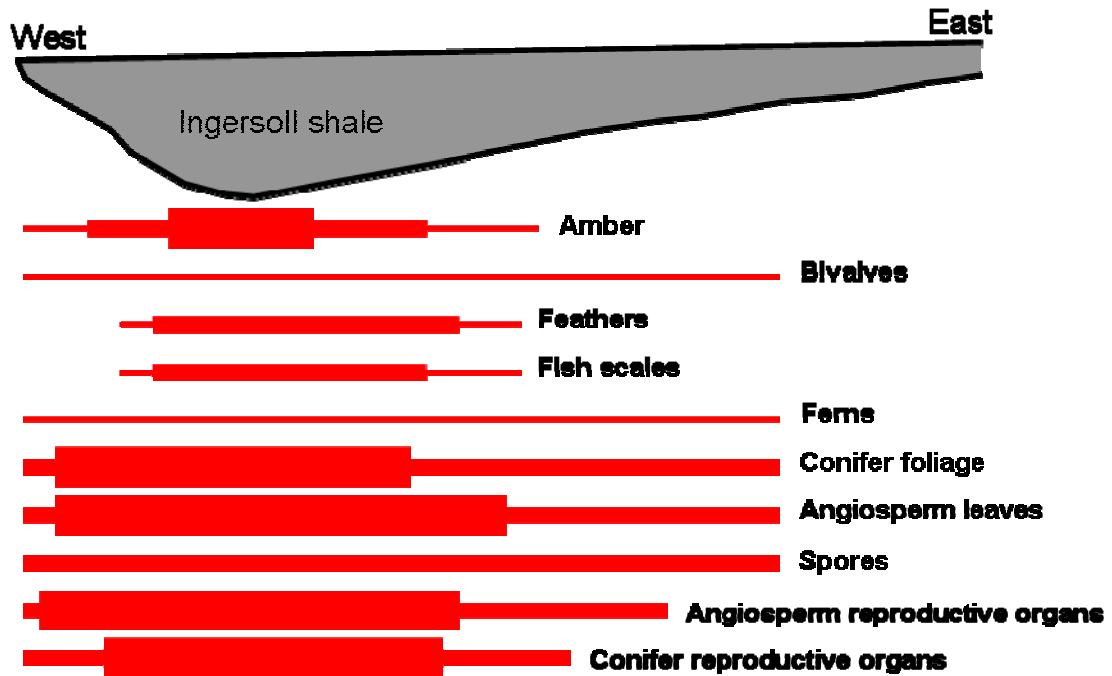


FIGURE 31—Lateral distribution and abundances of fossils in the Ingersoll shale. Bar widths qualitatively reflect abundances based on observations during quarrying. Note fossil abundance generally decreases away from axis of the clay lens.

6.0 LABORATORY OBSERVATIONS

6.1 Fabric Analysis

6.1.1 Tidal Rhythmicity in Subunit A

As described above, subunit A of the Ingersoll shale is characterized by couplets of graded sand and mud laminae that appear to be bundled into packages of relatively thick and thin laminae. This is suggestive of tidal laminites wherein the amount of sediment deposited during individual tidal cycles (i.e., individual sand-mud couplets) is governed by the neap-spring cycle (see Kvale and Archer, 1990). Laminae and bundles are apparent in the field (Fig. 12), in sample blocks (Fig. 23), and in CT scans of cores collected from subzone A (Fig. 32). However, the most accessible and continuous record of laminae was provided in polished slabs of epoxy-impregnated core and in the thin sections produced from those slabs (Fig. 33). Hence, these materials were used to evaluate the presence of a tidal signal, using the approach employed in previous studies of tidal laminites (e.g., Dalrymple and Makino, 1989; Kvale and Archer, 1990; Dalrymple, 1992).

Discrete sand-mud couplets were best developed in a ~13-cm-thick section of the 7.6-cm-diameter core, which includes the uppermost part of the oxidized zone (Fig. 33). Despite some deformation resulting from the coring process (e.g., laminae downwarp near core exteriors, compression or foreshortening of recovered sediment) and

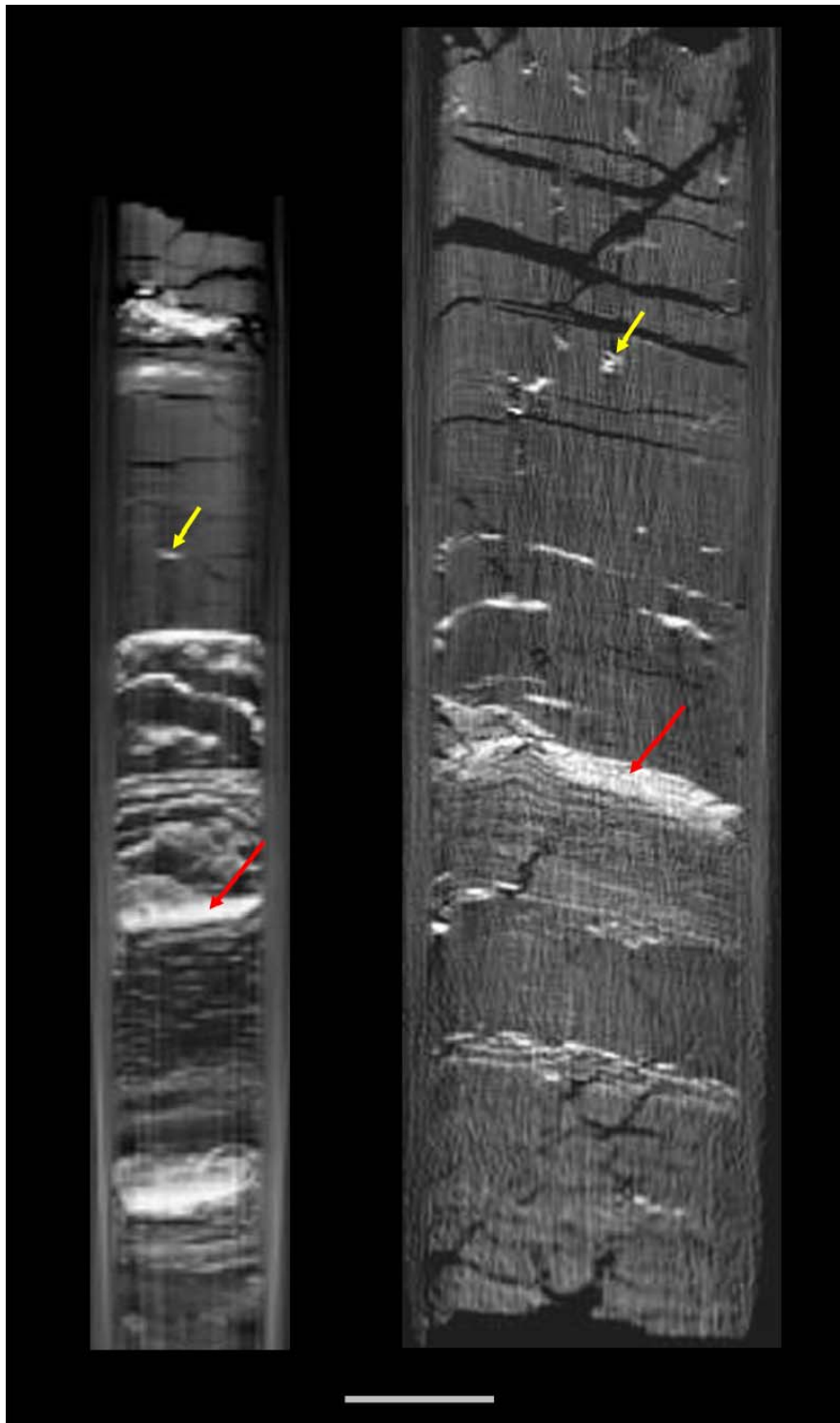


FIGURE 32—CT scans of 3.2-cm and 7.6-cm diameter cores taken from the Ingersoll shale. The cores show iron-cemented laminae (red arrows) and pyrite nodules (yellow arrows). The cores show alleged tidal laminae, but resolution is inadequate for measuring sand-mud couplets. Scale bar ~3.0 cm long.

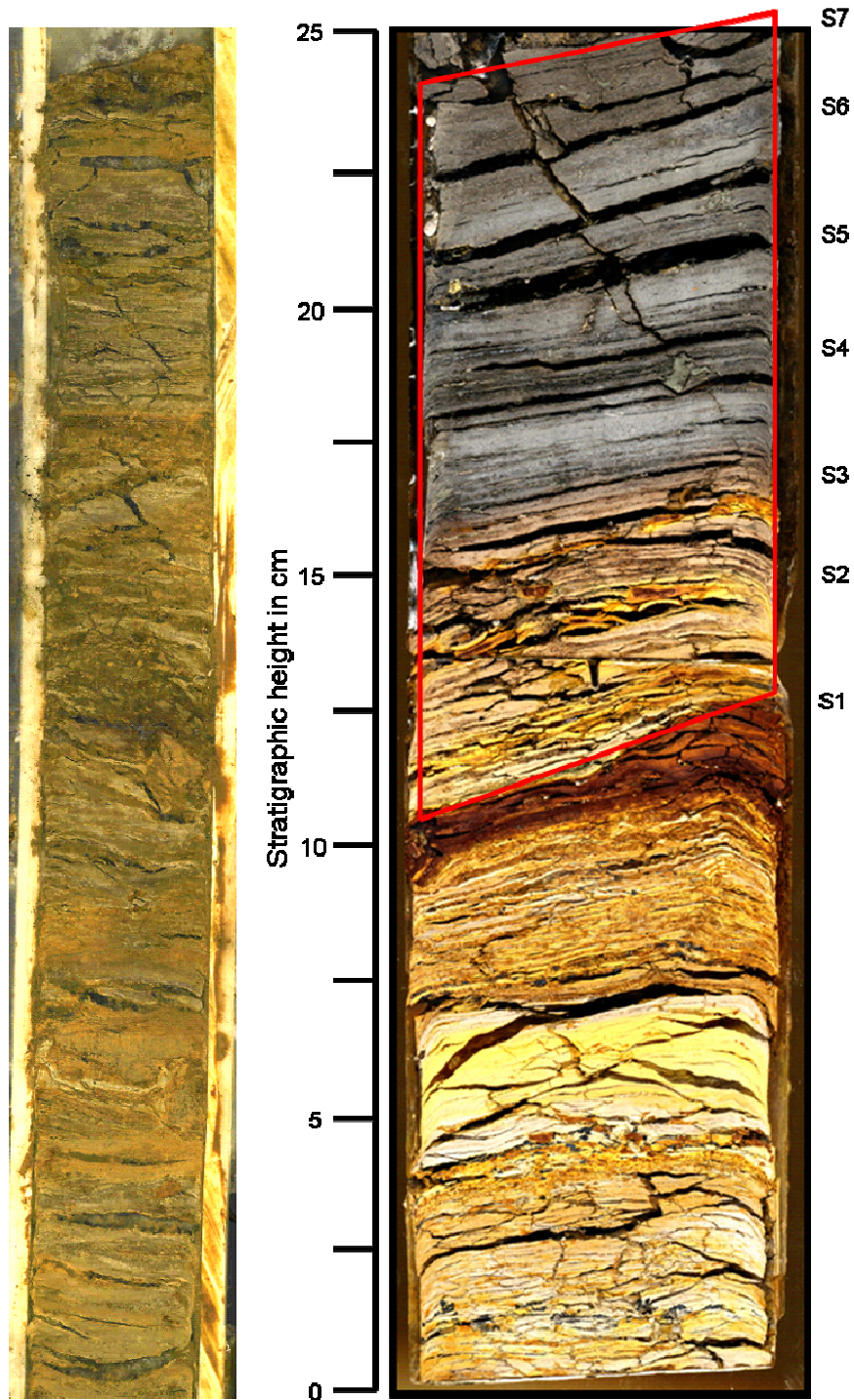


FIGURE 33—Photographs of Ingersoll shale core halves. Core on the left, encapsulated in paraffin wax, yielded poor resolution of individual lamina. Core on the right, encapsulated in epoxy resin, allowed for detailed observations of the graded sand-mud couplets. Red polygon highlights the interval used for tidal laminate analysis. S1-S7 refers to peaks in couplet thickness identified in figure 34.

subsequent formation of bedding-parallel cracks formed by desiccation, 91 couplets could be identified on enlarged core photographs (lowermost 61 couplets) or enlarged scanned images of thin sections (where photographic resolution was low, uppermost 30 couplets) of this interval. The thickness of each couplet was measured using calipers, corrected for enlargement, and plotted versus couplet number (Fig. 34).

The histogram in Figure 34 clearly indicates a cyclic fluctuation in laminae thickness, and the nature of these fluctuations is highly suggestive of tidal cyclicity. Six prominent cycles stand out in the data (numbered C1-C6 in Fig. 34A). Each of these cycles is defined by an average of 14 couplets (range 13 to 16 couplets). This pattern can be interpreted to reflect a tidal signal whereby each of the cycles records a tropical neap-spring cycle and each couplet records a mainly diurnal (daily) tidal rhythm (e.g., similar to that described in Visser, 1980; Kvale and Archer, 1990; Kvale et al., 1999). This interpretation is supported by the alternation of relatively high and low amplitudes of the peaks in couplet thickness (Fig. 34), which matches the pattern expected in response to the semi-monthly inequality; spring tides at perigee are higher than the spring tides at apogee during a lunar month (Kvale and Archer, 1990; Kvale et al., 1999).

The data from the Ingersoll shale are not as convincing or as clean as that derived from previously described tidal laminite sequences (Kvale and Archer, 1990). Notably, close examination of the histogram reveals the presence of what may be higher frequency cycles (C1-C11 in Fig. 34B) defined by an average of ~7 sand-mud couplets. This could reflect noise associated with lateral thickening and thinning of couplets, the inability to distinguish thinner couplets, and/or lack of deposition of sand and consequent mud

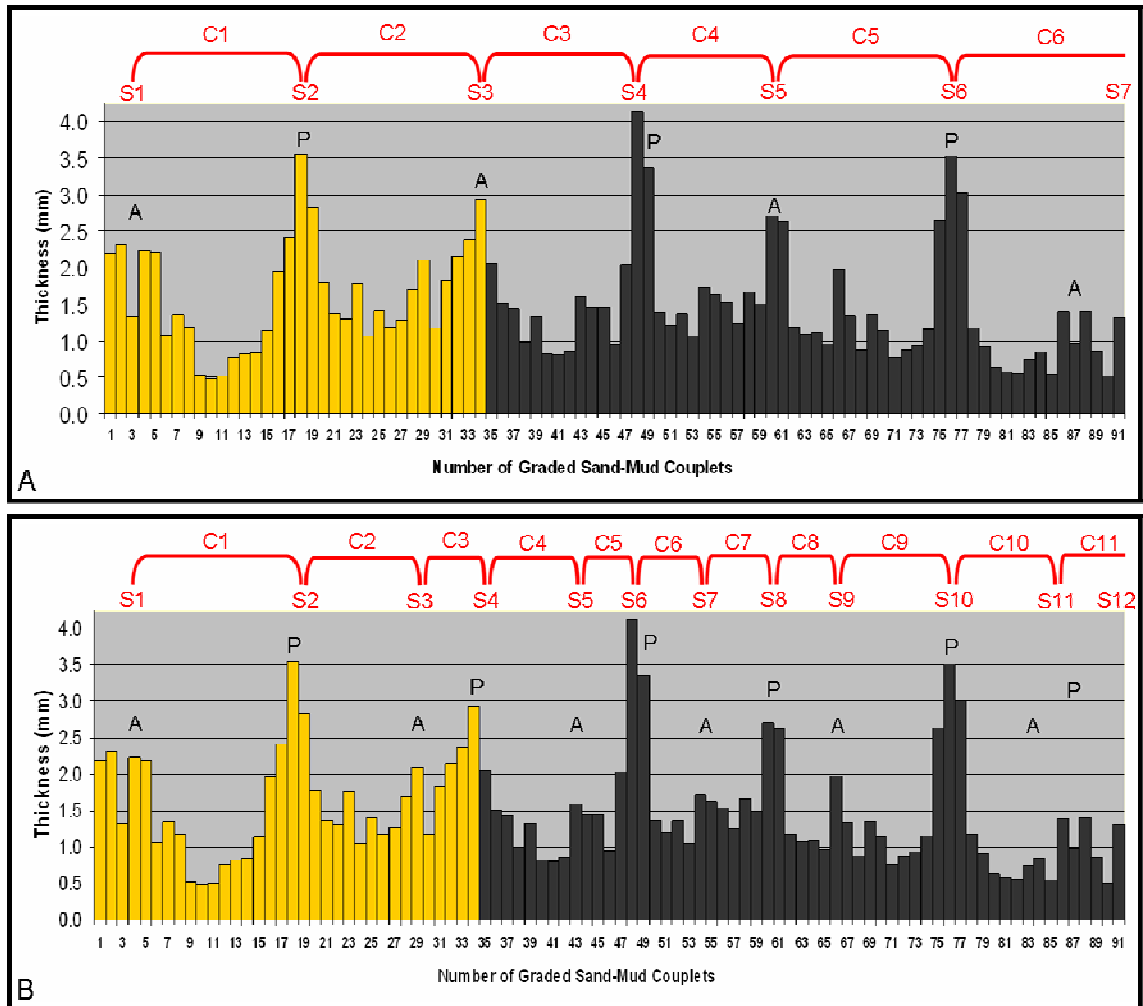


FIGURE 34—Histogram of graded sand-mud couplet thickness versus couplet number. Spring-neap cycles are shown in red lettering. Yellow histogram bars represent oxidized portion of Ingersoll shale core, gray bars represent unoxidized portion of core. Red lines and notations reflect possible interpretations of tidal signals. (A) C1 through C6 likely reflect semimonthly spring tide-to-spring tidal cycles (S1-S7 denote spring tide peaks). Note alternating high (S2, S4, S6) and low (S1, S3, S5) spring peaks that likely reflect perigee (P) and apogee (A), respectively. (B) A less likely alternate interpretation involving a higher number of incomplete cycles (C1-C11). As in A, S indicates spring tide peaks and A and P reflect apogee and perigee, respectively.

amalgamation during neap-phase tidal cycles. Alternatively, the higher frequency cycles could correspond to neap-spring cycles. In this scenario, a semi-monthly inequality is apparent. However, the presence of only ~7 couplets per cycle would indicate that the tidal record is incomplete and that deposition occurred only during spring tide phases.

6.1.2 Subunit B and C Fabrics

As previously noted in field observations (section 5.0), primary sedimentary structures (e.g., laminae) are less common or absent in subunits B and C. This is evident in CT images of cores from the middle and upper parts of Ingersoll. These images show homogeneous fabrics with abundant, small (<1 cm), commonly vertically oriented, high-density anomalies that reflect the distribution of pyrite (Fig. 35A). Although image resolution is too low to distinguish the nuclei of pyrite masses, many of these anomalies may reflect the position of the narrow pyritized burrows observed in the field and in sample blocks.

Thin sections and SEM observations of samples from subunits B and C reveal microfabrics that are not obvious in the CT images or in cores examined macroscopically. Continuous to weakly disrupted laminae of fine sand and silt are evident in thin sections (Fig. 35B). These laminae generally are very thin and commonly are defined by a single layer of grains. Although thin sections were not prepared for the entire interval represented by subunits B and C, observations of available thin sections indicate that sand-silt laminae are less common and thinner in the upper parts of the Ingersoll shale (i.e., subunit C). SEM images depict a strong preferred orientation: clay plates, which generally are less than < 4 μm across, and other platy minerals are preferentially oriented parallel to bedding (Fig. 35C).

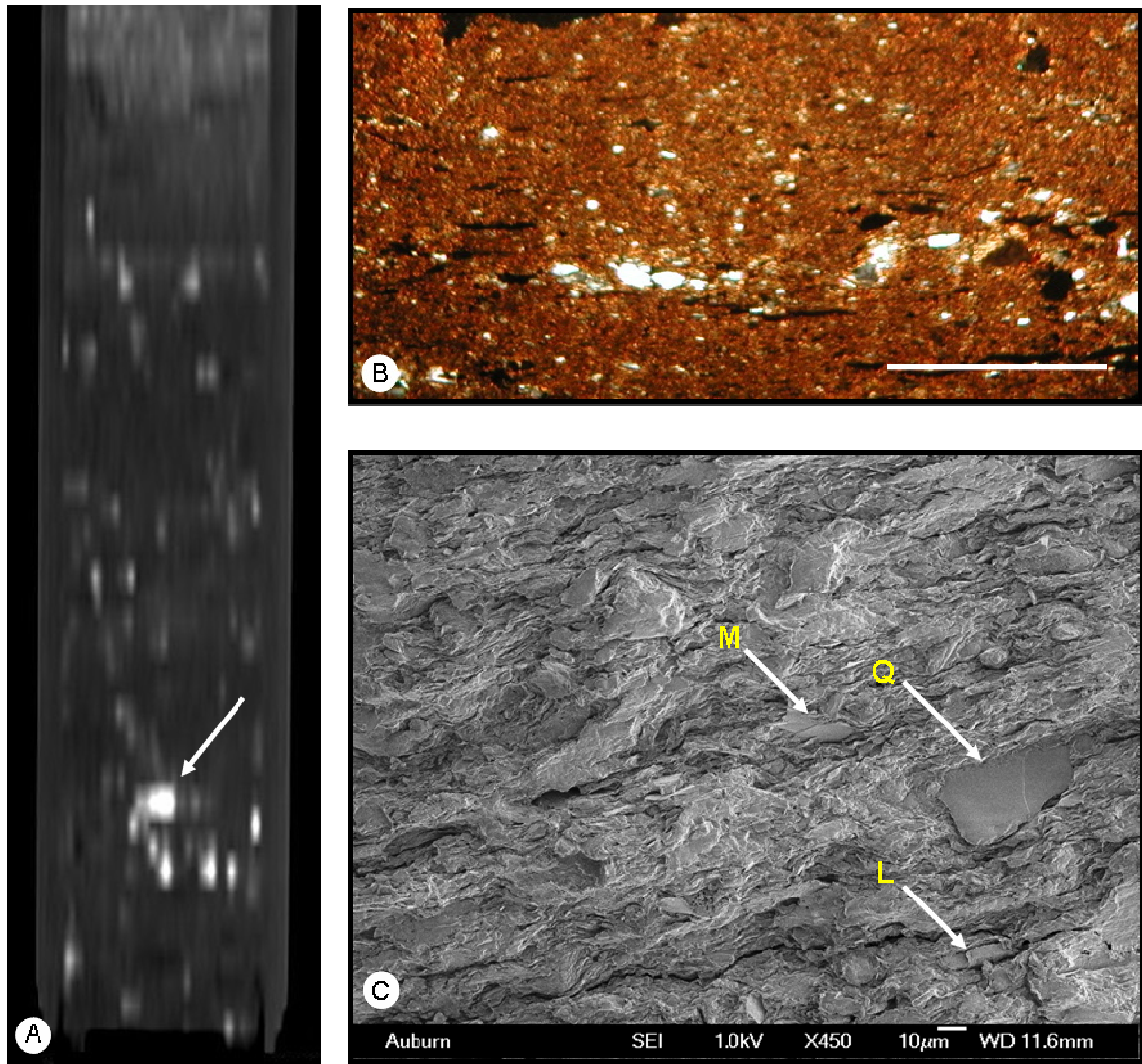


FIGURE 35—Subunit B and C fabrics. (A) CT scan of 3.2-cm core from subunit C shows high density (pyrite) anomalies (arrow). (B) Photomicrograph of thin-section from subunit C showing thin, discrete quartz silt lamina. Opaque objects are pyritized organic detritus. Scale bar ~1 mm long. (C) SEM image of subunit B showing strong preferred grain orientation parallel to bedding. M, Q, and L indicate mica plates, quartz grain, and lignite clast, respectively.

6.2 Textural Studies

Textural data derived from analyses of the 69 subsamples (Table 1) reflect the dominance of mud throughout the Ingersoll shale. Weight percent sand ranges from a low of ~0.60% to a high of ~20% (mean= 5.90%). A plot of weight percent sand versus stratigraphic height in the Ingersoll (Fig. 36) indicates a progressive fining upward trend; average weight percent sand in subunits A, B, and C, is 12.18, 3.21, and 2.04, respectively. Despite the overall trend of decreasing sand content towards the top of the Ingersoll, the textural plot in Figure 36 clearly reveals the presence of ~25 high-frequency textural cycles. Six of the peaks in weight percent sand (labeled 6 through 11 in Fig. 36) are apparently linked to the six main cycles in couplet thickness recognized in the tidal laminite study (see Fig. 34 section 6.1.1). The occurrence of roughly equally-spaced cycles in weight percent sand suggests that a tidal rhythm was influential throughout Ingersoll shale deposition. Specifically, each of the high-frequency textural cycles in Figure 36 could reflect the same neap-spring tidal cycle control inferred for the laminites in subunit A.

6.3 Organic Studies

6.3.1 Carbonate and Organic Carbon Contents

Acid digestion procedures indicate the virtual absence of carbonate in the Ingersoll shale samples. No effervescence was observed, and minor weight loss upon digestion (average 5.7% loss) can be attributed to loss of solids during filtering and dissolution of oxidation products of pyrite (e.g., jarosite).

Organic carbon contents derived from analysis of insoluble residues from the 69 Ingersoll shale subsamples are provided in Table 1 and plotted versus stratigraphic height

TABLE 1—Weight percent sand and organic carbon in the Ingersoll shale.

HEIGHT IN UNIT (CM)	SUBZONE	% SAND	% TOTAL ORGANIC CARBON	HEIGHT IN UNIT (CM)	SUBZONE	% SAND	% TOTAL ORGANIC CARBON
1.00	A	15.18	0.25	36.00	B	1.05	1.26
2.00		9.40	0.29	37.00		0.97	1.24
3.00		10.19	0.37	38.00		3.34	1.30
4.00		10.36	0.42	39.00		2.33	1.39
5.00		11.07	0.42	40.00		1.71	1.42
6.00		3.89	0.47	41.00		1.11	1.37
7.00		6.31	0.49	42.00		2.55	1.47
8.00		5.86	0.43	43.00		4.50	1.38
9.00		8.78	0.47	44.00		2.81	1.58
10.00		14.27	0.53	45.00		4.48	1.47
11.00		15.52	0.87	46.00		2.36	1.55
12.00		19.61	0.65	47.00		1.07	1.42
13.00		16.95	0.53	48.00		0.66	1.32
14.00		17.76	0.37	49.00		1.59	1.26
15.00		7.89	0.32	50.00		1.21	1.27
16.00		14.35	0.29	51.00		3.33	1.35
17.00		5.66	1.98	52.00		2.39	1.32
18.00		18.19	3.62	53.00		2.55	1.28
18.00		13.14	1.85	54.00		0.91	1.26
20.00		14.35	1.89	55.00		1.55	1.27
21.00		11.54	1.55	56.00		2.16	1.42
22.00		17.67	1.59	57.00		1.48	1.17
23.00		11.87	1.69	58.00		4.05	1.21
24.00	B	5.56	1.58	59.00	3.60	1.50	
25.00		1.76	1.42	60.00	1.07	1.32	
26.00		1.80	1.52	61.00	0.75	1.28	
27.00		3.06	1.47	62.00	0.88	1.36	
28.00		10.50	1.39	63.00	0.70	1.31	
29.00		1.53	1.32	64.00	3.42	1.31	
30.00		3.66	1.40	65.00	2.48	1.25	
31.00		3.83	1.65	66.00	2.22	1.30	
32.00		6.44	1.54	67.00	3.57	1.30	
33.00		11.43	1.39	68.00	0.97	1.19	
34.00		4.26	1.30	69.00	2.23	1.16	
35.00		1.92	1.38				

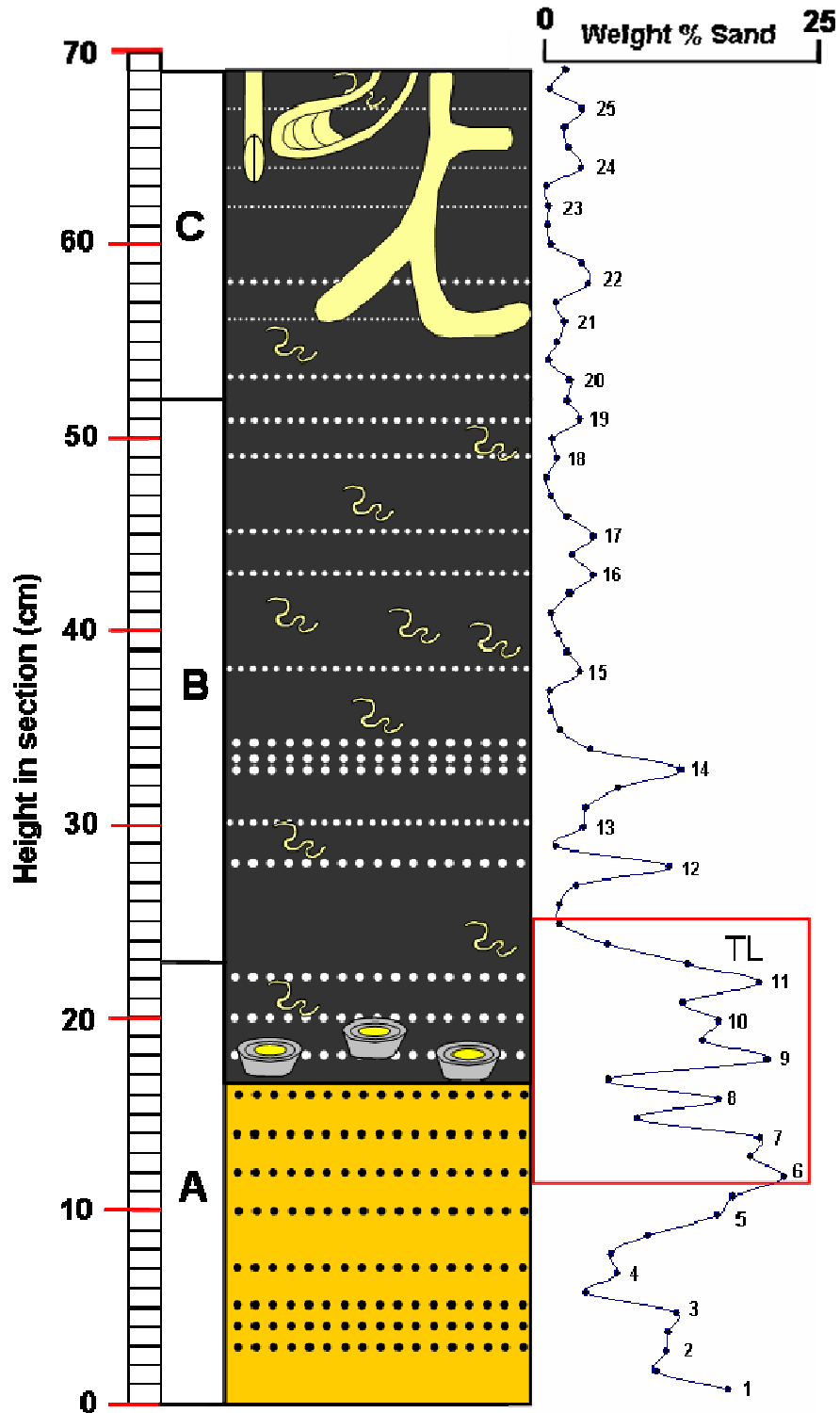


FIGURE 36—Textural data plotted against stratigraphic column of the Ingersoll shale. Peaks in weight percent sand are labeled 1 through 25. Red box indicates area of core containing sand-mud couplets used to study tidal rhythmicity and TL= tidal laminae.

in Fig. 37. Organic contents range from 0.25 to 3.62 weight % (mean= 1.22%). Organic contents are low (0.25 to 0.87; mean= 0.45%) in the highly oxidized basal part of subunit A. However, organic contents are relatively high throughout the unoxidized interval of the Ingersoll shale. Except for an anomalously high value of 3.62%, which was recorded immediately above the oxidized zone where plant macrodetritus is very abundant, organic contents for the Ingersoll vary between 1.16 and 1.89% (mean= 1.45%). For comparison, organic contents of subjacent clays in unit 6 and superjacent muddy sands of unit 8 average 0.31% and 0.39%, respectively.

6.3.2 Types of Organic Matter

A thorough characterization of organic matter was beyond the scope of the current study. It is obvious from field and laboratory observations that much of the organic carbon in the Ingersoll shale is in the form of terrestrial plant macro- and microdetritus. This is supported by qualitative palynological observations (by Richard Lupia and Ray Christopher; see Table 2) that indicate the prevalence of pollen and spores (Fig. 38A-D) and common mesofossils representative of the families Marsileaceae (heterosporous water ferns) and Isoetaceae (lycopsids) (Fig. 38E-H). However, palynological studies also indicate that marine dinoflagellates (Fig. 38I-L) are moderately abundant and diverse.

Palynomorphs also provided the basis for a general age assignment. Ingersoll shale palynomorphs can be assigned to the *Sohlipollis* Taxon Range Zone, which indicates a mid-Turonian through Santonian (Christopher et al., 1999; R.A. Christopher, personal communication, 2006).

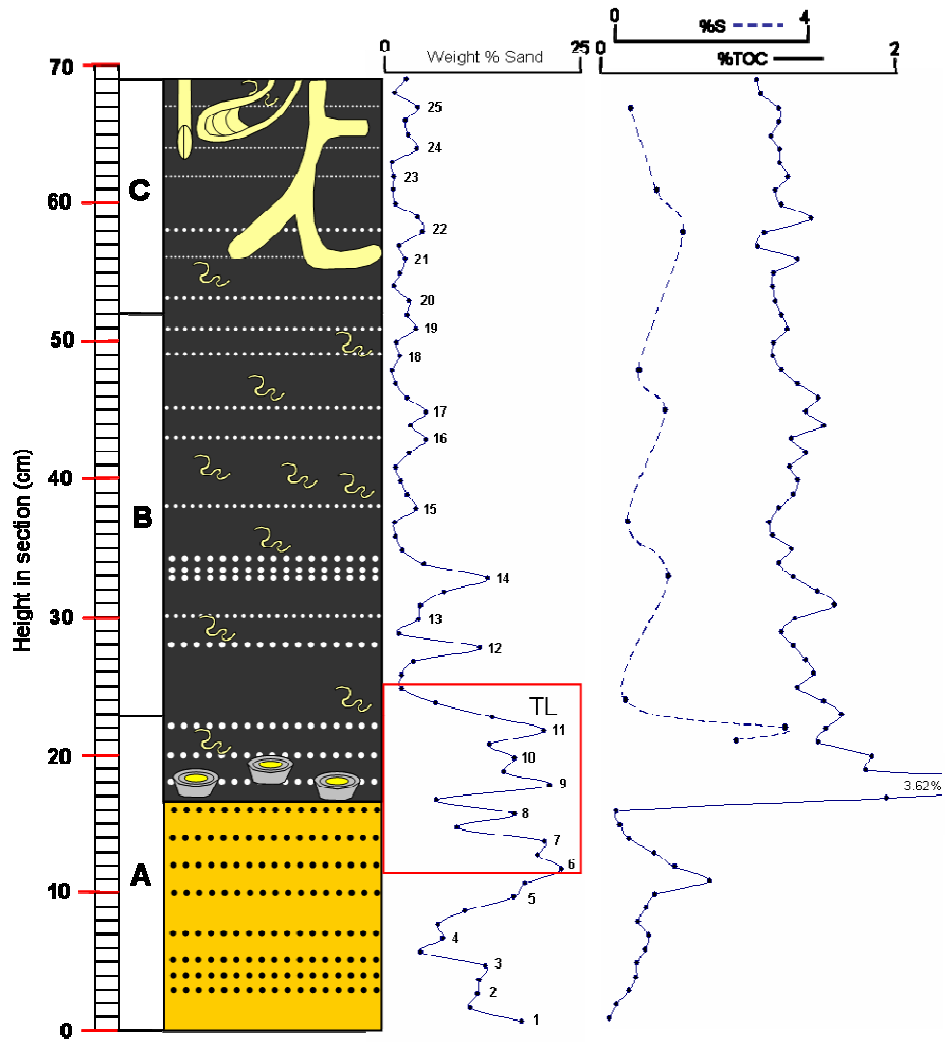


FIGURE 37—Total organic carbon (TOC) and sulfide sulfur (S) contents plotted against textural data.

TABLE 2—Palynomorphs identified in the Ingersoll shale.

Terrestrial Palynomorphs

Complexiopollis (“newer” forms)

Rugubivesicullites sp.

Taxodiaceapollenites hiatus

Sohlipollis sp.

Peromonolites allenensis

Complexiopollis exigua

Plicapollis sp.

Araucariacties australis

Fungal spores

Megaspores

Ariadnaesporites sp.

Arcellites sp.

Molospora lobata

Paxillitriletes sp.

Marine Palynomorphs

Dinoflagellate cysts (possibly including *Palaeohystrichophora infusoriodes*)

Acritarchs (including *Michrystridium* sp.)

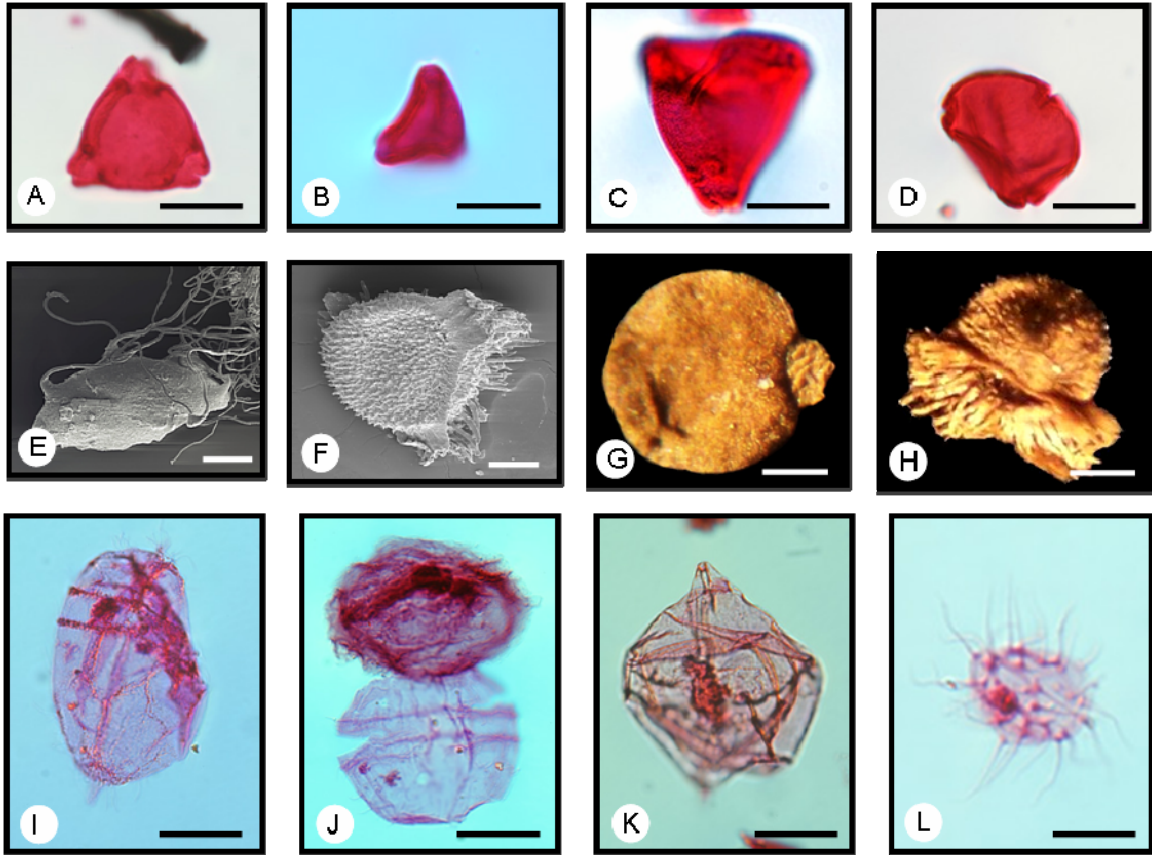


FIGURE 38—Photomicrographs of palynomorphs and megaspores isolated from the Ingersoll shale. (A-D) Pollen of the *Sohlipollis* Taxon Range Zone. (E-H) Megaspores, including *Ariadnasporites* sp. (E), *Paxillitriletes* sp. (F), *Molasporea lobata* (G), and *Paxillitriletes* sp. (H). (I-K) Marine dinoflagellate cysts. (L) Acritarch. Scale bars are ~20 μm long in A-D and ~100 μm long in E-L.

6.4 Pyrite and Sulfur Analyses

6.4.1 Pyrite

As noted initially during field observations, pyrite is extremely abundant in the Ingersoll shale. Pyrite is observed in association with many body fossils, either as a replacement product or as cavity fills (e.g., reproductive bodies, foliage, feather calami; e.g., see Fig. 7, section 3.2) and with some trace fossils (e.g., thin pyrite films on narrow burrow tubes, pyritized cores of *Rosselia*-like structures; e.g., Figs. 25C and D, 27B, section 5.3). It also occurs locally as relatively large, irregular nodules with unknown nuclei (Fig. 39). Sand-mud laminae pass through large pyrite concretions, whereas those in surrounding sediments are deformed around nodules (Fig. 39A, B). In thin section, pyrite occurs as isolated crystals, as aggregates of crystals replacing organic matter, and as burrow infills that have been partially compacted (Fig. 40A, B). Pyrite in SEM images appears as isolated crystals near organic material or as clusters of crystals and/or well-developed framboids within body fossils (Fig. 40C, D).

6.4.2 Sulfur and Sulfur Isotopic Analyses

Data from sulfur analyses (Table 3) reflect the abundance of pyrite. With the exception of a low value recorded for the one sample collected from the oxidized zone of subunit A (sulfide S= 0.03%), sulfide sulfur contents in the Ingersoll shale are high, ranging from 2.31 to 3.92 weight percent (n= 10; mean= 2.76%) sulfur. Sulfide S contents vary in proportion to sand and organic C contents (Fig. 37). Ratios of S to C are unusually high, ranging from 1.61 to 2.47 for unoxidized samples (Fig. 41). Sulfate S contents are generally very low (Table 3). Highest values are recorded near the interface between oxidized and unoxidized sediments in subunit A and in subunit C.

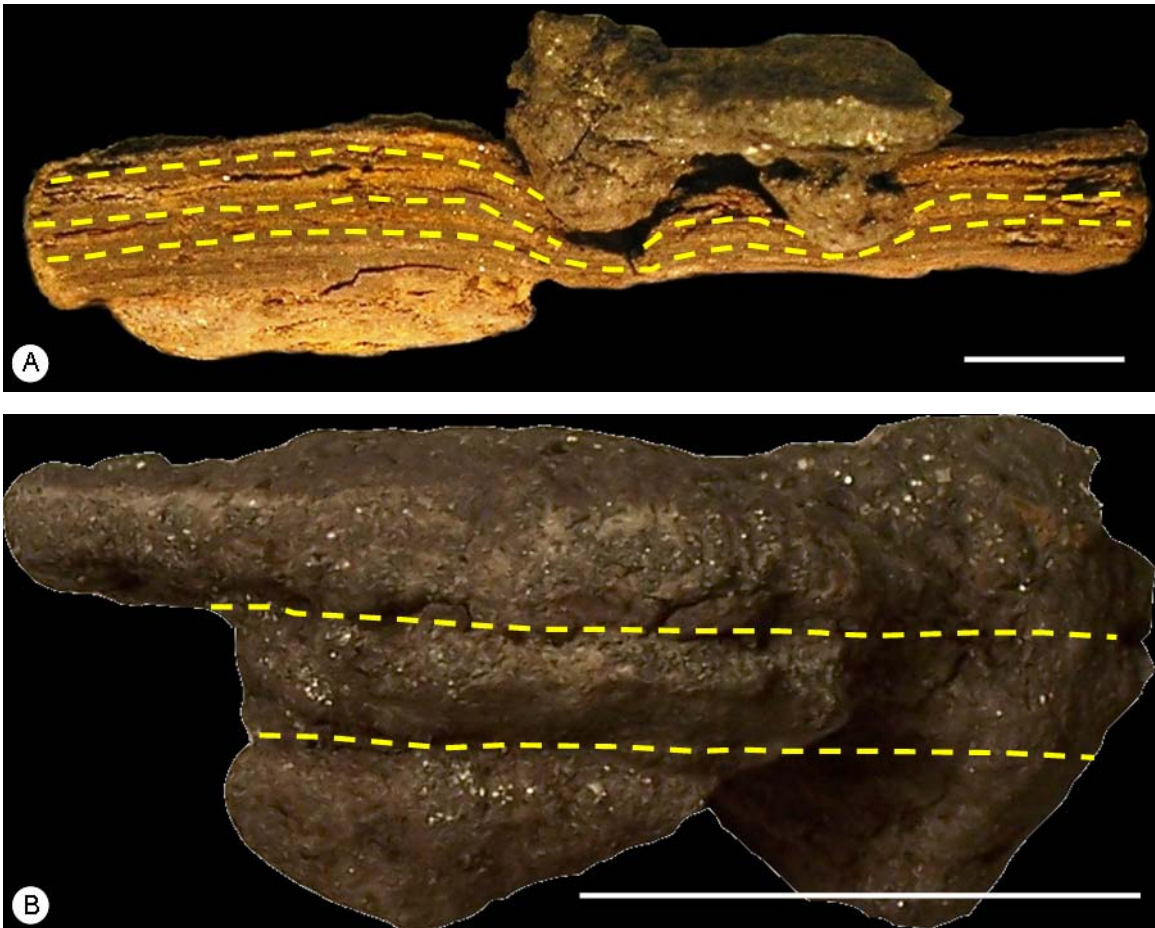


FIGURE 39—Pyrite concretion from subunit A of the Ingersoll shale. (A) Primary laminae (dashed yellow lines) are compacted around the pyrite concretion. (B) Same concretion shown in top photograph, rotated horizontally $\sim 90^\circ$ and enlarged to show horizontal traces of laminae within the concretion (dashed yellow lines). Scale bars are ~ 1 cm long.

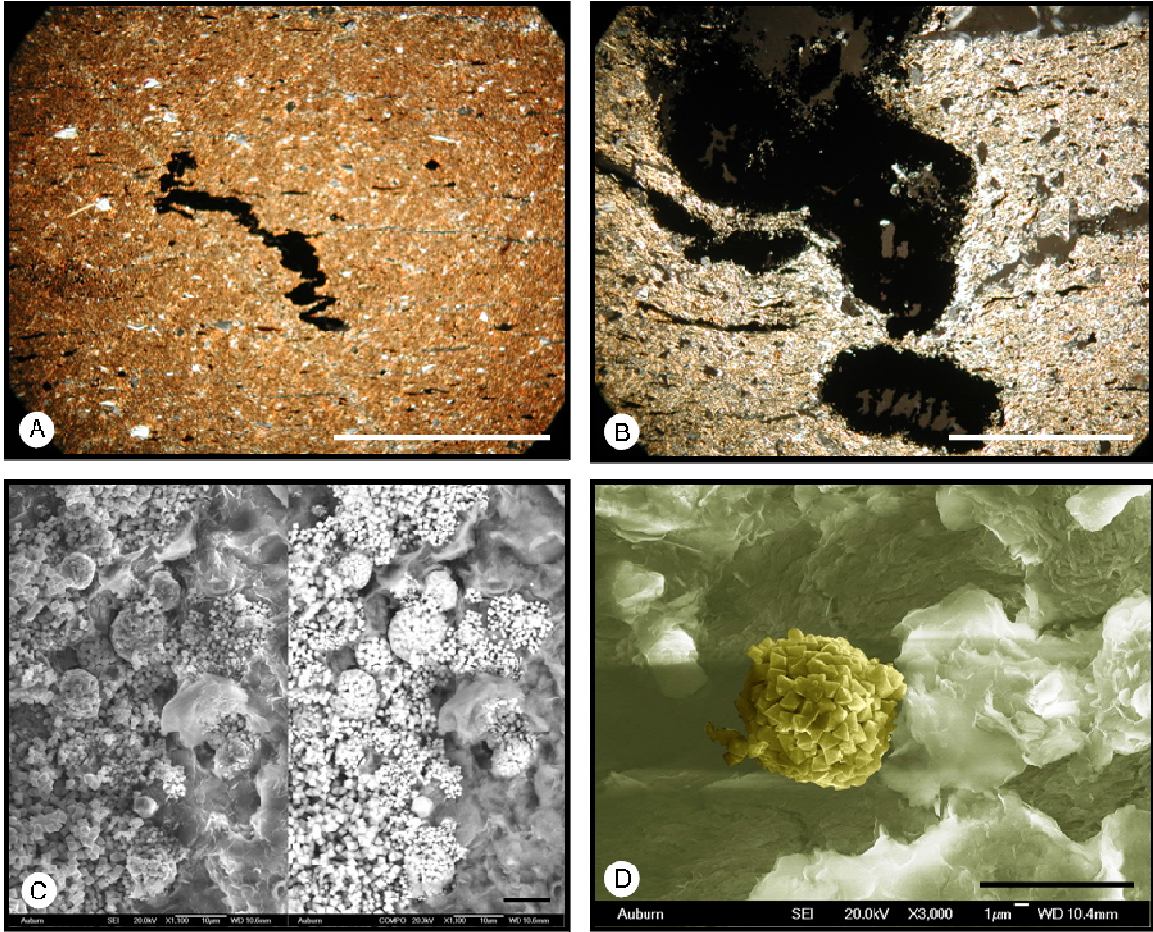


FIGURE 40—Forms of pyrite in Ingersoll shale. (A) Pyritized, compacted burrow(?). (B) Pyritized wood clasts. (C) Pyrite framboids from feather specimen. Image on right shows pyrite as bright white framboids and clusters, highlighted by backscatter elemental imaging (BSE). Clay matrix remains light gray. (D) False color image of a pyrite framboid in clay matrix. Scale bars are ~1 mm long in A and B, and 10 μ m long in C and D.

TABLE 3—Weight percent organic carbon, sulfide sulfur, and sulfate sulfur from the Ingersoll shale.

SAMPLE #	HEIGHT IN UNIT (cm)	%TOC	%SULFIDE SULFUR	%SULFATE SULFUR
18	8	0.43	0.03	0.03
31	21	1.55	3.42	0.32
32	22	1.59	3.92	0.26
35	24	1.42	2.29	0.26
43	33	1.39	2.73	0.23
47	37	1.24	2.31	0.17
55	45	1.47	2.69	0.26
58	48	1.32	2.43	0.37
68	58	1.21	2.88	0.35
71	61	1.28	2.61	0.37
77	67	1.30	2.34	0.35

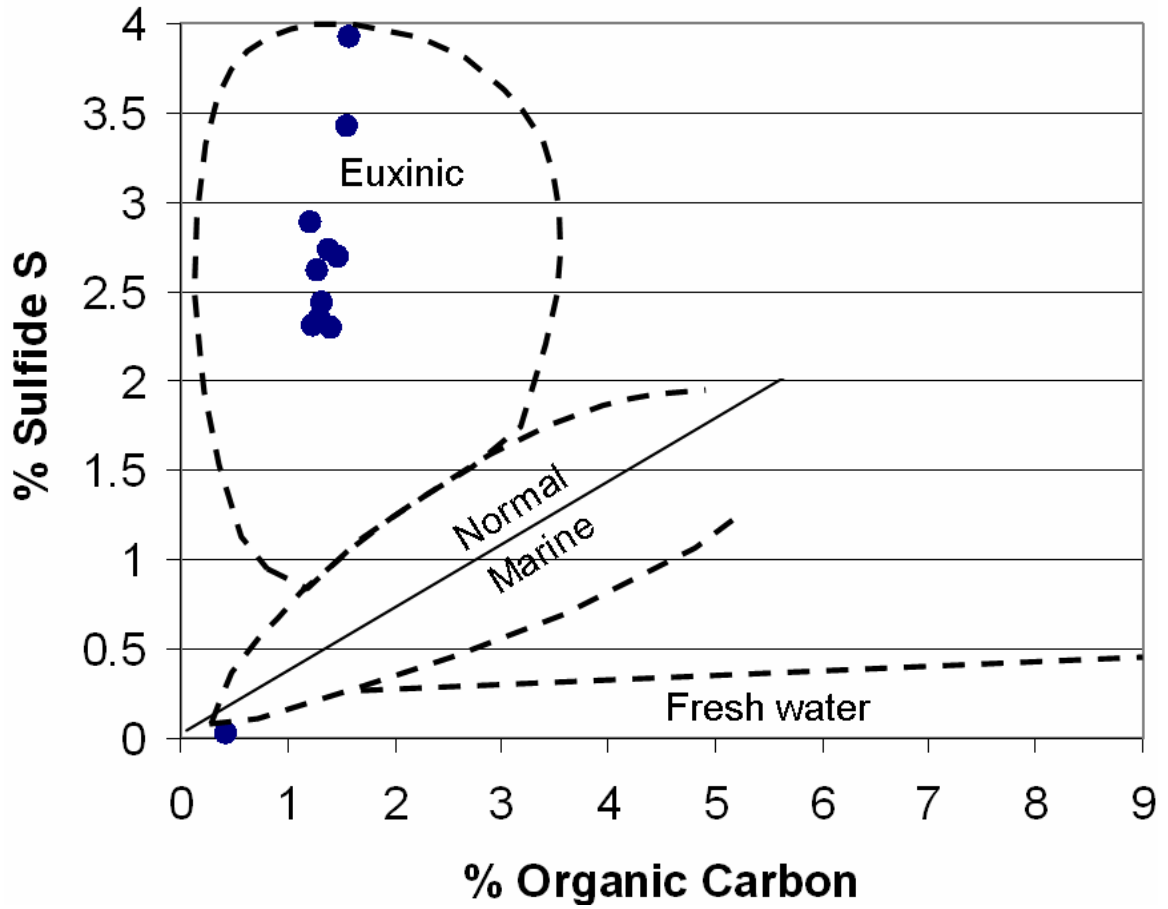


FIGURE 41—C versus S contents for Ingersoll shale samples (blue dots). Sulfur contents are generally much higher than those characteristic of normal marine and freshwater mudrocks as described by Berner and others (Berner, 1983, 1985; Berner and Raiswell, 1984).

Sulfate S may reflect the presence of minor sulfate mineralization associated with the oxidation of pyrite.

Data from isotopic analysis of pyrite samples are reported in Table 4. Values of $\delta^{34}\text{S}$ are all significantly low, ranging from -35.7 to -39.7 ± 0.1 per mil, relative to the Canyon Diablo troilite (CDT) standard.

TABLE 4—Sulfur isotopic compositions of Ingersoll shale pyrite samples.

SAMPLE #	HEIGHT IN UNIT (cm)	PYRITE SULFIDE $\delta^{34}\text{S}$ (RELATIVE TO CDT)
29	24	-39.7
48	45	-35.7
49	46	-35.7
80	47	-35.7
61	60	-38.3
62	61	-38.3
63	62	-38.3

7.0 INTERPRETATIONS

7.1 General Environmental Settings

7.1.1 Tuscaloosa Formation

The Tuscaloosa Formation in east central Alabama and west central Georgia has previously been interpreted to record deposition in continental, mainly fluvial environments (e.g., Frazier, 1982, 1997; Smith and King, 1983; Reinhardt and Donovan, 1986; Reinhardt et al., 1994). Strata are typically arranged in fining upward sequences interpreted to reflect the transitions from fluvial channel through point-bar to floodplain settings associated with low-sinuosity streams (Smith, 1984; Reinhardt and Donovan, 1986). Tops of sequences may include paleosols (Smith, 1984).

Observations of the Tuscaloosa Formation at the study site are consistent with previous interpretations. Unit 1 likely represents overbank mud facies, whereas units 2 through 4 appear to record a complete fining-upward fluvial cycle. Cross-stratified sands of unit 2 likely represent channel bar and/or point-bar deposits; homogeneous, rooted sands of unit 3 may be remnant bar or levee deposits modified by pedogenic processes; and unit 4 mud likely records floodplain overbank deposition.

7.1.2 Eutaw Formation

The Eutaw Formation records deposition in various marginal and shallow marine settings (Frazier and Taylor, 1980; Frazier, 1987, 1996, 1997; King, 1990, Savrda and Nanson, 2003); thus, its position above the fluvial Tuscaloosa Formation is recognized

as indicative of marine transgression. In the study area and most of the Chattahoochee Valley area, the Eutaw Formation has been attributed to deposition in variably tide- and storm-influenced estuarine settings (Frazier, 1996, 1997; Savrda and Nanson, 2003). Stratigraphic successions observed in the Eutaw in this region commonly include a lower “tidal sand” facies, which has been attributed to deposition in estuarine shoreline and bayhead-delta settings, and an upper package of “proximal lagoon” and/or “distal lagoon” facies (Frazier, 1997), which are interpreted to record subsequent transgression and deposition in estuarine central bay settings (Fig. 42; Frazier, 1997; Savrda and Nanson, 2003).

The gravelly sands with herringbone cross-stratification, clay drapes, and a low-diversity *Skolithos* ichnofacies trace fossil assemblage in the lowermost part of the Eutaw Formation in the study section (unit 5) are indicative of a relatively high-energy, tidal setting (Buatois et al., 2005). The character of these sediments is consistent with those previously placed in the tidal sand facies by Frazier (1997).

Units overlying the Ingersoll shale also are consistent with an estuarine interpretation. Relatively heavily bioturbated, fossiliferous, carbonaceous muddy sands with low-diversity trace fossil assemblages assignable to the *Cruziana* ichnofacies (i.e., units 8, 11, and 13) are similar to those interpreted as proximal central bay deposits at other localities in the region (Frazier, 1997; Savrda and Nanson, 2003). Well-sorted fine sand beds with large ball-and-pillow structures, like unit 9, also are common in proximal central bay facies recognized by earlier workers. Following previous interpretations (e.g., Savrda and Nanson, 2003), these can be attributed to major storm and/or flood events that resulted in rapid deposition of large volumes of sand along the submerged

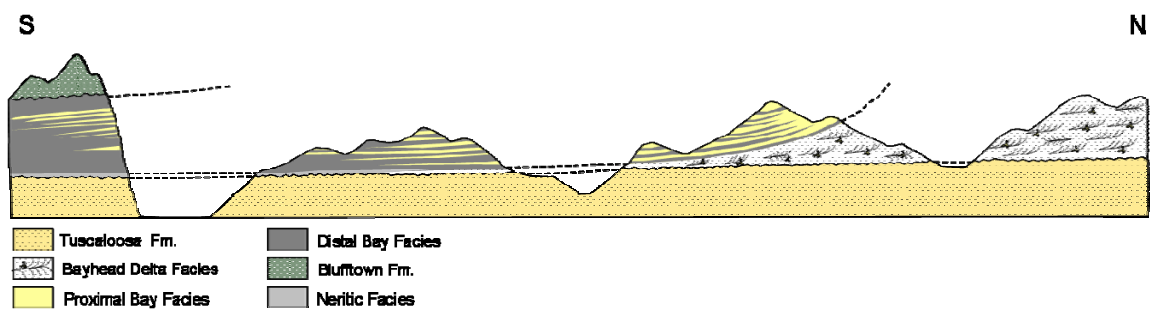


FIGURE 42—Generalized geologic cross-section of Eutaw lithofacies in east central Alabama and west central Georgia. Cross-section illustrates transition from bayhead delta facies to distal bay sediments down-dip and up section (modified from Frazier, 1997).

margins of a bayhead delta. Soft-sediment deformation may have occurred contemporaneously with deposition or sometime after deposition in response to shock-induced liquefaction. Notably, similar deformational features recognized elsewhere in the Eutaw and Blufftown formations may be indicative of paleoseismicity (Frazier, 1997). Units 10 and 12 are dominated by thinly intercalated sands and clays and are comparatively weakly bioturbated. These intervals preserve a record of fluctuating energy levels that are interpreted here to be related to tides. These units may reflect deposition at somewhat shallower depths closer to the estuarine shoreline.

7.1.3 Ingersoll Shale Channel Complex (Units 6 and 7)

Considering the interpretations described above, the channel-form complex formed by units 6 and the Ingersoll shale (unit 7) occurs at the transition from a relatively high-energy, tidally influenced bayhead delta setting (unit 5) to a comparatively quiet, central bay setting (unit 8). The geometry of this complex indicates deposition in a channel that was cut into the underlying tidal sand facies. The presence of thinly laminated sands and muds in unit 6 and the lower parts of the Ingersoll shale (subunit A) indicate the influence of tides. Based on stratigraphic context and sedimentologic character, unit 6 and the Ingersoll shale are interpreted to have accumulated within a north-south-trending tidal creek within an estuarine bayhead delta system (Figs. 43A, B). Specific physical and chemical conditions that prevailed in the Ingersoll creek are addressed in later sections of this thesis (section 7.3).

The modern-day Mahakam River delta, Indonesia (Gastaldo and Huc, 1992) provides possible modern analogs for the Ingersoll channel/creek. Modern tidal channel

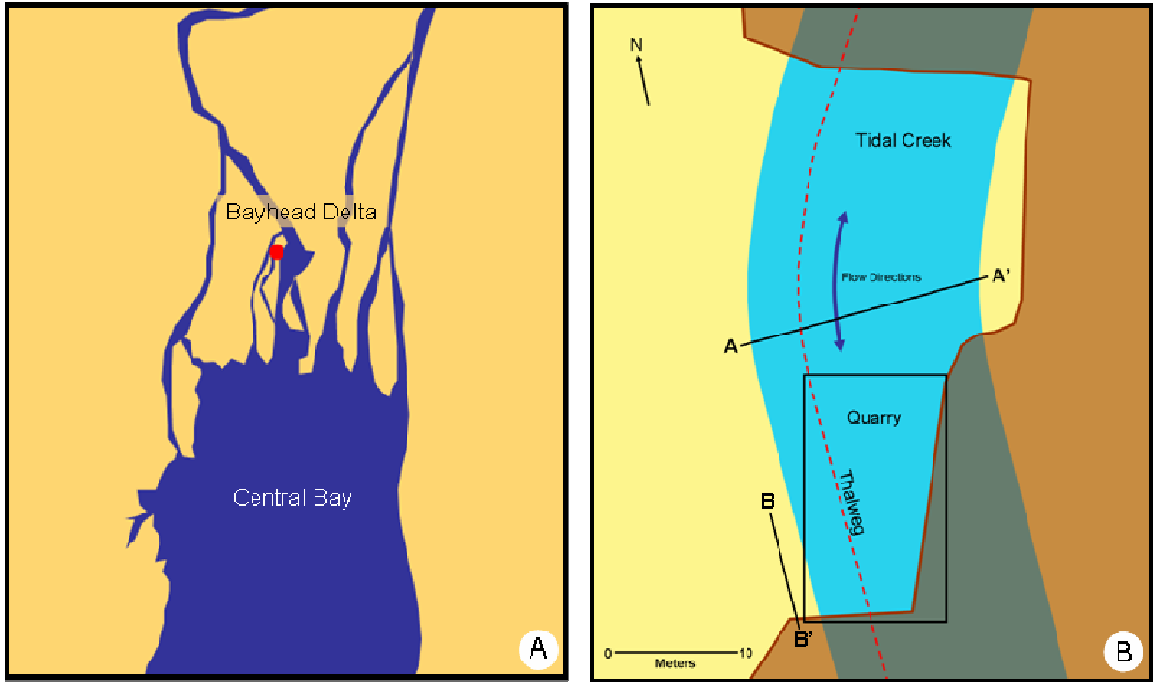


FIGURE 43—Interpretation of estuarine depositional setting for the Ingersoll shale. (A) Estuarine complex including bayhead delta in the Chattahoochee Valley. Red dot indicates inferred tidal creek setting for the Ingersoll shale. (B) Outcrop-scale reconstruction of the Ingersoll tidal creek in relation to quarry and trenches (lines A-A' and B-B').

fills within the Mahakam delta contain similar sedimentary structures and abundant plant litter. Where these channels are restricted by some obstacle (e.g., fallen trees, logs), they exhibit fining-upward sequences; rhythmically bedded sand-mud couplets grade upward into relatively structureless organic-rich muds.

7.2 Sea-level Dynamics

Estuarine deposits of the Eutaw Formation have been assigned to the lowstand systems tract of sequence UZAGC-3.0 (Mancini et al., 1995) and, in the sequence stratigraphic paradigm, can be considered as incised valley fill (IVF) (Mancini et al., 1995; Savrda and Nanson, 2003). The formation and preservation of lowstand incised valley fills involve several steps controlled by sea-level change (Van Wagoner et al., 1990). During sea-level fall and lowstand, subaerial exposure and erosion result in the formation of a sequence boundary (e.g., the Tuscaloosa/Eutaw contact). Base levels are lowered, and rivers deepen and widen their valleys (valley-incision stage). During the early stages of subsequent sea-level rise, drowning of river mouths results in elevated base levels and associated sediment aggradation by fluvial and/or estuarine processes (valley-filling stage; e.g., the Eutaw Formation in the Chattahoochee Valley region). As sea-level continues to rise and the shoreline migrates landward, tops of valley fills are truncated by shoreface ravinement to produce a transgressive surface (TS) that separates the IVF from overlying marine strata of the transgressive systems tract.

The formation of the Ingersoll shale channel-form complex can be explained by similar processes operating on a smaller scale and shorter time frame (Fig. 44). Narrow, shallow fluvial and/or tidal channels cut near the head of the estuary (within the interdistributary portions of a bayhead delta) may have begun to fill with sands and muds

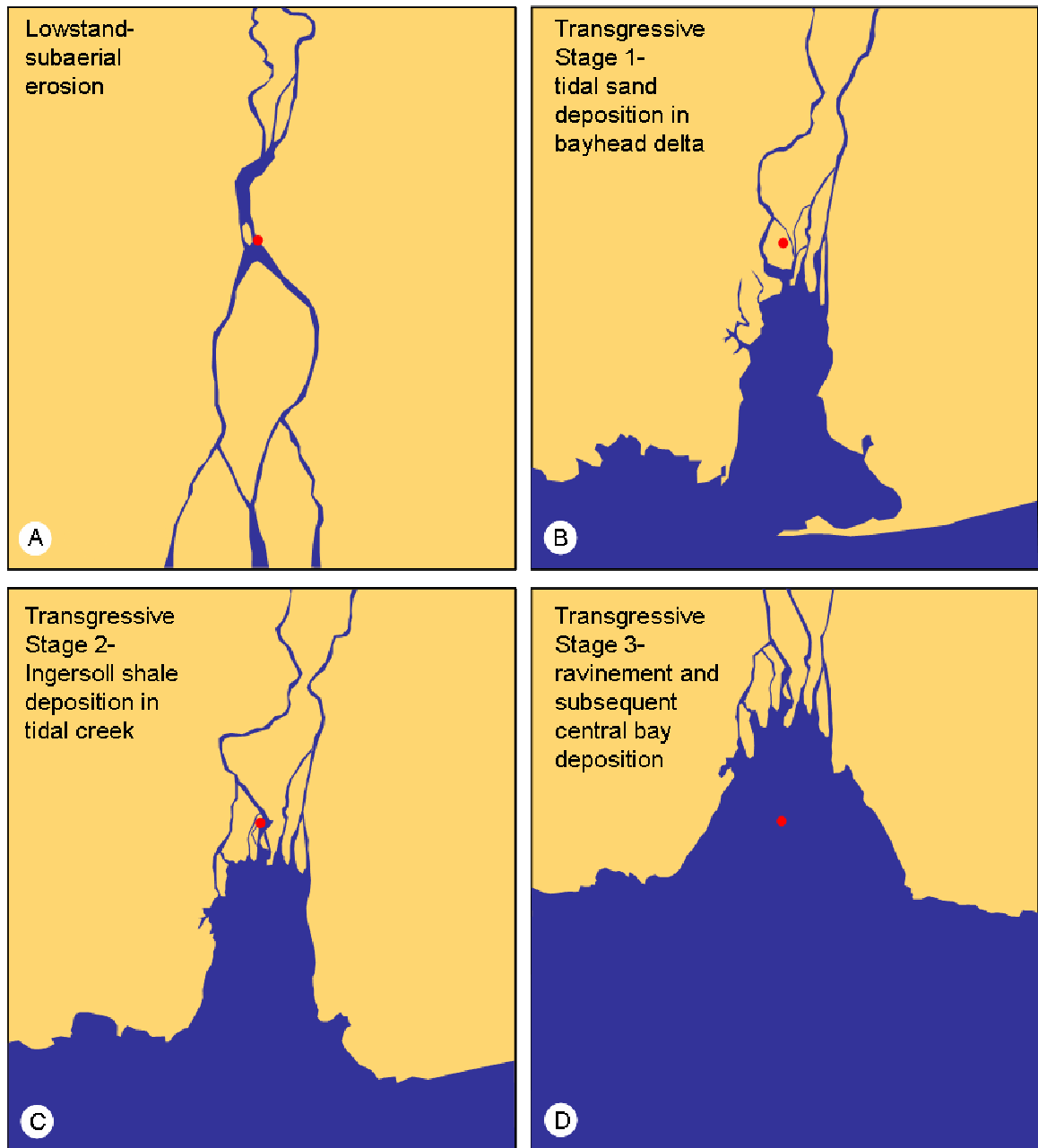


FIGURE 44—Reconstruction of estuary development within the Chattahoochee Valley in relation to the study location (red dots). (A) Subaerial exposure and erosion of the Tuscaloosa Formation during lowstand. (B) Initial transgressive flooding of river mouth and development of bayhead delta. (C) Cutting and progressive filling of tidal creek within bayhead delta. (D) Continued landward migration of bay shoreline and deposition of estuarine central bay deposits on top of truncated Ingersoll shale.

(i.e., units 6 and 7) in response to progressive transgression and drowning. As transgression continued and the central bay expanded landward, the top of the channel-fill was truncated by bay-shoreline ravinement. In this interpretation, the contact between the Ingersoll shale and unit 8 can be regarded as a transgressive surface of erosion within the larger lowstand IVF package.

7.3 Conditions in the Channel

7.3.1 Depositional Processes and Environmental Energy

As previously noted, rhythmically bedded sands and muds indicate that tidal processes were operating during deposition of the Ingersoll shale channel complex. As indicated by starved ripples, sand and hydrologically equivalent plant remains were transported into the tidal creek as traction load during higher-energy phases of daily tidal cycles. Mud and finer comminuted plant debris were likely transported in suspension and deposited during the slack-water phase of each tidal cycle.

Fluvial channels commonly are filled during point-bar migration. Similar lateral accretion in tidal creeks does occur, but tidal creeks are generally more stable than their fluvial counterparts (Fagherazzi et al., 2004). Tidal creeks and channels tend to widen by bank collapse (Fagherazzi et al., 2004), and channel filling does not occur unless the energy levels in the tidal channel decrease. Initial filling of the Ingersoll channel began during a relatively high-energy regime that included episodic erosional phases, which are indicated by truncation surfaces within and at the top of unit 6. A lower-energy tidal regime dominated the channel as deposition of the Ingersoll shale proper began. Decreasing sand content upward through the Ingersoll shale indicates that energy levels continued to decrease as the channel filled. The progressive decrease in energy indicated

by textural data could have been caused by a variety of local factors, including the restriction of flow by an obstacle (e.g., a fallen tree, etc.). However, this trend also could reflect the shift from a shallow, possibly intertidal channel to a deeper subtidal channel caused by sea-level rise and the landward migration of the bay shoreline.

7.3.2 Sedimentation Rates

Sedimentation rates for the Ingersoll shale can be estimated from the analysis of tidal rhythmites in subunit A and from textural data derived for the entire interval of the Ingersoll shale. Rate estimates depend on how the laminite data are interpreted (see section 6.1.1).

In the currently favored interpretation, the 13-cm-thick interval of subunit A analyzed for tidal rhythmicity contains ~6 spring-neap cycles (Fig. 34A). In the inferred diurnal system, each of these cycles represents ~13.66 days. Hence, this interval records ~3 tropical months (~27.32 days/month) of deposition at a rate of ~4.3 cm/month, or ~57 cm/year (assuming 13.36 tropical months/year), uncorrected for compaction.

Estimates of sedimentation rate for the entire Ingersoll shale interval can be made assuming that textural cycles recognized in Figure 36 are a pervasive signal of spring-neap cyclicity. If each of the 25 sand peaks recognized in the textural data reflect individual spring-tide phases, then the Ingersoll shale on the whole records 24 to 25 bimonthly cycles representing 12 to 12.5 tropical months, or slightly less than one year of deposition (328-342 days). If this is correct, the entire 69-cm-thick Ingersoll shale accumulated at a net rate of ~5.5-5.75 cm/tropical month, or 73-77 cm/year (again, uncorrected for compaction). This rate is higher than that inferred from tidal rhythmites in subunit A, and implies that the clay-rich parts of the Ingersoll shale (subunits B and C)

accumulated at higher rates than the sandier parts (subunit A), particularly considering that the clays undoubtedly experienced greater compaction. Alternatively, the 1-cm sampling interval for textural analysis is too coarse to effectively discriminate all sand peaks that are alleged here to reflect spring tidal phases.

Following the less favored alternative interpretation of laminite data (see Fig. 34B), the 13-cm-thick interval of subunit A analyzed for tidal rhythmicity would contain an incomplete record of ~11 spring-neap cycles, representing ~5.5 tropical months of deposition. In this scenario, this interval would have accumulated at a net rate of ~2.36 cm/tropical month, or ~31 cm/year. If this rate is extrapolated to the entire unit, the Ingersoll shale accumulated within ~2.2 years. In this alternative scenario, net sedimentation rates are lower than estimated above but are still rather high.

7.3.3 Substrate Consistency

The consistency of sediment that accumulated in the Ingersoll shale channel evolved through time. Sediments in lower parts of subunit A likely were mainly softgrounds. The sandier, more granular nature of that interval would have precluded development of more fluid or soupy substrates.

In contrast, the sediments that dominate the remainder of the Ingersoll shale likely were relatively fluid substrates (soupgrounds) during deposition. This can be inferred from both general sediment texture and from ichnologic evidence. Clay-rich sediments, particularly those that accumulate rapidly out of suspension, commonly are highly fluid (MacEachern et al., 2005). Moreover, these thixotropic substrates typically lack well-defined biogenic sedimentary structures because burrows tend to collapse immediately behind tracemakers as they “swim” through fluid sediments (Vadec and Schieber, 1999).

However, burrows of such sediment swimmers may be preserved where the tracemakers leave organic slime trails or mucus linings that form microenvironments favorable for early diagenetic pyrite mineralization (Vadec and Schieber, 1999; Schieber, 2002). The sparse, typically flattened, horizontal to subhorizontal, pyritized burrow segments that characterize the bulk of the Ingersoll shale are consistent with burrow production (presumably by vermiform organisms) and early mineralization in relatively fluid substrates.

The well-defined *Rhizocorallium* and *Thalassinoides* that cut the upper ~8 cm of the Ingersoll shale reflect a drastic change in substrate consistency. Sharp, commonly scratch-marked burrow walls in these structures are diagnostic of the firmground *Glossifungites* ichnofacies (Pemberton and Frey, 1985; Pemberton et al, 1992). They indicate that the once-fluid clays were buried, compacted, and then exhumed. Hence, these ichnofossils were emplaced after the top of the Ingersoll shale lens was truncated by bay shoreline ravinement (see section 7.2) or some other erosional mechanism.

7.3.4 Salinity

Based on the prevalence of a terrestrial fossil biota, it could be inferred that the Ingersoll shale accumulated beneath relatively fresh waters. However, palynologic and geochemical evidence indicate that the water in the Ingersoll shale channel was characterized by normal or near-normal salinities.

As previously noted, palynomorphs extracted from Ingersoll shale samples include abundant dinoflagellates and acritarchs. The forms that have been identified are indicative of marine waters (R. Lupia and R.A. Christopher, personal communication, 2006).

In freshwater or slightly brackish systems, low sulfate contents in waters limit the extent of sulfate reduction that can occur to form sulfides. Hence, sulfide S contents and S/C ratios in sediments are typically low (Fig. 41; Berner and Raiswell, 1984). In contrast, sulfate is not limiting in marine waters, and biogenic sulfate reduction in organic-rich sediments results in the production of sulfide and, ultimately, pyrite precipitation (Berner, 1970, 1983, 1985; Berner and Raiswell, 1984). The high sulfide sulfur contents within the Ingersoll shale, reflecting the abundance of pyrite, can therefore be taken as evidence for bacterial sulfate reduction under normal or near-normal marine conditions.

Sulfur isotopic compositions of Ingersoll shale pyrite also support bacterial reduction of marine sulfate. Bacterial sulfate reduction results in significant isotopic fractionation. In modern open systems with an unlimited supply of sulfate, precipitated sulfide phases may be up to 50-55‰ lighter than seawater sulfate (Thode et al., 1961; Holser and Kaplan, 1966; Claypool et al., 1980; Cecile et al., 1983; Faure, 1986). During the Late Cretaceous (Santonian), $\delta^{34}\text{S}$ values for seawater sulfate were within the approximate range of +15 to +18.00‰ (relative to CDT; Claypool et al., 1980). Assuming a 50-55‰ isotopic depletion, $\delta^{34}\text{S}$ values of pyrite formed by sulfate reduction in a Santonian open marine system would be on the order of -32 to -40‰. The range of $\delta^{34}\text{S}$ values for Ingersoll shale pyrite (-35.7 to -39.7‰) are consistent with these expected values.

It could be argued that an adequate supply of marine sulfate was not available to the Ingersoll sediments until after transgression and establishment of estuarine central bay conditions. That is, sulfate for sulfate reduction and pyritization was derived from

bay waters *after* Ingersoll shale deposition. However, this possibility can be excluded based on several lines of evidence. First, diffusion of marine waters at a later time cannot explain the abundance of marine palynomorphs within the shale. Second, the three-dimensional preservation of body fossils by pyrite and deformation of primary laminae around larger pyrite concretions indicate that mineralization occurred very early, prior to significant compaction of the Ingersoll muds. Finally, firmground burrows at the top of the Ingersoll shale indicate that muds were already dewatered and semiconsolidated by the time central bay conditions were established. Downward migration of sulfate-rich waters into this firm mud likely would have been limited and, hence, cannot explain the abundance of pyrite in the Ingersoll shale.

7.3.5 Oxygenation

The water column within the Ingersoll tidal channel likely was oxygenated. This would be expected, given the shallow depth of the channel and the evidence for at least periodic tide-driven currents that were strong enough to transport fine sands and silts. The presence, at least periodically, of bioturbating organisms also indicates sufficient levels of bottom-water oxygenation. However, pore waters likely were highly oxygen deficient, particularly during deposition of the clay-dominated parts of the Ingersoll shale. Highly fluid substrates would have precluded the formation of stable, open burrows and, thus, limited the diffusion of oxygen into the substrate. Oxygen-deficient, reducing (sulfidic) pore waters are indicated by high organic contents and the abundance of early-formed pyrite.

Notably, S/C ratios determined for the Ingersoll shale are unusually high compared to normal marine mudrocks. They fall within the range commonly associated

with euxinic marine basins (Fig. 41) wherein sulfate reduction begins in an anoxic water column well above the seafloor (Berner, 1984). As noted above, the water column in the Ingersoll channel was oxygenated and certainly not deep enough for the development of euxinic conditions. Rather, the unusually high S/C ratios in the Ingersoll shale may be attributed to enhanced sulfide precipitation related to the trapping and enrichment of both colloidal Fe and organic matter in the estuarine system (Morse and Berner, 1995; R. Raiswell, personal communication, 2006).

8.0 DISCUSSION

8.1 Factors Controlling Preservation in Fossil-Lagerstätten

8.1.1 Previous Studies

A variety of factors may contribute to exquisite preservation within conservation Lagerstätten. These include: (1) oxygen-deficiency; (2) rapid burial; (3) microbial processes (e.g., bacterial sealing); (4) early diagenetic mineralization; and (5) entombment in relatively sterile media (Seilacher et al., 1985; Allison, 1988; Babcock, 2001; Briggs, 2003). These factors are not mutually exclusive, and their relative roles vary significantly between deposits. Hence, classification of Lagerstätten based on formative processes may be difficult.

Oxygen deficiency generally leads to improved preservation by precluding bioturbation and limiting biochemical degradation. Oxygen deficiency may develop in basin bottom waters in response to the development of stable thermal or thermohaline water-mass stratification and/or high organic production and associated oxygen demand (Demaison and Moore, 1980). In other cases, bottom waters may be oxygenated but fossil preservation is enhanced by the development of anoxic conditions in pore waters at or just below the sediment-water interface in response to microbial degradation of sedimentary organic matter. The term stagnation deposit can be applied to a spectrum of Lagerstätten for which reducing conditions contributed in some way to fossil preservation (Seilacher et al., 1985). The Posidonienschiefer (Posidonia Shale) of southern Germany

is a good example of a stagnation deposit, as preservation was controlled primarily by oxygen deficiency that developed at various levels above the seafloor (Bottjer et al., 2002).

Rapid burial, or obrution, enhances preservation by isolating organisms from decay-promoting processes (e.g., oxidation, scavenging, and bioturbation) (Seilacher et al., 1985). Burial of organisms can occur during episodic events (e.g., sediment gravity flows, or storms), during the high-frequency periodic influx of sediment (e.g., that associated with tidal cycles), or through a combination of these processes. The Silurian Rochester Shale (New York) is an example of an obrution-type Lagerstätte containing echinoderms that were smothered by tempestites (Taylor and Brett, 1996). Following burial, other factors may enhance or lessen the preservation potential of fossils. Hence, rapid burial alone may not be sufficient for fossil preservation (Allison, 1988).

Bacterial sealing refers to the isolation of organic remains from decay processes via growth of microbial mats (Dunn et al., 1997; Toporski et al., 2002; Borkow and Babcock, 2003). Mat-forming microorganisms can alter the pH and Eh of the microenvironment surrounding soft body tissue (López-Cortés, 1999; Borkow and Babcock, 2003). Through this process, microbes can initiate precipitation of diagenetic minerals and, in some cases, are responsible for their own mineralization (bacterial autolithification of Wüttke, 1983). This mode of preservation is exemplified by the Eocene Messel Shale (Germany), wherein the finest details of soft-tissues are replicated by siderite bacterial pseudomorphs (Wüttke, 1983a). Alternatively, preservation of original bacterial carbon may occur without precipitation of minerals. This mode of preservation is exemplified by the Cretaceous Crato Formation (Brazil), which contains

fossil feathers preserved as mats of apparently unmineralized bacterial bodies (Briggs, 2003).

The taphonomic role of microbes is not limited to bacterial sealing (Allison, 1988). Bacterially-mediated, anaerobic decay processes can result in early diagenetic mineralization of labile tissue (Fisher and Hudson, 1985; Briggs, 2003; Martínez-Delclòs et al., 2004). The minerals that precipitate during early diagenesis are dependent on water chemistry (salinity, pH, Eh, etc.) and include pyrite, siderite, silica, apatite, carbonates, and clay minerals. These can be precipitated on or around soft body parts directly or, as described above, on microbial films that cover soft tissue (Briggs, 2003). Diagenetic mineralization contributed in some degree to the preservation of fossils in many well-known Lagerstätten. As examples, preservation of fossils in the Cambrian Burgess Shale was influenced by diagenetic growth of pyrite and clay (Orr et al., 1998), while fossil preservation in the Eocene Messel Oil Shale (Germany) (Wüttke, 1983) and the Carboniferous Francis Creek Shale (Mazon Creek biota of Illinois) (Babcock, 2001) was enhanced by early diagenetic siderite growth.

Entombment of organisms in sterile media, such as ice, asphalt, peat, and amber, produces conservation traps within which even more labile tissue may be preserved (Seilacher et al., 1985). Peat bogs have yielded examples of Iron-Age cadavers that include all internal organs, skin, hair, and even clothing (Glob, 1969). Fossilized tree resin, or amber, represents a more common medium within which fossils may be exquisitely preserved as unmineralized inclusions (Grimaldi et al., 2000). Important fossil-bearing amber deposits occur in the Cretaceous of New Jersey, the Eocene-Oligocene of northern Europe (Baltic amber), and the Miocene of the Dominican

Republic (Dominican amber) (Poinar, 1998; Grimaldi et al., 2000; Martínez-Delclòs et al., 2004; Grimaldi and Engel, 2005).

8.1.2 Factors Controlling Fossil Preservation in the Ingersoll Shale

All of the taphonomic factors described above contributed in some way to the preservation of the Ingersoll shale fossil biota. While rapid burial may be the most important factor, pore-water anoxia, early diagenetic mineralization, bacterial sealing, and preservation in amber also played a role.

Rapid burial is considered to be the key agent in the preservation of Ingersoll shale fossils. Extremely high net sedimentation rates (up to 77 cm/yr) associated with cyclic tidal deposition led to rapid burial and isolation of animal and plant remains. Moreover, rapid deposition of clays (e.g., in subunits B and C) resulted in relatively inhospitable soupy substrates that inhibited bioturbation and facilitated development of reducing pore waters and consequent sulfide mineralization.

Reducing pore waters at or just below the sediment-water interface also likely enhanced the preservation of Ingersoll fossils. Sulfidic conditions induced by bacterial degradation of abundant organic matter in the sediments not only inhibited the physical destruction of plant and animal parts by scavenging and bioturbation, but also directly led to early diagenetic pyrite mineralization of some fossils.

Although not pervasive, many Ingersoll fossils were replaced in whole or in part by early diagenetic pyrite. In some cases, pyritization destroyed fine morphological or structural details that are otherwise preserved in carbonized plant fossils. Nevertheless, early diagenetic mineralization played an important role in preserving some plant and animal tissues in three dimensions.

Although the role of bacterial sealing in the preservation of Ingersoll fossils has not been completely assessed, this process clearly was important in the preservation of the fossil feathers recovered from the deposit. Fossil feathers are completely replaced by mainly rod-shaped bacteria, which preserve the finest details of the feather structure. Although some feather elements have been selectively pyritized (e.g., three-dimensionally preserved feather calami) and pyrite occurs as randomly dispersed crystals in other parts of feathers, the bacteria replacing the bulk of the feathers are not pyritized. Rather, EDS analyses of the fossil bacteria (see Knight, 2007) indicate the presence of carbon and clay minerals. The carbon may represent original bacterial carbon or plant kerogens similar to those observed in autolithified soft tissue from the Messel Shale (see Wuttke, 1983, Franzen, 1985; Briggs, 2003). Clay minerals may have precipitated in response to the metabolic activity of the bacteria themselves, or they may be the result of some later abiogenic diagenetic process.

The role of conservation and concentration traps is exemplified by the relatively abundant, inclusion-bearing amber recovered from the sandier parts of subunit A of the Ingersoll shale. Much of this amber is allochthonous or para-autochthonous (i.e., derived from plants in proximity to the channel). The formation of fossil resins and the inclusion of fossils therein mainly reflect preservational factors operating outside of the channel itself. However, relatively strong tidal currents in the Ingersoll channel served to transport and concentrate amber clasts (concentration trap). Moreover, upon burial, oxygen-deficient pore waters likely inhibited the degradation and destruction of the amber (Martínez-Delclòs et al., 2004).

8.2 Comparison with Other Lagerstätten

Fossil-Lagerstätten, although generally rare, have been recognized in a variety of deposits representing a broad range of environmental facies and geologic ages. Each is unique with respect to the types of fossils preserved, modes of preservation, and the combination of environmental and diagenetic factors that contributed to preservation. A complete comparative description of all Lagerstätten discovered to date is beyond the scope of this thesis. Herein, only four well-known conservation Lagerstätten are reviewed and compared to the Ingersoll shale Lagerstätte. These are the Cambrian Burgess Shale, Pennsylvanian Francis Creek Shale, Eocene Messel Shale, and Cretaceous South Amboy fire clay. These deposits were chosen for comparison because they exemplify a broad range of depositional regimes and preservation styles.

8.2.1 Burgess Shale

The Burgess Shale (British Columbia, Canada) is perhaps the most well-known Cambrian conservation Lagerstätte. The Burgess shale is composed of thinly laminated to massive, dark gray, fine-grained mudstone and graded turbidites deposited ~530 Ma in a fully marine basin near the western edge of the Laurentian continental platform (Fletcher and Collins, 1998). Fossils recovered from the Burgess Shale are diverse and include trilobites, brachiopods, annelids, chordates, priapulids, and other unassigned forms with no clear affinity to modern organisms. Skeletal hard parts and some soft parts occur as carbonized films, while some labile tissues are replaced with diagenetic pyrite or clay minerals (Orr et al., 1998). The Burgess Shale can be characterized as an obrution/stagnation deposit. Deposition involved episodic sediment-gravity flows that transported marine organisms along with clastic sediment (mud) down a limestone

escarpment into deeper and presumably anoxic waters. Fossils were quickly entombed and smothered in sediment (Orr et al., 1998; Babcock, 2001).

The marine shelf/slope setting of the Burgess Shale contrasts markedly with the depositional environment of the Ingersoll shale. However, as with the Ingersoll shale, deposition is thought to have occurred rapidly, thereby burying the organisms and, in combination with reducing pore waters, inhibiting their decay. The episodic nature of sediment influx into the Burgess Shale anoxic marine basin differs from the more continuous or high-frequency periodic tidal deposition that filled the Ingersoll shale tidal channel. In the case of the Burgess Shale biota, organisms are believed to have been transported alive and, upon burial, were preserved more or less intact. In contrast, the predominately allochthonous and para-autochthonous fossil biota of the Ingersoll shale consists primarily of isolated organs (e.g., leaves, feathers, etc.) (see Knight, 2007).

8.2.2 Francis Creek Shale

The Pennsylvanian Francis Creek Shale Member of the Carbondale Formation in the Mazon Creek area of Illinois is known for exquisite preservation of non-biomineralized marine and terrestrial biotas within siderite concretions (Baird et al., 1985, 1986). This unit accumulated in estuarine distributary bays in a prograding deltaic setting. Fossils include a diverse carbonized terrestrial plant assemblage, fish, crustaceans, insects, bivalves, polychaetes, and medusae. Fossil preservation was enhanced by several factors. Deposition in this setting was very rapid; studies of tidal laminites contained in silty mudstones indicate that sedimentation rates may have exceeded 100 cm/yr (Babcock, 2001). Moreover, episodic influxes of turbid fresh water and sediment from distributary and tidal channels resulted in the transport of terrestrial

organisms and the death and rapid burial of marine forms. Variable salinities and turbidity in this setting also enhanced preservation by inhibiting bioturbation and scavenging. Most important, preservation of soft parts was favored by entombment in early diagenetic siderite concretions that formed under primarily fresh- and brackish-water conditions. In associated, more fully marine facies, deposited when water chemistry was less favorable for siderite mineralization, concretions are less common and the quality of fossil preservation is lower (Babcock, 2001).

The Ingersoll shale and the Francis Creek Shale are similar in several respects. Both accumulated in marginal marine settings. The Ingersoll shale was deposited in a tidal creek within a bayhead delta setting during marine transgression, while the Francis Creek Shale was deposited farther down stream in an estuary during delta progradation. Moreover, both deposits contain tidal rhythmites that reflect very high rates of sedimentation and burial. However, there are notable differences. For the Francis Shale, early diagenetic mineralization of siderite, which reflects a significant freshwater influence, played a central role in fossil preservation. In contrast, pyrite mineralization reflecting predominantly marine waters was a subordinate factor in the preservation of the Ingersoll biota. Oddly, the Francis Shale biota includes common marine elements, whereas the Ingersoll shale, thus far, has failed to yield marine macrofossils other than rare casts and molds of bivalves (in subunit C only) and possibly marine fish scales.

8.2.3 Messel Shale

The middle Eocene Messel Shale in West Germany contains a fossil biota that includes, among other components, terrestrial and avian vertebrates, fish, and insects. This Lagerstätte was deposited in a small (~2.3 km²), relatively deep (>10 m), stagnant,

subtropical lake of tectonic origin (Franzen, 1985). The lake was part of a river system, as evidenced by fossils of organisms that are typical of running water (Franzen, 1985). Depositional rates were low in this quiet-water environment. Terrestrial animals preserved within the shale were drowned by occasional floods and drifted down stream and settled to the bottom of the lake (Franzen, 1985). Fossils of flying animals may have been introduced to the lake bottom after mass killings caused by CO₂ escape from nearby volcanic eruptions (Franzen, 1985). Fossil preservation was enhanced by periodic basin anoxia that developed in response to dinoflagellate blooms (Franzen, 1985). Oxygen-depletion and associated microbial production of H₂S limited scavenging and bioturbation of lake bottom.

The paleoenvironments and preserved biotas of the Messel Shale and Ingersoll shale are very different. However, these two units have some similarities with respect to style of soft-tissue preservation. In the Messel Lagerstätte, fossil feathers, skin, and hair are preserved as body silhouettes wherein labile tissues have been replaced by rod- and coccoid-shaped bacteria, which in turn were preserved via autolithification by siderite (Wuttke, 1983; Franzen, 1985). Mats of comparable bacteria, albeit apparently unmineralized, have preserved all of the fossil feathers from the Ingersoll shale.

8.2.4 South Amboy Fire Clay

The Turonian South Amboy fire clay, part of the Raritan Formation exposed in New Jersey, contains an extraordinarily diverse, carbonized and locally pyritized terrestrial plant assemblage (Newberry, 1895). However, these deposits are best known for their abundant amber and associated inclusions. The latter include, among other things, well-preserved insects, spiders, mites, flowers, mushrooms, and bird feathers (see

Grimaldi et al., 2000). The sedimentologic context of the South Amboy fire clay is seemingly poorly documented. However, previous studies indicate that plants and amber accumulated within interdistributary channels and restricted, anaerobic slackwater channels that ran through brackish, deltaic swamps (Grimaldi et al., 2000).

The South Amboy fire clay and Ingersoll shale Lagerstätten compare favorably with regard to depositional environment, fossil biota, and modes of fossil preservation. Both accumulated in restricted channels within marginal marine settings and both contain amber and well-preserved, carbonized and variably pyritized terrestrial flora. Given the similarities, more detailed comparative studies of sedimentologic context and paleoenvironments would be useful.

8.3 Prospecting for Comparable Conservation Lagerstätten

Prospecting for conservation Lagerstätten is a realistic objective since the causative factors that lead to their formation are finite (Seilacher et al., 1985; Allison, 1988). It seems reasonable to assume that the paleoenvironmental conditions responsible for the deposition of the Ingersoll shale have recurred in time and space and that similar deposits containing comparably well-preserved fossil biotas exist elsewhere in the stratigraphic record. Accordingly, observations on and interpretations made for the Ingersoll shale may be of use in developing a predictive strategy for locating similar Lagerstätten.

The Ingersoll shale accumulated in a narrow and shallow, marine-influenced tidal channel wherein a mainly terrestrial biota was preserved due to rapid deposition of organic-rich, clay-dominated sediments and consequent pore-water anoxia and early sulfide precipitation. This restricted channel developed in an estuarine delta-head delta

setting in response to regional transgression. This paleoenvironmental framework can be used to prospect for other conservation Lagerstätten. As an example, the Cretaceous system of the eastern Gulf coastal plain is dominated by stacked marginal marine, predominately estuarine successions that formed in response to sea-level dynamics (e.g., Eutaw and Blufftown formations, Cusseta Sand; Frazier, 1996, 1987; King, 1993). Based on our understanding of the Ingersoll shale, other isolated, fossil-rich channel deposits can be sought in these successions, particularly in intervals that preserve bayhead-delta facies. These may occur in the lower parts of transgressive estuarine packages (as is the case for the Ingersoll shale). However, similar deposits could occur higher in these packages as a result of bayhead-delta progradation during highstand or regressive phases.

Notably, other unusually fossiliferous clay lenses previously have been described from the Eutaw Formation and equivalent Santonian units from the eastern Gulf coastal plain (e.g., Hilgard, 1860; Konopka et al., 1997; Herendeen et al., 1999; Sims et al., 1999). Predictably, these may reflect deposition in settings similar, if not identical, to that of the Ingersoll shale. However, the paleoenvironmental and sequence stratigraphic contexts of these clay lenses are not well documented. Comparative sedimentologic and stratigraphic studies of such previously identified deposits would provide another way of testing the prospect value of observations made in the study of the Ingersoll shale.

9.0 SUMMARY AND CONCLUSIONS

The Ingersoll shale, a thin (<1 m) clay lens in the Cretaceous Eutaw Formation exposed in eastern Alabama, contains an unusually well-preserved, mainly terrestrial biota. The biota is dominated by a diverse, carbonized and variably pyritized flora consisting of macrofossils (isolated and articulated leaves, stems, cones, flowers, etc.), megaspores, and palynomorphs. However, it also contains abundant amber with fossil inclusions, rare invertebrates (e.g., bivalves and arthropods parts), and, most notably, common feathers preserved by dense mats of fossil bacteria. Studies were undertaken in order to establish the formative processes responsible for this conservation Lagerstätte. The main findings of this work are summarized below.

(1) Unit geometry, internal sedimentologic characteristics, and stratigraphic position between high-energy tidal sand facies below and estuarine central bay facies above indicate that the Ingersoll shale accumulated during estuarine transgression in a narrow, shallow, restricted channel within the lower reaches of a bayhead delta.

(2) Tidal laminites represented by bundled couplets of carbonaceous sand and mud laminae dominate the base of the Ingersoll shale, while organic-rich clay becomes more prevalent through the middle and upper parts of the unit. Analysis of tidal laminites and textural analyses of the entire Ingersoll shale suggest that deposition occurred very rapidly (as high as 77 cm/year) in response to diurnal tidal currents that transported sediment as traction and/or suspended load. Upward fining indicates that tidal current

strengths decreased through time, perhaps in response to transgressive flooding/ deepening of the channel.

(3) Limited bioturbation (reflected by sparse, narrow, flattened burrows), high organic contents, and abundant early-formed pyrite indicate that, during deposition of the clay-rich parts of the Ingersoll shale, substrates were relatively fluid and highly reducing.

(4) Despite the prevalence of a terrestrial biota, abundant marine palynomorphs and geochemical evidence (pyrite content, S/C ratios, and stable isotopic signatures of pyrite sulfur) indicate that the Ingersoll shale was deposited beneath normal to near-normal marine waters.

(5) All of the main factors that contribute to fossil preservation within conservation Lagerstätten are manifest in the Ingersoll shale. High sedimentation rates resulted in the rapid burial (obration) of fossil remains. Preservation of buried remains was further enhanced by anoxic pore-water (stagnation) and consequent pyritization, which, in some cases, resulted in three-dimensional preservation of fossils (diagenetic mineralization). Reducing conditions also likely contributed to the formation of bacterial mats that preserved feathers and, perhaps, other fossil elements (bacterial sealing). Although entombment of fossil inclusions in Ingersoll amber (conservation traps) occurred outside of the channel, amber clasts were hydraulically concentrated by tidal currents and their preservation was enhanced by reducing conditions.

(6) The Ingersoll shale is unique among previously described fossil Lagerstätte but closely resembles the Cretaceous South Amboy fire clay (New Jersey) with respect to depositional setting, fossil assemblage composition, and modes of preservation. Knowledge of the stratigraphic and paleoenvironmental context of the Ingersoll shale

may be of use in predicting the locations of other deposits that may contain comparable unusually well-preserved fossil biotas.

10.0 REFERENCES

- ALLISON, P.A., 1988, Konservat-Lagerstätten: cause and classification: *Paleobiology*, v. 14, p. 331-334.
- ARCHER, A.W., 1998, Hierarchy of controls on cyclic rhythmites: Carboniferous basins of eastern and mid-continental U.S.A., *in* Alexander, M.R., Davis, R.A., and Henry, V.J., eds., *Tidalites: Processes and products: Society for Sedimentary Geology Special Publications 61*, p. 151-173.
- BABCOCK, L.E., 2001, Explaining ancient fossil motherlodes: Depositional circumstances of Cambrian Burgess Shale-type deposits: *American Paleontologist*, v. 9, p. 2-5.
- BAIRD G.C., SHABICA, C.W., ANDERSON, J.L., and RICHARDSON, E.S., JR, 1985, Biota of a Pennsylvanian muddy coast: Habitats within the Mazonian delta complex, Northeast Illinois: *Journal of paleontology*, v. 59, p. 253-281.
- BAIRD G.C., SROKA, S.D., SHABICA, C.W., and KUECHER, G.J., 1986, Taphonomy of Middle Pennsylvanian Mazon Creek area fossil localities, Northeast Illinois: Significance of exceptional fossil preservation in syngenetic concretions: *Palaios*, v. 1, p. 271-285.
- BERNER, R.A., 1970, Sedimentary pyrite formation: *American Journal of Science*, v. 268, p. 1-23.

- BERNER, R.A., 1983, Sedimentary pyrite formation: An update: *Geochimica et Cosmochimica Acta*, v. 48. p. 605-615.
- BERNER, R.A., 1985, Sulphate reduction, organic matter and pyrite formation: *Philosophical Transactions of the Royal Society of London*, v. A 315, p. 25-28.
- BERNER, R.A., and RAISWELL, R., 1984, C/S method for distinguishing freshwater from marine sedimentary rocks: *Geology*, v.12, p. 65–68.
- BINGHAM, P.S., and FRAZIER, W.J., 2004, Paleogeographic reconstruction of Upper Cretaceous southwest Georgia and east central Alabama using the GIS method (DIGGH) to analyze the disconformity separating Tuscaloosa sediments from the Eutaw Formation: *Geological Society of America, Abstracts with Programs*, v. 36, no. 2, p. 137.
- BLOTT, S.J., and PYE, K., 2001, Gradistat: a grain size distribution and statistics package for the analysis of unconsolidated sediments: *Earth Surface Processes and Landforms*, v. 26, p. 1237-1248.
- BORKOW, P.S., and BABCOCK, L.E., 2003, Turning pyrite concretions outside-in: Role of biofilms in pyritization of fossils: *The Sedimentary Record*, v. 1, p. 1-7.
- BOTTJER, D.J., ETTER, W., HAGADORN, J.W., and TANG, C.M., eds., 2002, *Exceptional Fossil Preservation: A Unique View on the Evolution of Marine Life*: Columbia University Press, New York, 403 p.
- BRIGGS, E.G., 2003, The role of decay and mineralization in the preservation of soft-bodied fossils: *Annual Review of Earth and Planetary Sciences*, v. 31, p. 275-301.

- BUATOIS, A., GINGRAS, M.K., MACEACHERN, J., MÀNGANO, M.G., ZONNEVELD, J.P., PEMBERTON, S.G., NETTO, R.G., MARTIN, A., 2005, Colonization of brackish-water systems through time: Evidence from the trace-fossil record: *Palaios*, v. 20, p. 321-347.
- CECILE, M.P., SHAKUR, M.A., and KROUSE, H.R., 1983, The isotopic composition of western Canadian barites and the possible derivation of oceanic sulphate $\delta^{34}\text{S}$ and $\delta^{18}\text{O}$ age curves: *Canadian Journal of Earth Science*, v. 20, p. 1528-1535.
- CHRISTOPHER, R.A., SELF-TRAIL, J.M., PROWELL, D.C., and GOHN, G.G., 1999, The stratigraphic importance of the Late Cretaceous pollen genus *Sohlipollis* gen. nov. in the Coastal Plain Province: *South Carolina Geology*, v. 41, p. 27-44.
- CLAYPOOL, G.E., HOLSER, W.T., KAPLAN, I.R., SAKAI, H., and ZAK, I., 1980, The age curves of sulfur and oxygen isotopes in marine sulfate and their mutual interpretations: *Chemical Geology*, v. 28, p. 199-260.
- DALRYMPLE, R.W., 1992, Tidal depositional systems, *in* Walker, R.G., and James, N.P., eds., *Facies Models and Sea Level Changes*: Geological Association of Canada, p. 195-218.
- DALRYMPLE, R.W., and MAKINO, Y., 1989, Description and genesis of tidal bedding in the Cobequid Bay-Salmon River Estuary, Bay of Fundy, Canada, *in* Taira, A., and Masuda, F., eds., *Sedimentary Facies of the Active Plate Margin*: Terra Scientific, Tokyo, p. 151-177.
- DAVIS, P., and BRIGGS, D.E.G., 1995, Fossilization of feathers: *Geology*, v. 23, p. 783-786.

- DEMAISON, G.J., and MOORE, G.T., 1980, Anoxic environments and oil source bed genesis: American Association of Petroleum Geologists Bulletin, v. 64, p. 1179-1209.
- DUNN, K.A., MCLEAN, R.J.C., UPCHURCH, G.R., JR., and FOLK R.L., 1997, Enhancement of leaf fossilization potential by bacterial biofilms: Geology, v. 25, p. 1119-1112.
- EARGLE, D.H., 1955, Stratigraphy of the outcropping Cretaceous rocks of Georgia: U.S. Geological Survey Bulletin 1014, 101 p.
- FAGHERAZZI, S., GABET, E.J., and FURBISH, D.J., 2004, The effect of bidirectional flow on tidal channel planforms: Earth Surface Processes and Landforms, v. 29, p. 295-309.
- FAURE, G. 1986, *Principles of Isotope Geology*, second edition: New York, John Wiley and Sons, 589 p.
- FISHER, I. ST. J., and HUDSON, J.D., 1985, Pyrite geochemistry and fossil preservation in shales: Philosophical Transactions of the Royal Society of London, v. B 311, p. 167-169.
- FLETCHER, T.P., and COLLINS, D.H., 1998, The Middle Cambrian Burgess Shale and its relationship to the Stephen Formation in the southern Canadian Rocky Mountains: Canadian Journal of Earth Sciences, v. 35, p. 413-436.
- FRANZEN, J.L., 1985, Exceptional preservation of Eocene vertebrates in the lake deposit of Grube Messel (West Germany), *in* Extraordinary Fossil Biotas: Their Ecological and Evolutionary Significance: Philosophical Transactions of the Royal Society of London v. 311B, p.181-186.

- FRAZIER, W.J., 1982, Sedimentology and paleoenvironmental analysis of the Upper Cretaceous Tuscaloosa and Eutaw Formations in western Georgia, *in* Arden, D.D., and Beck, B.B., eds., Second Symposium on Geology of the Southeastern Coastal Plain: Georgia Geological Society, Information Circular, p. 39-52.
- FRAZIER, W.J., 1987, A guide to the facies stratigraphy of the Eutaw Formation in western Georgia and eastern Alabama, *in* Frazier, W.J., and Hanley, T.B., eds., Geology of the Fall Line: A Field Guide to Structure and Petrology of the Uchee Belt and Facies Stratigraphy of the Eutaw Formation in Southwestern Georgia and Adjacent Alabama: Georgia Geological Society, 22nd Annual Field Trip Guidebook, p. B1-B25.
- FRAZIER, W.J., 1996, Estuarine deposits in the Eutaw and Blufftown Formations (Santonian and Campanian) of southwestern Georgia and adjacent Alabama and their sequence stratigraphic significance: Geological Society of America, Abstracts With Programs, v. 28, no. 2, p. 12.
- FRAZIER, W.J., 1997, Upper Cretaceous strata in southwestern Georgia and adjacent Alabama: Atlanta Geological Society Field Trip, Guidebook, p. 1-22.
- FRAZIER, W.J., and TAYLOR, R.S., 1980, Facies changes and paleogeographic interpretation of the Eutaw Formation (Upper Cretaceous) from western Georgia to central Alabama, *in* Tull, J.F., ed., Field Trips for the Southeastern Section of the Geological Society of America, Birmingham, Alabama, p. 1-27.

- GASTALDO, R.A., and HUC, A.Y., 1992, Sediment facies, depositional environments, and distribution of phytoclasts in the recent Mahakam River delta, Kalimantan, Indonesia: *Palaios*, v. 7, p. 574-590.
- GLOB, P.V., 1969, *The Bog People*: London, Faber, 200 p.
- GRIMALDI, D., and ENGEL, M.S., 2005 *Evolution of the Insects*: New York, Cambridge University Press, 755 p.
- GRIMALDI, D., SHEDRINSKY, A., and WAMPLER, T.P., 2000, A remarkable deposit of fossiliferous amber from the Upper Cretaceous (Turonian) of New Jersey, *in* Grimaldi, D., ed., *Studies On Fossils In Amber, With Particular Reference To The Cretaceous Of New Jersey: Paleontology of New Jersey Amber Part VII*, p. 1-76.
- HERENDEEN, P.S., MAGALLÓN-PUEBLA, S., LUPIA, R., CRANE P.R., and KOBYLINSKA, J., 1999, A preliminary conspectus of the Allon flora from the Late Cretaceous (Late Santonian) of Central Georgia, U.S.A.: *Annals of the Missouri Botanical Garden*, v. 86, p. 407-471.
- HILGARD, E.W., 1860, *Report on the geology and agriculture of the state of Mississippi*: Mississippi State Geological Survey, Jackson, MS, 391 p.
- HOLSER, W.T., and KAPLAN, I.R., 1966, Isotope geochemistry of sedimentary sulfates: *Chemical Geology*, v. 1, p. 93-135.
- KELLNER, A.W.A., 2002, A review of avian Mesozoic fossil feathers, *in* Chiappe, L.M., and Witmer, L.M., eds., *Mesozoic Birds: Above the Heads of Dinosaurs*, p. 389-404.

- KING, D.T., JR., 1990, Facies stratigraphy and relative sea-level history-Upper Cretaceous Eutaw Formation, central and eastern Alabama: Transactions, Gulf Coast Association of Geological Societies, v. 40, p. 381-387.
- KING, D.T., JR., 1993, Eustatic and tectonic effects within sequence stratigraphy of the outcropping paralic-marine section, Upper Cretaceous, Alabama: Transactions, Gulf Coast Association of Geological Societies, v. 43, p. 157-171.
- KING, D.T., JR., and SKOTNICKI, M.C., 1986, Facies relations and depositional history of the Upper Cretaceous Blufftown Formation in eastern Alabama and coeval shelf sediments in central Alabama, *in* Reinhardt, J., ed., Stratigraphy and Sedimentology of Continental, Nearshore, and Marine Cretaceous Sediments of the Eastern Gulf Coastal Plain: Society of Economic Paleontologists and Mineralogists Foundation, Annual Research Conference, p. 10-26.
- KNIGHT, T.K., 2007, Biotic composition and taphonomy of an Upper Cretaceous Konservat-Lagerstätte, Eutaw Formation, eastern Alabama: Unpublished M.S. thesis, Auburn University, Auburn, 237 p.
- KONOPKA, A.S., HERENDEEN, P.S., MERRILL, G.L.S., and CRANE, P.R., 1997, Sporophytes and gametophytes of polytrichacea from the Campanian (Late Cretaceous) of Georgia, U.S.A.: International Journal of Plant Sciences, v. 158, p. 489-499.
- KVALE, E.P., and ARCHER, A.W., 1990, Tidal deposits associated with low-sulfur coals, Brazil Fm. (Lower Pennsylvanian), Indiana: Journal of Sedimentary Petrology, v. 60, p. 563-574.

- KVALE, E.P., JOHNSON, H.W., SONETT, C.P., ARCHER, A.W., and ZAWISTOSKI, A., 1999, Calculating lunar retreat rates using tidal rhythmites: *Journal of Sedimentary Research*, v. 69, p. 1154-1168.
- LOPÉZ-CORTÉS, A., 1999, Paleobiological significance of hydrophobicity and adhesion of phototrophic bacteria from microbial mats: *Precambrian Research*, v. 96, p. 25-39.
- MACEachern, J.A., BANN, K.L., BHATTACHARYA, J.P., and HOWELL, C.D., JR., 2005, Ichnology of Deltas: Organism response to the dynamic interplay of rivers, waves, and tides, *in* *River Deltas-Concepts, Models, and Examples: Society for Sedimentary Geology Special Publication no. 83*, p. 49-85.
- MANCINI, E.A., PUCKETT, M.T., TEW, B.H., and SMITH, C., 1995, Upper Cretaceous sequence stratigraphy of the Mississippi–Alabama area: *Transactions, Gulf Coast Association of Geological Societies*, v. 45, p. 377-384.
- MARTÍNEZ-DELCLÒS, X., BRIGGS, D.E.G., and PEÑALVER, E., 2004, Taphonomy of insects in carbonates and amber: *Palaeogeography, Palaeoclimatology, Palaeoecology*, v. 203, p. 19-64.
- MORSE, J.W., and BERNER, R.A., 1995, What determines sedimentary C/S ratios? *Geochemica et Cosmochimica Acta*, v. 59, p. 1073-1077.
- NEWBERRY, J.S., 1895, The flora of the Amboy Clays, *in* Hollick, A., ed., *Monographs of the United States Geological Survey*, v. 26, p. 260.
- NORELL, M.A., and XU, X., 2005, Feathered dinosaurs: *Annual Review of Earth and Planetary Science*, v. 33, p. 277-299.

- O'BRIEN, N.R., and SLATT, R.M., 1990, *Argillaceous Rock Atlas*: New York, Springer-Verlag, 141 p.
- ORR, P.J., BRIGGS, D.E.G., and KEARNS, 1998, Cambrian Burgess Shale animals replicated in clay: *Science*, v. 281, p. 1173-1175.
- PEMBERTON, S.G., and FREY, R.W., 1985, The *Glossifungites* ichnofacies: Modern examples from the Georgia coast, U.S.A. in Curran, H.A., ed., *Biogenic Structures: Their Use in Interpreting Depositional Environments*: Society of Economic Paleontologists and Mineralogists, Special Publication no. 35, p. 237-259.
- PEMBERTON, S.G., MACCEACHERN, J.A., and FREY, R.W., 1992, Trace fossil facies models: Environmental and allostratigraphic significance, in Walker, R.G., and James, N.P., eds., *Facies Models—Response to Sea Level Change*: Geological Association of Canada, p. 47-72.
- POINAR, G. JR., 1998, Trace fossils in amber: a new dimension for the ichnologist: *Ichnos*, v. 6, p. 47-52.
- REINHARDT, J., and DONOVAN, A.A., 1986, Stratigraphy and sedimentology of Cretaceous continental and nearshore sediments in the eastern Gulf Coastal Plain: in Reinhardt, J., ed., *Stratigraphy and Sedimentology of Continental, Nearshore, and Marine Cretaceous Sediments of the Eastern Gulf Coastal Plain*: SEPM Field Trip Guidebook, v. 3, 99 p.
- REINHARDT, J., SCHINDLER, S., and GIBSON, T.G., 1994, Geologic map of the Americus 30'x 60' quadrangle, Georgia and Alabama: Department of the Interior, U.S. Geological Survey, map 1-2174.

- SAVRDA, C.E., and KING, D.T., JR., 1993, Log-ground and *Teredolites* Lagerstätte in a transgressive sequence, Upper Cretaceous (Lower Campanian) Mooreville Chalk, central Alabama: *Ichnos*, v. 3, p. 69-77.
- SAVRDA, C.E., and NANSON, L.L., 2003, Ichnology of fair-weather and storm deposits in an Upper Cretaceous estuary (Eutaw Formation, western Georgia, USA): *Palaeogeography, Palaeoclimatology, Palaeoecology*, v. 202, p. 67-83.
- SAVRDA, C.E., LOCKAIR, R.E., HALL, J.K., SADLER, M.T., SMITH, M.W., and WARREN, D., 1998, Ichnofabrics, ichnocoenoses, and ichnofacies implications of an Upper Cretaceous tidal-flat sequence, (Eutaw Formation, central Alabama): *Ichnos*, v. 6, p. 53-74.
- SCHIEBER, J., 2002, The role of an organic slime matrix in the formation of pyritized burrow trails and pyrite concretions: *Palaios*, v. 17, p. 104-109.
- SEILACHER, A., REIF, W.-E., and WESTPHAL, F., 1985, Sedimentological, ecological and temporal patterns of *Fossil-Lagerstätten*: *Philosophical Transactions of the Royal Society of London*, v. B 311, p. 5-23.
- SIMS, H.J., HERENDEEN, P.S., LUPIA, R., and CHRISTOPHER, R.A., 1999, Fossil flowers with normapolles pollen from the Upper Cretaceous of southeastern North America: *Review of Palaeobotany and Palynology*, v. 106, p. 131-151.
- SMITH, L.W., 1984, Depositional Setting and Stratigraphy of the Tuscaloosa Formation, Central Alabama to West-Central Georgia: Unpublished M.S. thesis, Auburn University, Auburn, 139 p.

- SMITH, L.W., and KING, D.T., JR., 1983, The Tuscaloosa Formation: Fluvial facies and their relationship to the basement topography and change in paleoslope, *in* Carrington, T.J., ed., Current Studies of Cretaceous Formations in Eastern Alabama and Columbus, Georgia: Twentieth Annual Field Trip of the Alabama Geological Society, p. 11-16.
- TAYLOR, W.L., and BRETT, C.E., 1996, Taphonomy and paleoecology of echinoderm Lagerstätten from the Silurian (Wenlockian), Rochester shale: *Palaios*, v. 11, p. 118-140.
- THODE, H.G., MONSTER, J., and DUNFORD, H.B., 1961, Sulphur isotope geochemistry: *Geochimica et Cosmochimica Acta*, v. 25, p. 150-174.
- TOPORSKI, J.K.W., STEELE, A., WESTALL, F., AVCI, R., MARTILL, D.M., and MCKAY, D.S., 2002, Morphologic and spectral investigation of exceptionally well-preserved bacterial biofilms from the Oligocene Enspel Formation, Germany: *Geochimica et Cosmochimica Acta*, v. 66, p. 1773-1791.
- VADEC, L., and SCHIEBER, J., 1999, Biogenic Structures produced by worms in soupy, soft muds; observations from the Chattanooga Shale (Upper Devonian): *Journal of Sedimentary Research*, v. 69, p. 1041-1049.
- VAN WAGONER, J.C., MITCHEM, R.M., CAMPION, K.M., and RAHMANIAN, V.D., 1990, Siliciclastic sequence stratigraphy in well logs, cores, and outcrops: Concepts for high-resolution correlation of time and facies: American Association of Petroleum Geologists Methods in Exploration Series, no. 7, 55 p.
- VISSER, M.J., 1980, Neap-spring cycles reflected in Holocene subtidal large-scale bedform deposits, a preliminary note: *Geology*, v. 8, p. 543-546.

WÜTTKE, M. 1983, 'Weichteil-Erhaltung' durch lithifizierte Mikroorganismen bei mittel-eozänen Vertebraten aus den Ölschiefern der 'Grube Messel' bei Darmstadt: Senck. Lethaea, v. 64, p. 509-527.